

Tryptophan Coordinates cGAS/STING Signaling in the Intestinal Epithelium

Dissertation

zur Erlangung des Doktorgrades
der Mathematisch-Naturwissenschaftlichen Fakultät
der Christian-Albrechts-Universität zu Kiel

vorgelegt von

Julia Kugler

Kiel, 2023

Erster Gutachter: Prof. Dr. Philip Rosenstiel

Zweiter Gutachter: Prof. Dr. Thomas Roeder

Tag der mündlichen Prüfung: 08.02.2024

Zum Druck genehmigt: 08.02.2024

Gez. Dekan

Table of Contents

List of Abbreviations	1
Summary	5
Zusammenfassung	6
1. Introduction	8
Inflammatory bowel disease (IBD)	8
Intestinal Physiology	8
Pathophysiology	8
Predispositions to IBD	10
ER Stress	11
Autophagy	12
Diagnosis and Epidemiology	13
Therapeutic approaches	14
1.3 Inflammation	15
Nucleic acid recognition	15
cGAS/STING pathway	15
NF- κ B pathway	17
Cytokines	18
Immunometabolism	20
1.4 Tryptophan	22
Sources and fates of Trp	22
Trp in inflammation	25
1.5 Aim	26
2. Materials and Methods	27
2.1 Cell biological methods	27
Cell culture	27
CRISPR/Cas	28
Crypt isolation	28
Organoid culture	29
MTS assay	29
Transfections	30
2.2 Molecular biological methods	30
RNA isolation	30
cDNA synthesis	31
qPCR	31
Consumption release rate (CORE)/Analysis of Medium Exchange Rates	31
Glucose tracing	32
2.3 Biochemical methods	33
Protein lysates and total protein concentration determination	33
WB	34
2.4 Cohorts and bioinformatical analysis	34
2.5 Statistical analysis	35
3. Results	36

3.1 The intestinal mucosa of IBD patients exhibits shortage of Trp	36
3.2 Trp starvation decreases the cell viability <i>in vitro</i>	38
3.3 Trp starvation sensitizes cells to NF- κ B activation	39
3.4 Trp starvation lowers STING protein levels	41
3.5 Trp starvation impairs the cGAS/STING response	43
3.6 Replenishing Trp restores STING expression	46
3.7 Starvation-induced STING decrease is specific to Trp	46
3.8 Trp starvation does not affect the cellular ATP levels	47
3.9 Autophagy inhibition does not rescue STING levels	52
3.10 Trp starvation does not affect STING via ER stress	56
3.11 Trp starvation decreases Tmem173 mRNA levels	60
3.12 Trp starvation requires protein translation for STING degradation	63
4. Discussion	64
4.1 Trp levels are decreased in the inflamed intestinal epithelium	64
4.2 Trp starvation sensitizes cells to NF- κ B activation	65
4.3 Trp starvation impairs the cGAS/STING response	67
4.4 Replenishing Trp restores STING after starvation	70
4.5 Trp starvation does not affect cellular ATP levels	71
4.6 Inhibition of autophagy does not restore STING levels under Trp starvation	73
4.7 Trp starvation affects STING independent of oxidative stress	75
4.8 Trp starvation decreases Tmem173 mRNA expression	78
4.9 Inhibition of protein synthesis rescues Trp starvation-induced STING loss	80
4.10 Conclusion	82
4.11 Outlook	83
References	84
Appendix	96
Materials	96
Chemicals	96
Consumables	97
Kits	98
Media/Buffer compositions	98
Stimulants and inhibitors	101
siRNAs	101
qPCR Assays/Primers	102
Antibodies for WB	102

Supplements	103
List of Figures	103
List of Tables	103
Acknowledgements	104
Eidesstattliche Erklärung	105

List of Abbreviations

The abbreviations used in this thesis are listed in the following table.

3-HAA	3-hydroxyanthranilic acid
3-HK	3-hydroxykynurenine
5-HT	5-hydroxy-tryptamine/serotonin
5-HTrp	5-hydroxytryptophan
4-OI	4-octyl-itaconate
AA	Amino acid
ActD	Actinomycin D
AD	Alzheimer's disease
ADF	Advanced DMEM/F12
ADP	Adenosine diphosphate
AhR	Aryl hydrocarbon receptor
Akt	Protein kinase B
Amp	Ampicillin
AMP	Adenosine monophosphate
AMPK	AMP-activated protein kinase
APCs	Antigen-presenting cells
ATF	Activating transcription factor
ATG	Autophagy-related
ATG16L1	Autophagy-related protein 16-like 1
ATP	Adenosine triphosphate
Asp	Aspartate
BBB	Blood-brain barrier
BMDCs	Bone marrow-derived dendritic cells
BMDMs	Bone marrow-derived macrophages
BSA	Bovine serum albumin
Cas	CRISPR-associated protein 9
CasR	Calcium-sensing receptor
CD	Crohn's disease
CD4	Cluster of differentiation 4
CDNs	Cyclic dinucleotides
cDNA	Complementary DNA
cGAMP	Cyclic GAMP-AMP
cGAS	Cyclic GMP-AMP synthase
CHX	Cycloheximide
CMA	Chaperone-mediated autophagy
CMV	Cytomegalovirus
c-myc	Cellular Myc
CNS	Central nervous system
CORE	Consumption release rate
CREB	Cyclic-AMP response element binding
CRISPR	Clustered regularly interspaced short palindromic repeats
CRP	C-reactive protein
crRNA	CRISPR RNA
CTT	Carboxy-terminal tail
CXCL	C-X-C motif chemokine ligand
Cyp1A1	Cytochrome p450 family 1 subfamily A member 1
DCs	Dendritic cells
DMEM	Dulbecco's Modified Eagle Medium

DMSO	Dimethyl sulfoxide
DMXAA	5,6-dimethylxanthenone-4-acetic acid
DNA	Deoxyribonucleic acid
dNTPs	Deoxynucleotide triphosphates
dsDNA	Double-stranded DNA
DSS	Dextran sulfate sodium
E-4P	Erythrose 4-phosphate
EC	Enterochromaffin cell
ECL	Enhanced chemiluminescence
EDTA	Ethylenediamine tetraacetic acid
EIF-2	Eukaryotic translation initiation factor 2
EIF2αK	Eukaryotic translation initiation factor 2 α kinase
EIF2αK4	Eukaryotic translation initiation factor 2 α kinase 4
ER	Endoplasmic reticulum
ERAD	ER-associated protein degradation
ERK	Extracellular signal-regulated kinase
ERN1/IRE1	Endoplasmic reticulum to nucleus signaling 1
FBS	Fetal bovine serum
GAS	IFN- γ -activated site
GC-MS	Gas chromatography–mass spectrometry
Gclm	Glutamate-cysteine ligase modifier subunit
GCN2	General control nonderepressible 2
gDNA	Genomic DNA
GDP	Guanosine diphosphate
GPX4	Glutathione peroxidase 4
gRNA	Guide RNA
GSH	Glutathione
GTP	Guanosine triphosphate
GWASs	Genome-wide association studies
HBSS	Hanks' balanced salt solution
hEGF	Human epidermal growth factor
HEPES	N-2-hydroxyethylpiperazine-N-2-ethane sulfonic acid
HSPA5/GRP78	Heat shock 70kDa protein 5
IBD	Inflammatory bowel disease
IDO1	Indoleamine 2,3-Dioxygenase 1
IECs	Intestinal epithelial cells
IEX-1	Immediate early gene X-1
IFN	Interferon
IFNAR	IFN α / β receptor
IKK	I κ B kinase
IL	Interleukin
IL-10R	Interleukin-10 receptor
IL-4I1	Interleukin-4-induced-1
IRE1	Inositol-requiring enzyme 1
IRF	Interferon regulatory factor
ISGF3	IFN-stimulated gene factor 3
ISRE	IFN-stimulated response elements
IκBs	Inhibitors of NF- κ B
JAK	Janus kinase
KA	Kynurenic acid
KD	Knockdown
Keap1	Kelch-like ECH-associated protein 1

KO	Knockout
KP	Kynurenine pathway
KYA	Kynurenic acid
Kyn	Kynurenine
LB	Lysogeny broth
LC3	Microtubule-associated protein 1 light chain 3
LC-MS	Liquid chromatography–mass spectrometry
LPS	Lipopolysaccharide
MAMPs	Microbe-associated molecular pattern
MAPKs	Mitogen-activated protein kinases
MEFs	Murine embryonic fibroblasts
MHC	Major histocompatibility complex
mRNA	Messenger RNA
mTOR	Mammalian target of rapamycin
MTORC1	Mammalian target of rapamycin complex 1
MTS	(3-(4,5-dimethylthiazol-2-yl)-5-(3-carboxymethoxyphenyl)-2-(4-sulfophenyl)-2H-tetrazolium)
NA	Nucleic acid
NAC	N-acetylcysteine
NAD	Nicotinamide adenine dinucleotide
NAM	Nicotinamide
NEAA	Non-essential amino acids
NF-κB	Nuclear factor κB
NLRP3	NLR family pyrin domain containing 3
NOD2	Nucleotide binding oligomerization domain containing 2
NR	Nicotinamide ribose
Nrf2	Nuclear factor erythroid 2-related factor 2
OD	Optical density
OXPHOS	Oxidative phosphorylation
p53	Tumor protein 53
P/S	Penicillin / streptomycin
pANCA	Perinuclear antineutrophil cytoplasmic antibodies
PAM	Protospacer adjacent motif
PAMPs	Pathogen-associated molecular patterns
PBS	Phosphate buffered saline
PC	Pyruvate carboxylase
PCV	Packed cell volume
PCR	Polymerase chain reaction
PD1	Programmed cell death ligand
PDH	Pyruvate dehydrogenase
PE	Phosphatidylethanolamine
PEP	Phosphoenolpyruvate
PERK/EIF2AK3	Eukaryotic translation initiation factor 2-a kinase 3
Phe	Phenylalanine
PIC	Picolinic acid
PKR, EIF2αk2	Protein kinase R
PMS	Phenazine methosulfate
PRRs	Pattern-recognition receptors
PtdCho	Phosphatidylcholine
PUFA	Poly-unsaturated fatty acids
PVDF	Polyvinylidene difluoride
QA	Quinolinic acid

qPCR	Quantitative PCR
RA	Rheumatoid arthritis
RIPA	Radioimmunoprecipitation assay
RNA	Ribonucleic acid
ROS	Reactive oxygen species
rRNA	Ribosomal RNA
RT	Room temperature
SBEs	STAT3-binding elements
SCFA	Short chain fatty acid
SDS-PAGE	Sodium dodecyl sulfate polyacrylamide gel electrophoresis
SEM	Standard error of the mean
SI	Small intestine
siRNA	Small interfering RNA
SLC6A19/BOAT1	Solute carrier family 6 member 19/system B(0) neutral amino acid transporter 1
SNPs	Single nucleotide polymorphisms
STAT	Signal transducer and activator of transcription
STING	Stimulator of interferon genes
SQSTM1/p62	Sequestosome-1
TBK1	TANK binding kinase
TBS-T	Tris-buffered saline with tween
TCA	Tricarboxylic acid cycle
TDO	Tryptophan 2,3-dioxygenase
TGS	Tris-glycine-SDS
TLR	Toll-like receptor
TM	Tunicamycin
TNBS	2,4,6-trinitrobenzene sulfonic acid
TNF	Tumor necrosis factor
TrpH1	Trp hydroxylase 1 enzyme
TrpH2	Trp hydroxylase 2 enzyme
TPM	Transcript per million
Trex1	3' repair exonuclease 1
TRIM	Tripartite motif
tRNA	Transfer RNA
Trp	Tryptophan
TYK2	Non-receptor tyrosine kinase 2
Tyr	Tyrosine
UC	Ulcerative colitis
ULK	Unc-51-like kinase family
UPR	Unfolded protein response
WARS	Tryptophanyl-tRNA synthetase
WB	Western blot
XA	Xanthurenic acid
XBP1	X-box-binding protein 1
ZO-1	Zonula occludens-1
α-KG	α-ketoglutarate
β-ME	β-mercaptoethanol

Summary

Inflammatory bowel disease (IBD) is characterized by a breakdown of the intestinal barrier function and a dysregulated inflammatory response to the microbiota for which currently no cure is available. Disease activity of IBD patients negatively correlates with serum levels of the essential amino acid Tryptophan (Trp), which is known to play a regulatory role in the intestine. Microbial pathogens can be sensed via cyclic GMP-AMP synthase (cGAS) / stimulator of interferon genes (STING), an innate immune sensor complex involved in the detection of both foreign and self double-stranded DNA resulting in type I interferon (IFN) production. The hitherto existing investigations of either Trp or STING have focused on professional immune cells while little is known about the mutual influence of Trp and STING in intestinal epithelial cells. Thus, this study aimed to understand the role of Trp in coordinating the cGAS/STING response in murine enterocytes.

The present work shows that intracellular Trp differentially coordinates immune responses in enterocytes. In experiments employing the murine enterocytic cell line ModeK, it was shown that Trp starvation augmented the nuclear factor κ B (NF- κ B) response to lipopolysaccharide (LPS) or interleukin (IL)-1 β stimulation, while it significantly impaired the cGAS/STING response to DMXAA, cyclic GAMP-AMP (cGAMP), or dsDNA via decreasing STING levels. Despite Trp starvation, the ATP levels of the cells were not affected. The effect on STING, however, seemed to be rather specific to Trp starvation, as general autophagy inducers did not affect STING levels, and supplementation with the Trp metabolite Kyn did not provide rescue. The marked decrease in STING protein levels was independent of autophagy since neither a KO of *autophagy-related protein 16-like 1 (Atg16l1)*, nor a KO of *EIF2 α K (Eif2ak4)* rescued the phenotype. Although ER-stressed cells were more sensitive to Trp reduction, post-translational modifications by reactive oxygen species (ROS) induced by Trp starvation are an unlikely cause since supplementation with the ROS scavenger N-acetylcysteine (NAC) did not restore STING levels. Importantly, STING exhibited a long half-life time exceeding the starvation period, and the effect of Trp starvation on STING was abrogated by blocking the protein synthesis. Thus, Trp starvation seemed to induce the synthesis of a STING-degrading factor. Additionally, Trp starvation decreased Tmem173 mRNA levels.

This study demonstrates that Trp starvation impairs the cGAS/STING response via decreasing STING at both protein and mRNA levels. Although the precise mechanism remains unknown, the results suggest that Trp starvation leads to the synthesis of a STING-degrading factor. It remains to be investigated whether the impaired STING response under Trp starvation occurs in a multicellular organism, and it likely is dependent on the type of pathogen whether this would render the individual immunocompromised or unaffected.

Zusammenfassung

Chronisch entzündliche Darmerkrankungen (CED) unterliegen einer multifaktoriellen Genese und sind besonders durch eine infunktionale intestinale Barriere und eine fehlregulierte, überschießende Immunantwort auf das Mikrobiom gekennzeichnet. Bislang existieren keine kausalen medikamentösen Therapieansätze. Die Krankheitsaktivität der CED-Patienten korreliert negativ mit den Serumwerten der essenziellen Aminosäure Tryptophan (Trp), welche homöostatische und immunologische Prozesse im Darm reguliert.

Mikrobielle Krankheitserreger können über den cGAS/STING Signalweg detektiert werden, einem angeborenen Immunsensorkomplex, welcher sowohl zellfremde als auch zelleigene doppelsträngige DNS erkennt, und konsekutiv die Produktion von Typ I Interferonen induziert. Bisherige wissenschaftliche Studien haben die Funktion von Trp oder STING in professionellen Immunzellen untersucht, wohingegen wenig über den gegenseitigen Einfluss von Trp und STING in intestinalen Epithelzellen bekannt ist. Ziel dieser Studie war es, die Rolle von Trp in der Koordination des cyclic GMP-AMP synthase (cGAS) / stimulator of interferon genes (STING) Signalwegs in murinen Enterozyten zu analysieren.

Die vorliegende Arbeit zeigt, dass intrazelluläres Trp die Immunantworten in Enterozyten auf unterschiedliche Weise koordiniert. In Experimenten mit der enterozytären Zelllinie ModeK konnte gezeigt werden, dass Trp-Mangel die nuclear factor κ B (NF- κ B) Antwort nach Lipopolysaccharide (LPS)- oder Interleukin (IL)-1 β Stimulation verstärkt, die cGAS/STING Antwort auf DMXAA, cyclic GAMP-AMP (cGAMP), oder dsDNS durch Herunterregulierung der STING-Proteinexpression jedoch signifikant beeinträchtigt. Trotz des Aminosäuremangels zeigten sich ATP-Werte unverändert. Jene Herunterregulierung von STING schien spezifisch für Trp-Mangel zu sein, da generelle Autophagie-Induktoren keine Auswirkungen auf den STING-Proteinspiegel zur Folge hatten, und eine Supplementierung mit dem Trp Metaboliten Kynurenin den Effekt ebenfalls nicht aufheben konnte. Eine deutliche Reduktion des STING-Proteinspiegels durch gesteigerte zelluläre Autophagie konnte ausgeschlossen werden, da weder ein Knockout von *autophagy-related protein 16-like 1 (Atg16l1)* noch von *EIF2 α K (Eif2ak4)* den Phänotypen aufheben konnte. Obwohl ER-gestresste Zellen sensitiver auf den Trp-Mangelzustand reagierten, war der supprimierende Effekt einer Trp-Depletion auf STING am ehesten nicht auf posttranslationale Modifikationen durch reaktive Sauerstoffspezies (ROS) zurückzuführen, da die Supplementierung mit dem ROS-Fänger N-Acetylcysteine (NAC) keine resolutionierende Wirkung zeigte. Da das STING Protein eine lange Halbwertszeit aufwies, welches die Dauer der Trp-Mangel Experimente überschritt, und durch Blockierung der Proteinsynthese die Wirkung von Trp-Mangel auf STING aufgehoben werden konnte, liegt die Vermutung nahe, dass Trp-

Mangel die Synthese eines STING-degradierenden Faktors induziert. Darüber hinaus bewirkte Trp-Mangel eine Herabregulierung der Tmem173 mRNA.

Diese Studie hat gezeigt, dass Trp-Mangel die cGAS/STING Antwort durch Herunterregulierung von STING sowohl auf Protein- als auch auf mRNA-Ebene beeinträchtigt. Obwohl der exakte Mechanismus unbekannt bleibt, deuten die Ergebnisse darauf hin, dass durch Trp-Mangel die Synthese eines STING-degradierenden Faktors induziert wird. Es bleibt offen, ob Trp-Mangel die STING Antwort ebenfalls in einem multizellulären Organismus beeinträchtigen würde, da die Art des proinflammatorischen Stimulus bedingt, ob sich die Trp-Depletion in einer Immunschwäche widerspiegeln oder keine Konsequenzen nach sich ziehen würde.

1. Introduction

Inflammatory bowel disease (IBD)

Intestinal Physiology

The intestinal lumen is colonized by a diverse microbiota which form a symbiotic relationship with the human body: The microbiota enhances food digestion efficacy and restricts pathogen colonization; the human gut, on the other hand, provides a nutrient-rich and rather safe environment for the microbes (Duerkop et al., 2009; Mahapatro et al., 2021). Bacteria, as diverse as 500-1000 different species, make up the majority of the estimated 10-100 trillion organisms of the microbiota, but viruses and archaea also colonize the gut (Duerkop et al., 2009). The unsterile lumen and the host tissue are separated by a complex intestinal barrier formed by a single layer of columnar intestinal epithelial cells (IECs) coated by a mucus gel. IECs comprise four different cell types, of which enterocytes are the most abundant. They are responsible for the absorption and are joined by apical junctional complexes. The mucus is secreted by goblet cells and serves to limit the number of microbes that reach the epithelium. Paneth cells (only present in the small intestine (SI)) contribute to the barrier function by secreting antimicrobial peptides known as defensins which, together with secretory IgA antibodies, are retained in high concentrations in the mucus. Enteroendocrine cells produce hormones that are important for tissue repair, enterocyte differentiation, and angiogenesis. These four IEC types share a common progenitor, the multipotent stem cells located at the base of the crypts. Differentiated cells then migrate toward the top of the villus until they are shed into the lumen after 4-5 days (Roda, 2010; Maloy and Powrie, 2011; Mahapatro et al., 2021). Discrimination between commensal and pathogenic bacteria is achieved by a cross-talk between IECs as non-professional antigen-presenting cells (APCs), immune cells (professional APCs), and intestinal microbes. Thereby, IECs are able to activate T cells and lamina propria immune cells, in turn, secrete cytokines and growth factors to stimulate IECs (Roda, 2010; Maloy and Powrie, 2011). The cross-talk between IECs, gut microbiota, and immune cells is of utmost importance to ensure intestinal homeostasis (Maloy and Powrie, 2011). Inflammation per se is a protective mechanism triggered by injury or infection, however, when the inflammatory response to the microbiota gets dysregulated in a genetically susceptible host, chronic intestinal disorders such as inflammatory bowel disease (IBD) can arise (Abraham and Cho, 2009).

Pathophysiology

IBD is a heterogeneous chronic inflammatory disease with its two main clinical forms being Crohn's disease (CD) which affects the entire gastrointestinal tract, and ulcerative colitis (UC) restricted to the colonic mucosa (Kaser et al., 2010; Andreou et al., 2020). Common to both UC and CD is a breakdown

of the intestinal epithelial barrier which leads to translocation of microbial antigens from the lumen, initiating a self-perpetuating cycle of inflammation where the triggered inflammation causes further barrier damage (Taylor and Colgan, 2007). The exact cause of IBD is unknown, but it is hypothesized that the chronic inflammation of IBD arises from either a change in the composition of the microbiota, from an abnormal immune response, or from a dysregulated host-microbe interaction, together with environmental and genetic predispositions as discussed below (Wen and Fiocchi, 2004).

It has yet been debated whether IBD can be classified as an autoimmune or rather as immune-mediated disease. Classical autoimmune characteristics comprise the presence of autoreactive T- and B-cells and the circulation of autoreactive antibodies. For instance, even though perinuclear antineutrophil cytoplasmic antibodies (pANCA) were found in UC patients, their presence could not be associated with disease activity, neither was their presence a precondition nor specific for the development of IBD. As research on other autoantibodies has been aborted, the concept of IBD as immune-mediated disease is favored (Wen and Fiocchi, 2004). As such, pro-inflammatory mediators, mainly tumor necrosis factor α (TNF α) and interleukin (IL)-1 β , are released in elevated levels by peripheral monocytes as well as lamina propria macrophages of IBD patients and are central to the initiation and perpetuation of the inflammation (Schreiber et al., 1995).

In case of a mild or transient inflammation, the inevitably arising tissue damage can be restored normally (Rieder and Fiocchi, 2009). After successful elimination of the trigger, mostly macrophages are responsible for removing the dead cells, and their switch from a pro- to an anti-inflammatory phenotype is essential for the resolution phase, as they secrete factors that aid in tissue healing (Fullerton & Gilroy, 2016; Ortega-Gomez et al., 2023). The mucosal healing requires the proliferation of IECs to reconstruct the barrier and this process depends on the cytokine microenvironment. Studies have shown that, for example, TNF α and IL-6 both drive inflammation but IL-6 additionally stimulates IECs proliferation together with IL-10 (Mahapatro et al., 2021). A frameshift mutation of the nucleotide binding oligomerization domain containing 2 (NOD2) gene was associated with increased susceptibility to CD development. Whereas IECs poorly respond to lipopolysaccharide (LPS) stimulation under healthy conditions, elevated activation of nuclear factor κ B (NF- κ B) upon TNF α and interferon (IFN) γ exposure leads to an upregulation of NOD2 in IECs. This, in turn, increases the responsiveness of IECs to LPS followed by overexpression of the chemotactic IL-8 cytokine, which might aggravate barrier disruption (Rosenstiel et al., 2003). If the resolution of inflammation fails and proceeds to a chronic inflammation, the tissue's regenerative capacity may be unable to cope with the extent of tissue damage and the healing attempt may result in the formation of scar tissue. In simple terms, this process of fibrosis underlies the deposition of collagen by fibroblasts which consequently leads to

narrowing of the intestinal lumen and is accompanied by obstructive symptoms of the patients (Rieder and Fiocchi, 2009).

Certain associated conditions of IBD can set the patients at an increased risk of infection, such as malnutrition or chronic airway disease. Moreover, treatments with some immunosuppressive drugs can predispose the patients to infections. Common types of infections can be either reactivation of latent viruses such as cytomegalovirus (CMV), or opportunistic infections such as enteropathogenic *Escherichia coli*. In this way, infections play a big role in the pathogenesis of IBD and even though it may not be the underlying cause, it can worsen the course of the disease or contribute to disease relapse. Most importantly, infections represent an increased cause of death among IBD patients (Irving and Gibson, 2008).

Predispositions to IBD

Antibiotic treatments, especially tetracyclines, have been shown to increase the risk of IBD. As this is only an association, further research is required since IBD patients often require antibiotic treatment so that the causative may be attributed to the patient's immunity rather than the treatment. The Westernized lifestyle that confers higher risk also has led to the 'hygiene hypothesis', according to which the lack of natural stimulation of the intestinal immune system under supernatural hygienic conditions can be a causative agent for IBD (Rogler et al., 2016).

Genome-wide association studies (GWASs) have contributed to an advanced identification of potential risk genes and, despite a substantial overlap, some of the single nucleotide polymorphisms (SNPs) are unique to either UC or CD (Schreiber et al., 2005; Kaser et al., 2010). For example, CD has been specifically linked to variants in autophagy genes (e.g. ATG16L1, IRGM) or NOD-like receptors (e.g. NOD2), whereas UC has been uniquely associated with loci related to IEC function (e.g. ECM1) or E3 ubiquitin ligase (e.g. HERC2). Those risk genes, however, show striking variances between different populations and most of them seem to set the individual at modest risk only (Kaser et al., 2010), highlighting the necessary interplay between both genetic and environmental factors.

Although those SNPs likely have been prevalent for hundreds of years, the incidence of IBD in Westernized countries has increased over the past 100 years, which also emphasizes the importance of environmental agents triggering IBD (Rogler et al., 2016). Amongst others, the environmental risk factors for IBD flares comprise low vitamin D levels, dysregulated hormone levels, and the diet. In specific, an increase in poly-unsaturated fatty acids (PUFA) and saturated fats is associated with an increased risk of CD flares, whereas an increase in fibers might have a protective role during remission (Ananthakrishnan et al., 2018; Rogler et al., 2016). Westernized diets are enriched in the ω -6 PUFA

arachidonic acid, which triggers inflammation that can be alleviated by lipid peroxidation via glutathione peroxidase 4 (GPX4). The activity of GPX4, however, is reduced in the inflamed epithelium of CD patients (Mayr et al., 2020). Cigarette smoking is a clear risk factor for CD, but interestingly seems to be protective against UC flares (Podolsky, 2002; Rogler et al., 2016).

ER Stress

Protein folding takes place in the endoplasmic reticulum (ER) with the aid of molecular chaperones, but the complexity of the process makes it prone to errors so that the capacity will be saturated especially in the context of infections, glucose starvation, cellular injury, or excessive demand of protein synthesis. As a first approach to alleviate the stress, the cell will halt the general protein translation and instead prioritize proteins required for the unfolded protein response (UPR) which will boost the folding machinery. Next, the un- or misfolded proteins are degraded. During ER-associated protein degradation (ERAD), the proteins are transported to the cytosol to be degraded via the ubiquitin-proteasome system. If the cell cannot cope with the stress and reaches a certain threshold, it will initiate apoptosis (Rashid et al., 2015; Chino and Mizushima, 2020). Three ER stress sensors survey the ER protein folding status and initiate UPR signal transduction, namely endoplasmic reticulum to nucleus signaling 1 (ERN1/IRE1), eukaryotic translation initiation factor 2- α kinase 3 (PERK/EIF2AK3) and activating transcription factor (ATF)6. Under homeostatic conditions, they are bound by and thus inhibited by heat shock 70kDa protein 5 (HSPA5/GRP78). However, when unfolded proteins accumulate, they recruit and bind to HSPA5, liberating the sensors (Rashid et al., 2015). Further, ER stress can activate autophagy via the PERK-eIF2 α axis (Kaser et al., 2010).

Of the three pathways activated by the UPR, isoform inositol-requiring enzyme 1 (IRE1) resembles the evolutionary most conserved pathway and further seems to be of utmost importance in the intestinal epithelium as it uniquely features the additional IRE1 β (Kaser et al., 2008; Kaser et al., 2010). The activation of IRE1 leads to splicing of X-box-binding protein 1 (XBP1) to yield XBP1s which induces the transcription of genes required for ER maintenance and expansion, and even genes involved in secretory cell differentiation (Kaser et al., 2008). Deep sequencing revealed SNPs of *XBP1* that may set an individual at increased risk of IBD. Likewise, the intestinal epithelium of IBD patients features increased ER stress (Kaser et al., 2008). Mice with a specific knockout (KO) of *Xbp1* in the intestinal epithelium were unable to resolve the ER stress and were more susceptible to dextran sulfate sodium (DSS) colitis. This was accompanied by reduced numbers of both Paneth and goblet cells and a hyperresponsive state of IECs to inflammatory mediators (Kaser et al., 2008). Likewise, *Xbp1*-deficient ModeK cells featured increased activation of signal transducer and activator of transcription (Stat)3 and secretion of IL-6 and IL-11 (Niederreiter et al., 2013). The inflammatory state of *Xbp1* KO cells could

be alleviated via inhibiting the ATF6 branch (Stengel et al., 2020). Loss of *Xbp1* induces autophagy in Paneth cells as both processes UPR and autophagy function to compensate for each other's impairment to alleviate inflammatory conditions (Adolph et al., 2013).

Autophagy

Recently, GWASs have discovered the autophagy-related protein 16-like 1 (*ATG16L1*) as a risk factor for CD (Hampe et al., 2007). CD patients that harbor the T300A risk allele of the *ATG16L1* gene were found to have morphological abnormalities in Paneth cells (Maloy and Powrie, 2011). *ATG16L1* is a protein with a fundamental role in autophagy, which refers to a recycling process during which intracellular constituents are transported to and broken down in lysosomes. Autophagy is essential to the cellular homeostasis, but it is increased under conditions of nutrient shortage, or in response to cellular stress or infections conducive to fuel biosynthetic processes or energy generation (Parzych and Klionsky, 2014). This evolutionary highly conserved process can broadly be divided into the three types microautophagy, macroautophagy, and chaperone-mediated autophagy (CMA). After chaperones recognize cargo proteins based on a particular pentapeptide motif, these proteins are unfolded and translocated to the lysosome, known as CMA; whereas the cargo is directly taken up by the lysosome during microautophagy. Macroautophagy describes the *de novo* formation of double-membrane vesicles called autophagosomes which engulf the cargo and then fuse with the lysosome to create the autolysosome (Parzych and Klionsky, 2014).

When the cell experiences a lack of nutrients or energy, the mammalian target of rapamycin complex 1 (MTORC1) dissociates from the induction complex which leads to dephosphorylation and thus activation of the Unc-51-like kinase family (ULK)1/2 and autophagy-related (ATG)13 followed by the induction of macroautophagy (Parzych and Klionsky, 2014). This starts with the initiation of an isolation membrane (or phagophore) from a yet unknown origin and involves either ULK1 or -2 and ATG13 in mammals (amongst others). The formed isolation membrane is elongated by means of the ATG12–ATG5–ATG16L1 complex (amongst others). Thereby, the ATG12-5-16L1 complex aids lipidation of the microtubule-associated protein 1 light chain 3 (LC3-I) with phosphatidylethanolamine (PE) to give rise to the hydrophobic LC3-II that facilitates the elongation of the isolation membrane until it fully engulfs its cargo and is then called an autophagosome. LC3-II is then cleaved from the outer membrane and allows the fusion with the lysosome resulting in the formation of an autolysosome. The engulfed constituents are hydrolyzed by lysosomal enzymes at low pH and become available for anabolism in the cytoplasm (Galluzzi et al., 2014; Haq et al., 2019; Parzych and Klionsky, 2014). When specific cargos are recycled during selective autophagy, the adaptor protein sequestosome-1 (SQSTM1/p62) aids in

delivering the cargo to the autophagosome by binding to ubiquitinated proteins or organelles and attaching them with LC3-II (Haq et al., 2019).

Deficiency of *Atg16/1* disturbs the recruitment of ATG12-ATG5 conjugate and thus the formation of the autophagosome, and consequently severely impairs the recycling of proteins. A bone marrow-specific KO of *Atg16/1* (or hypomorphic *Atg16/1* variants) did not lead to spontaneous enteritis, but the mice were more susceptible to DSS colitis (Saitoh et al., 2008). In *Atg16/1* KO cells, the ATF6 branch mediating ER stress was overactivated, and blocking the ATF6 upstream signaling could alleviate the inflammatory status of these cells (Stengel et al., 2020). Along the same line, *Atg16/1^{ΔIEC}* mice showed IRE1 α accumulation in Paneth cells (Tschurtschenthaler et al., 2017), again highlighting the interplay of autophagy and UPR as previously described by Adolph et al. (2013) in inflamed Paneth cells.

Diagnosis and Epidemiology

IBD patients present with diarrhea, or even dysentery, and abdominal pain accompanied by fever, and anemia (Baumgart and Le Berre, 2021; Tontini et al., 2015). Moreover, they are frequently diagnosed with extraintestinal manifestations that may comprise joint pain, psoriasis, or ankylosing spondylitis (Mahapatro et al., 2021). The determination of the biomarkers C-reactive protein (CRP) in the serum, or calprotectin and lactoferrin in the stool are frequently used to identify active or inactive IBD cases and therapy responders but cannot help discriminating between CD and UC. Histological and endoscopic investigations revealing the affected regions of the intestine forms the basis for the differential diagnosis of IBD, yet diagnosing the non-classical forms of either of the disease subtypes remains challenging as no gold standard has been established (Tontini et al., 2015). IBD can affect both children and adults with an onset of CD typically between 15-35 years of age, while UC usually starts before the age of 20 (Saeid Seyedian et al., 2019). Generally, IBD is considered a gender-independent disease in the West, although a slight female dominance of CD was reported in otherwise inconsistent studies. This contrasts with a slight male dominance of both UC and CD in Asia (Mak et al., 2020).

The epidemiological trends of IBD remarkably vary between geographic regions. It is estimated that a total of 2.5-3 million people has been diagnosed with IBD in Europe which accounts for 0.3 % of the population, and this prevalence tends to steadily increase (Mak et al., 2020). Traditionally described as a disease of the Western world, the incidence of IBD has been rising in the Eastern world over the past decades with higher occurrences in Asian industrializing countries (Ananthakrishnan et al., 2018; Mak et al., 2020).

Therapeutic approaches

As an incurable disease, lifelong medication is required to restrain disease progression that otherwise would expand to digestive and malignant processes and uncontrolled inflammation affecting the whole body. Current treatment strategies focus on both clinical and endoscopic remission as a hard end point and target inflammatory cascades on the molecular level (Baumgart and Le Berre, 2021), trying to restore the normally delicate balance between pro- and anti-inflammatory cytokines which is shifted towards a pro-inflammatory signature in IBD (Schreiber et al., 2002). Amongst the approved therapeutics are different antibodies against TNF α , anti-integrin antibodies, an inhibitor of the Janus kinase (JAK), and a biologic agent against the p40 subunit of IL-12/23, for which strategies are required to facilitate initial choices and follow-up treatments (Baumgart and Le Berre, 2021). Anti-TNF α antibodies (e.g. infliximab) provide alleviation as they restore the intestinal barrier function of CD patients (Noth et al., 2012). The use of immunosuppressive or immunomodulatory agents including corticosteroids, however, increases the risk for opportunistic infections. As standard therapy, antibiotics seem to be beneficial to treat CD rather than UC patients (Podolsky, 2002). In case of therapy resistance, a partial removal of the intestine by surgery may be helpful (Tontini et al., 2015). All in all, currently available treatment options can, in the best-case, lead to a durable remission only, while patients struggle to bear potentially life-threatening side effects (Baumgart and Le Berre, 2021). This highlights the urgent necessity of developing new targets to combat IBD. One such new strategy may be a change of the diet, which has been successfully tested in a pediatric CD clinical trial. The partial enteral nutrition combined with an exclusion diet (anti-inflammatory diets) lead to a better adverse-event profile for most children, microbiota recomposition, and higher rates of glucocorticoid-free clinical remission (Baumgart and Le Berre, 2021). However, changing the diet can be difficult for many patients (Podolsky, 2002). In this way, patients may benefit from nutritional supplementation.

Given the many contributors environment, lifestyle, genetics, gut microbiota composition, and diet, it is unlikely that the majority of patients will benefit from the same medication that targets just one pathway. To pave the way for personalized medicine, a key research area should focus on identifying disease pattern in patient subgroups so that the therapy can be tailored to either suppress or enhance certain immunologic responses or how to stably change the individual microbiota aiming to restore homeostasis (Maloy and Powrie, 2011).

1.3 Inflammation

Nucleic acid recognition

The innate immune system represents the first line of defense to detect both extra- and intracellular pathogens based on their pathogen-associated molecular patterns (PAMPs) by means of germline-encoded pattern-recognition receptors (PRRs). Cytosolic sensors can recognize intracellular pathogens via toxins, cellular damage, microbial molecules (e.g. LPS), or nucleic acids (NAs) (reviewed in Chen et al., 2016; Roers et al., 2016). As deoxyribonucleic acid (DNA) is the carrier of genetic information in all living organisms and viruses, except for ribonucleic acid (RNA) viruses, its intracellular detection serves as a general molecular pattern to mount an immune response (reviewed in Chen et al., 2016). The most important viral microbe-associated molecular pattern (MAMPs) are NAs, which is why NA recognition is of utmost importance in fighting viral infections (reviewed in Roers et al., 2016). Therefore, tight regulations are necessary to avoid autoimmune reactions such as the containment of DNA sensors in the endolysosome or cytosol which, under homeostatic conditions, is devoid of self-DNA. Extracellular self-DNA originating from tissue damage is rapidly degraded by restriction enzymes, and only NAs of microbial origin reach the endolysosomes. Further, endogenous NAs are kept below an immunostimulatory threshold via restriction enzymes such as 3' repair exonuclease 1 (Trex1) in the cytoplasm or DNase I in human serum; also, damaged DNA can be removed via autophagy for recycling (reviewed in Roers et al., 2016). While the eukaryotic genome is restricted to the nucleus or mitochondria, respectively, DNA can leak into the cytosol under pathologic conditions such as stress or DNA instability and/or damage. The massive amount of DNA leaking into the cytosol can overwhelm the regulation processes and activate PRRs to cause sterile inflammation (reviewed in Roers et al., 2016; Bai and Liu, 2019). Although generally undesired, sensing of self-DNA that has reached the cytoplasm after phagocytosis of dead tumor cells can promote anti-tumor responses (reviewed in Chen et al., 2016).

cGAS/STING pathway

The main cytosolic DNA-sensing mechanism is the cGAS-STING pathway, consisting of the PRR cytosolic DNA sensor cyclic GMP-AMP synthase (cGAS) and the adaptor stimulator of interferon genes (STING, also known as MPYS, MITA, ERIS, and TMEM173) which responds to cGAMP and initiates the signal transduction (Li et al., 2013; Sun et al., 2013). The sequence-independent activation of this cascade by either intrinsic or extrinsic DNA leads to an innate immune response and subsequent IFN production. cGAS is present in an autoinhibitory state under homeostatic conditions, and binding of DNA leads to a conformational change in the active site (reviewed in Chen et al., 2016). Thereby, cGAS senses exogenous and endogenous DNA equally well as the only molecular requirement is double-stranded

DNA (dsDNA) in B-form confirmation with a length of at least 24-40 bp in human cells, the murine cGAS seems to have a lower threshold (reviewed in Roers et al., 2016). As a cytoplasmic nucleotidyltransferase, the activated cGAS then catalyzes the synthesis of the signaling molecule 2'3'-cyclic GAMP-AMP (2'3'-cGAMP) from both adenosine triphosphate (ATP) and guanosine triphosphate (GTP) with two phosphodiester linkages (Li et al., 2013; Sun et al., 2013). This and other cyclic dinucleotides (CDNs) from microbial sources (i.a. cyclic di-AMP or cyclic di-GMP) serve as second messengers to bind to STING (Burdette et al., 2011) and subsequently induce its extensive conformational change, whereby 2'3'-cGAMP has the highest binding affinity for STING than other CDNs (reviewed in Chen et al., 2016; Bai and Liu, 2019). Located at the ER, the activated STING then traffics to an ER-Golgi intermediate and finally to the Golgi apparatus. En route, it rapidly recruits and activates the TANK binding kinase (TBK1) via its carboxy-terminal tail (CTT) which resembles a TBK1 substrate. TBK1, in turn, phosphorylates the CTT of STING at several serine and threonine residues, so that STING can bind to a positively charged region of the transcription factor interferon regulatory factor (IRF)3. IRF3 is then recruited to also be phosphorylated by TBK1 and is thereby activated, leading to its dimerization and translocation to the nucleus (Ishikawa and Barber, 2008; Zhong et al., 2008; Ishikawa et al., 2009; Zhang et al., 2019; reviewed in Chen et al., 2016; Bai and Liu, 2019). As TBK1 is a broadly activated kinase, this licensing mechanism that first requires the phosphorylation of STING to allow for the phosphorylation of IRF3 by TBK1, critically restricts the IFN response to be activated during infection only and thus prevents aberrant IFN production (reviewed in Chen et al., 2016). STING further activates the I κ B kinase (IKK) ultimately leading to the release of NF- κ B to enter the nucleus. These transcription factors induce the expression inflammatory mediators (reviewed in Chen et al., 2016; Bai and Liu, 2019). Interestingly, infected cells can also alert neighboring cells via transferring cGAMP through gap junctions (reviewed in Chen et al., 2016; Bai and Liu, 2019).

A consequence of pro-inflammatory responses, in particular type I IFN, is the upregulation of PRRs and thus increased sensitivity of the NA recognition system. In this way, many NA-sensing receptors were initially discovered as IFN-responsive gene before identified as PRR. Thus, caution must be taken with the administration of IFN therapeutics to avoid a potential occurrence of autoimmune diseases (reviewed in Roers et al., 2016).

To ensure a sensitive response to foreign DNA, several regulatory steps at the translational or post-translational level exist to avoid unspecific activation. The increased expression of both cGAS and STING in response to IFN I represents a positive feedback mechanism to enhance the detection and thus to amplify the signal. In line with this, it is little surprising that many cancer cell lines were found to have suppressed or even lost the expression of cGAS and/or STING as an escape strategy from immune surveillance. On the other hand, phosphorylation of cGAS at Ser305 (in human; Ser291 in

mice) by the protein kinase B (Akt) can inhibit cGAS and implies a possible crosstalk between these pathways (reviewed in Chen et al., 2016). Excessive STING activation is prevented due to its subsequent degradation via autophagy (Saitoh et al., 2009; Prabakaran et al., 2018). STING can be inhibited when it is palmitoylated at Cys88 and Cys91 at the Golgi apparatus. Another regulation mechanism of STING is achieved via ubiquitination, both positively and negatively. When polyubiquitinated at Lys63 (K63) by the E3 ligases tripartite motif (TRIM)56 and TRIM32, STING activation and downstream signaling was found to be enhanced, whereas polyubiquitination at K48 by the E3 ligases RNF5 and TRIM30a results in proteasomal degradation of STING (reviewed in Chen et al., 2016).

NF- κ B pathway

In IECs, the master immunologic transcription factor NF- κ B, discovered by Sen and Baltimore in 1986 (Sen and Baltimore, 1986), is key to maintaining the epithelial barrier integrity and to the crosstalk between microbes and immune cells (Nenci et al., 2007). NF- κ B forms a complex as either homo- or heterodimers of its different members RelA (p65), RelB, c-Rel, p50/p105, and p52/p100 in mammalian cells (Ghosh et al., 1990; Kieran et al., 1990; Nolan et al., 1991; reviewed in Chen et al., 2003; Perkins, 2007). The NF- κ B complex is bound by inhibitors of NF- κ B (I κ Bs) that retain it in the cytoplasm, and activation of the NF- κ B pathway in response to stress, inflammatory stimuli, or infections is initiated when IKK phosphorylates I κ B. I κ B consequently gets degraded relieving NF- κ B to enter the nucleus where it induces or represses gene expression (Baeuerle and Baltimore, 1988; Ghosh and Baltimore, 1990; reviewed in Chen et al., 2003; Perkins, 2007). Amongst the cellular processes that NF- κ B can influence are proliferation and apoptosis, inflammation and tissue repair, emphasizing that although NF- κ B activation traditionally has been regarded as mainly pro-inflammatory, it became apparent that it also contributes to the resolution of inflammation (reviewed in Chen et al., 2003; Lawrence et al., 2001; Perkins, 2007). The complexity of the pathway includes self-regulatory processes by inducing counter-regulatory target genes. For instance, the activation of NF- κ B can protect against apoptosis via inducing several anti-apoptotic genes, while at the same time inducing the immediate early gene X-1 (IEX-1). IEX-1, in turn, directly blocks NF- κ B activation and thereby halts further expression of anti-apoptotic genes (Arlt et al., 2008). A deficiency of the murine IEX-1 homolog gly96 led to an aggravation of both acute and chronic inflammation in a mouse colitis model (Sina et al., 2010). This emphasizes the necessity for NF- κ B regulation as, nevertheless, NF- κ B activation positively correlates with inflammation in general, and its increased activation in macrophages and in IECs is associated with both CD and UC (reviewed in Kaser et al., 2010).

Cytokines

The cytokines TNF α and IL-1 β mainly exert their pro-inflammatory actions via engaging the NF- κ B pathway, and TNF α itself represents an NF- κ B target gene (Schreiber et al., 2002; Rosenstiel et al., 2003). As important regulator, the anti-inflammatory cytokine IL-10 can dampen the production of both TNF α and IL-1 β in macrophages (Schreiber et al., 1995). Many other cytokines instead, such as IL-6 and IFNs, signal via the transcription factor STAT family. Its member STAT1 is overactivated especially in UC and, to a lesser extent, in CD (Schreiber et al., 2002). IFNs were first described in 1957 by Isaacs and Lindenmann (1957a, 1957b), and are mediators of the immune-epithelial crosstalk with immune stimulating effects. They fall into three main categories: Type I IFNs (IFN α , IFN β , IFN κ , IFN ϵ , IFN ω , IFN τ , IFN δ) together with type III (IFN λ 1, - λ 2, - λ 3) are secreted in response to viral infections, and IFNs type II (IFN γ) mediate immune responses against a broad variety of pathogens (Wheelock, 1965; Havell et al., 1975; Stewart et al., 1977; Rubinstein et al., 1981; Derynck et al., 1982; reviewed in Sadler and Williams, 2008; Schneider et al., 2014; Takaoka and Yanai, 2006). The type I IFN signal through the IFN α/β receptor (IFNAR) that consists of the IFNAR1 and IFNAR2 subunits and is expressed nearly ubiquitously. JAK1 and non-receptor tyrosine kinase 2 (TYK2) are associated with IFNAR, and their activation in turn engages the STAT family (Novick et al., 1994; Darnell et al., 1994; Gonzalez-Navajas et al., 2012; Schneider et al., 2014), whose members STAT1, -2, -3, and -5 are activated in most cell types, and STAT4 and -6 additionally in lymphocytes. IRF9 is recruited in response to STAT1 and STAT2 activation to form the STAT1-STAT2-IRF9 complex. This IFN-stimulated gene factor 3 (ISGF3) complex then initiates gene transcription upon binding to IFN-stimulated response elements (ISREs) present in the promoters of ISGs. On top of that, both IFN I can activate other STAT complexes without engaging IRF9, e.g. STAT1 homodimers, which then bind to IFN- γ -activated site (GAS) enhancer elements also present in the promoters of ISGs. In contrast, IFN II (IFN γ) only can activate genes with a GAS site in their promoters as it cannot stimulate ISGF3 complex formation (Darnell et al., 1994; Gonzalez-Navajas et al., 2012; Schneider et al., 2014). Again common to both IFN I and IFN II is the activation of STAT3 and the following promotion of STAT3-binding elements (SBEs) (Gonzalez-Navajas et al., 2012). Next to the JAK/STAT pathway, IFN I can also activate mitogen-activated protein kinases (MAPKs) pathways, in particular p38 and extracellular signal-regulated kinase 1 and 2 (ERK1 and ERK2) to mount antiviral effects such as growth inhibition (Gonzalez-Navajas et al., 2012; Takaoka and Yanai, 2006).

The ISGs induced in response to IFN I comprise a variety of over 300 different genes, of which many genes encode for PRRs or transcription factors to initiate an amplification loop aiming to intensify pathogen sensing and further IFN production. Some ISGs instead execute direct antiviral actions to limit the virus spread, such as inducing apoptosis, regulating post-transcriptional events and protein translation, or aid in cytoskeletal remodeling (Der et al., 1998; de Veer et al., 2001). An example is the

protein kinase R (PKR; also known as EIF2 α K2), which is a member of the protein kinase family that regulate protein synthesis upon activation under conditions of environmental stress. Other members of this eukaryotic translation initiation factor 2 alpha kinase (EIF2 α K) family are EIF2 α K1 (HRI), EIF2 α K3 (PERK), and EIF2 α K4 (GCN2). These proteins phosphorylate EIF2 α resulting in preventing EIF2 β activity by sequestration. This abolishes the recycling of guanosine diphosphate (GDP) and leads to a translational arrest and a halt in proliferation (Sadler and Williams, 2008).

CD and UC differ in that CD is described as a primarily type 1-predominated disease associated with elevated levels of T_H1 and T_H17 cells and their cytokine profiles IL-12, -23, -17, -18 and IFN γ , whereas UC is characterized by a type 2-driven phenotype in which Th2 and Th9 cells, and the cytokines IL-13, -5, -9 prevail (Schreiber et al., 2002; Mahapatro et al., 2021; Wen and Fiocchi, 2004). This, however, may be an oversimplification of the human pathology as, for instance, an overactivation of STAT1 was primarily seen in UC and only to a lesser extent in CD, which should be considered when interpreting data from animal studies (Schreiber et al., 2002). Nonetheless, CD Patients have increased levels of IFN λ in serum and inflamed ileal tissues that, as shown in a mouse model, induced Paneth cell death via STAT1 activation (Günther et al., 2019).

Type I IFN play a dual role in IBD: being protective in the stage of acute inflammation by reducing the release of IL-1 β , the harmful effects prevail during the chronic recovery phase such as enhancing the infiltration of immune cells (Li et al., 2021). On the other hand, there is evidence suggesting that a chronic secretion of IFN I in virus infection, however, can even lead to a state of immunosuppression because of increased T cell apoptosis triggered by IL-10, programmed cell death ligand (PD1), and indoleamine 2,3-dioxygenase 1 (IDO1) signaling. This attenuates pathogen clearance and the resolution of inflammation (Fullerton and Gilroy, 2016). Thus, anti-IFN-therapies for IBD patients must achieve a delicate balance between stimulating and repressing IFN-I signaling to overcome the difficulties of possible side effects that can manifest as either destructive tissue damage or increased risk of cancer.

As IBD patients were found to have increased mucosal levels of IL-6 (Nikolaus et al., 2018), blocking the trans-signaling of IL-6 bound to its soluble receptor complex was studied in a recent phase 2a clinical trial (Schreiber et al., 2021). The IL-6 cytokine family signals via a complex of the α -receptor IL-6R and β -receptors, most commonly gp130. In cells that do not express the membrane-bound IL-6R, IL-6 can bind the soluble form of IL-6R to activate gp130, inducing the so-called trans-signaling (Waetzig et al., 2010). In contrast to the severe immunosuppression induced by inhibiting the membrane-bound IL-6R, targeting the soluble receptor seemed to be well-tolerated and effective (Schreiber et al., 2021).

Immunometabolism

Metabolism plays an important role in every cellular process and cell fate decision. The finetuning between metabolic pathways that a cell switches on and off is influenced by growth factors, nutrients, stimulants, and metabolites, whose levels are further determined by competing cells and reactive oxygen species (ROS) (Buck et al., 2017). The influx of immune cells to the side of inflammation intensifies the competition for nutrients between different cell types. Further, the increased synthesis of inflammatory mediators and cytokines makes inflammation a metabolically intense process (Cummins et al., 2016). Immune cells have to rapidly respond to the environmental changes in form of infections, different stimuli, and changes in nutrient availability in order to exert their unique range of effector functions such as migrating towards and infiltrating the target tissue, fighting pathogens, and influence other cells (Buck et al., 2017). An extensive body of research has focused on the metabolic switches that both determine and accompany immune cell activation or quiescence (O'Neill et al., 2016; Buck et al., 2017); thus, this project focusses on IEC metabolism given their utmost importance at barrier defenses.

Although the gut is a nutrient-rich environment (Buck et al., 2017), the intestinal mucosa, and IECs which line the mucosa, experience unique fluctuations of perfusion rates each day when the blood volume is low during fasting periods but raises significantly after food ingestion (Taylor and Colgan, 2007). Thus, the metabolic activity and function of IECs is also controlled by their location (Buck et al., 2017): Owing to the unique anatomy of the gut with the juxtaposition of the richly perfused mucosa and the anerobic, microbiota-colonized lumen, IECs must metabolically adapt to an impressive range of pO_2 fluctuations to maintain their barrier function (Taylor and Colgan, 2007). The hypoxic response facilitates the metabolic switch from oxidative phosphorylation (OXPHOS) to glycolysis (Taylor and Colgan, 2017), and further exerts barrier protective functions via promoting mucin production or xenobiotic clearance (Taylor and Colgan, 2007). On top of that, IECs also provide a metabolic barrier in a way that they protect their progenitor cells. As aforementioned, the IEC layer is a site of active proliferation as IECs are constantly renewed and migrate from the crypt up the villi during their maturation. By utilizing the short chain fatty acid (SCFA) butyrate to fuel OXPHOS, the differentiated cells prevent it from reaching the stem cells as butyrate can inhibit their proliferation (Kaiko et al., 2016; Buck et al., 2017). Proliferation in general is also controlled by the mammalian target of rapamycin (mTOR) pathway, which is closely linked to amino acid (AA) metabolism. mTOR can sense the levels of AAs and growth factors to stimulate proliferation via messenger RNA (mRNA) translation and lipid synthesis under conditions favorable for growth.

In the future, the growing recognition of immunometabolism will likely benefit a broad scope of application such as co-treatment with nutritional supplements, or metabolic profiles as biomarkers for

diagnostics or to aid in assessing the right treatment options. For instance, the study by Aden et al. (2019) found that IBD patients who achieved clinical remission after anti-TNF treatment featured elevated levels of butyric acid in the stool (Aden et al., 2019). Another metabolite that was found to be altered in serum levels of IBD patients compared to healthy controls is Trp (Nikolaus et al., 2017).

1.4 Tryptophan

Sources and fates of Trp

Trp is of importance when studying immunometabolism as it was shown that, for example, the tumor microenvironment is depleted of Trp but enriched for its immunosuppressive metabolite kynurenine (Kyn) (reviewed in Buck et al., 2017; Opitz et al., 2020). As Trp is required for T cell proliferation, excessive Trp catabolism by competing cells limits T cell activation (O'Neill et al., 2016).

Trp was isolated in 1901 by Hopkins and Cole, and first synthesized in 1908 by Ellinger and Flamand (Ellinger and Flamand, 1908). Trp belongs to the essential AAs, meaning it must be taken up by the diet because it cannot be synthesized by the human body (Hopkins, 1912). Recommended Trp doses approximate to 4 mg/kg/day for adults, however, this varies within the lifespan as e.g. children require higher doses. Whereas an excessive dietary intake of Trp has not been associated with any side effects in humans, a deficiency of Trp, on the contrary, severely impacts the health status. A diet insufficient in Trp and vitamin B₃ can, when becoming chronic, lead to a metabolic dysfunction called pellagra whose symptoms mainly manifest in skin, gut, and brain alterations (Agus et al., 2018; Palego et al., 2016).

When Trp is taken up by food, it first is absorbed in the intestine and then transported to all main tissues via the blood stream to finally be taken up by all cells as fuel for biosynthesis of proteins (Palego et al., 2016). Its transport via the bloodstream is unique as Trp requires binding to albumin because of its hydrophobic nature conferred by its indole ring, which is a chemical structure present only in Trp amongst all AAs (Palego et al., 2016).

On the molecular level, AAs are loaded onto their respective transfer RNA (tRNA) by the aid of aminoacyl-tRNAs, so that the ribosomes can then attach the AAs to the growing protein chain. Two different forms of human tryptophanyl-tRNA synthetase (WARS) carry out the incorporation of Trp into proteins either in the cytoplasm (encoded by the gene *WARS1*) or in mitochondria (encoded by the gene *WARS2*) (Hoagland et al., 1958; Jorgensen et al., 2000).

When the demand for Trp exceeds its supply, this condition of AA shortage results in the accumulation of uncharged tRNAs which are then sensed via the protein kinase general control nonderepressible 2 (GCN2). GCN2 then phosphorylates eukaryotic translation initiation factor 2 (EIF-2) to mediate general translational repression while supporting the translation of key genes of the general AA control pathway such as GCN2 (Wek et al., 1989; Dever et al., 1992; Wek et al., 1995).

Next to being incorporated into proteins/peptides, Trp derivatives are of bioactive importance, influencing different cellular metabolic pathways and physiologic responses (Palego et al., 2016). Its metabolic importance is highlighted by the finding that, in nitrogen balance, the amount of Trp required for protein synthesis is mainly matched by that degraded. Trp is the least abundant AA found in proteins. Thus, less than 1 % of dietary Trp is incorporated into proteins with the remaining dietary Trp being utilized for metabolism (Bender, 1983; Badawy, 2015; Palego et al., 2016). Thereby, the fate of Trp can follow three distinct degradative pathways, of which ~ 95 % of overall Trp is metabolized along the kynurenine pathway (KP) in the liver, making it the metabolically most active pathway (Badawy, 2015). Although only accounting for 5 – 10 % of the Trp degradation under physiologic conditions, the extrahepatic KP gains increasing significance under immune activation. Yet widely distributed, it does not contain all the enzymes present in the liver, so that the type of derivative produced is determined by the presence of the KP enzymes (Badawy, 2017). The flux of Trp down the KP also is influenced by the amount of Trp in the free (not bound to albumin) state that is immediately available for tissue uptake (Badawy, 2017; Badawy, 2015).

This ratio between free and bound Trp even influences the passage of Trp into the brain where it will be metabolized into serotonin (5-hydroxy-tryptamine, 5-HT) by Trp hydroxylase 2 enzyme (TpH2), the final derivative of another Trp degradation pathway (Etienne et al., 1976; Yuwiler et al., 1977; Palego et al., 2016; Agus et al., 2018). Enterochromaffin cells (ECs) in the gut express the Trp hydroxylase 1 enzyme (TpH1) and synthesize most of the body's serotonin (> 90 %) that cannot cross the blood-brain barrier. As a neurotransmitter, serotonin mediates the communication between the gut and both extrinsic and intrinsic neurons to regulate secretory and peristaltic reflexes (Agus et al., 2018).

Next to the oral intake of Trp from sources such as bananas, milk, tuna, bread, or peanuts, Trp can be produced by bacterial members of the microbiota including *E. coli* (Agus et al., 2018), via the so-called shikimate pathway shared between bacteria, plants, and even fungi. Phosphoenolpyruvate (PEP) and erythrose 4-phosphate (E-4P) are converted in a seven-step metabolic process to yield chorismite as the precursor for tyrosine (Tyr), phenylalanine (Phe), and Trp (Ely and Pittard, 1979; Palego et al., 2016). The microbiota also metabolizes Trp into indole and indole derivatives, representing the third pathway of Trp metabolism (Agus et al., 2018; Lanis et al., 2017). These function as ligands of the aryl hydrocarbon receptor (AhR) transcription factor (Miller, 1997; Heath-Pagliuso et al., 1998). The AhR signaling pathway regulates both intestinal immune responses and barrier integrity and thus maintains intestinal homeostasis. Next to indoles, AhR can also be activated by xenobiotics or other dietary components, but the contribution of the microbiota is highlighted by the finding that no AhR ligands are present in the intestines of germ-free mice. Instead, members of the cytochrome p450 protein family can modify the ligands in a way to abolish AhR signaling. One such member is cytochrome p450

family 1 subfamily A member 1 (Cyp1A1), that, in turn being transcriptionally regulated by AhR, creates a negative feedback loop for this pathway (Agus et al., 2018; Lanis et al., 2017).

The central metabolite Kyn of the aforementioned KP also serves as an AhR ligand (Lanis et al., 2017). The rate-limiting step of the KP is the oxidation of the indole ring, that converts Trp to *N*-formylkynurenine. The respective enzymes are IDO1, found in most peripheral tissues and the immune system, and tryptophan 2,3-dioxygenase (TDO) in the liver. While both use molecular O₂ as a co-substrate, only TDO requires heme as a co-factor (Badawy and Evans, 1973; Hirata and Hayaishi, 1975; Palego et al., 2016; Badawy, 2017). In contrast to the wide expression of IDO1, the isoform IDO2 is restricted to APCs, liver, kidney, and few brain tissues. If IDO2 contributes to Trp conversion to Kyn, its contribution is only minimal, but both IDO isoforms are of immunologic importance (Badawy, 2015). All further metabolites and enzymes of the KP can be taken from Figure 1.1.

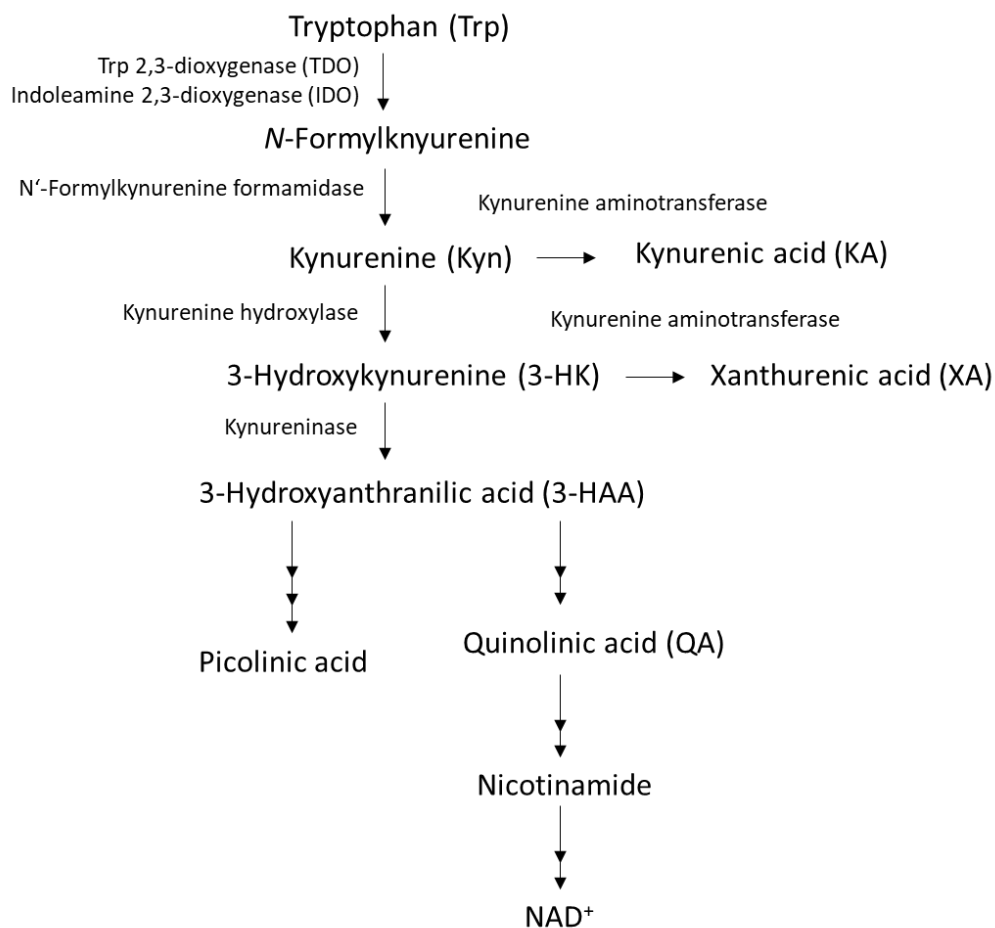


Figure 1.1 Tryptophan metabolism through the kynurenine pathway (KP)

Overview of the Trp derivatives and the respective enzymes.

Figure adapted from Badawy (2015).

Importantly, the different metabolites have been associated with either cytoprotective (kynurenic acid (KA)), or toxic (e.g. quinolinic acid (QA), 3-hydroxykynurenine (3-HK)) effects (Palego et al., 2016).

Particularly noteworthy is the immunomodulating effect of KP metabolites, so that the former concept of fetal tolerance during pregnancy had to be revised and a Trp utilization concept was suggested instead. Pregnancies are based on an increased demand for protein building blocks which would be counteracted by Trp depletion (Badawy, 2017). The KP pathway results in the formation of nicotinamide (vitamin B₃) and nicotinamide adenine dinucleotide (NAD⁺) (Bender, 1983), the latter is important not only for the energy balance of the cell, but also is involved in DNA repair, and inflammation. During redox reactions, NAD⁺ is reduced to NADH that, in turn, drives biochemical reactions by means of its cellular reducing power. Thus, NAD⁺ can be an interesting target in inflammatory disorders (Navarro et al., 2021).

Trp in inflammation

Importantly, the consequences of IDO activation also combine metabolic and immunomodulating functions, as balancing Trp catabolism aids in mediating immune tolerance during pregnancy, and Trp retention protects from extensive tissue damage via preventing aberrant immune activation (Palego et al., 2016). It was shown that a Trp-free diet administered to mice alleviated central nervous system (CNS) autoimmunity via impairing encephalitogenic T cell responses which seemed to have been microbiota-dependent (Sonner et al., 2019). Along the same lines, IDO1 can be activated by IFN γ (Feng and Taylor, 1989), that is induced during colitis, and the resulting depletion of Trp suppresses T cell proliferation. IDO1 expression in IECs likewise ameliorates colitis in mice. Indeed, next to its pro-inflammatory actions, IFN γ may direct inflammatory resolution also via inducing IL-10 receptor (IL-10R) on IECs which is crucial for wound healing and barrier integrity. This IL-10R expression is attributable to the IDO1-mediated conversion of Trp to Kyn, which in turn activates the AhR (Lanis et al., 2017).

The many properties of Trp derivatives and the respective catabolizing enzymes have been exploited for different kinds of therapies such as administration of a derivative and pharmacological modulation of the enzyme activity or the receptors to which the derivatives bind (Modoux et al., 2021). For instance, a combined treatment of IDO1 inhibitors and immune checkpoint inhibitors is under investigation for cancer treatment whose efficacy may potentially be enhanced when additionally combining with an interleukin-4-induced-1 (IL-4I1) inhibitor (Modoux et al., 2021). Another promising strategy may represent the research on probiotics to make use of bacteria producing AhR agonists as the inoculation of *Lactobacillus* strains has been proven to attenuate colitis in a mouse model (Lamas et al., 2016).

1.5 Aim

Up to date, there is no treatment available to cure a patient from IBD, and current therapy options set the patient at the risk of developing severe side effects. Since inflammation is frequently accompanied by a change in metabolism, the growing field of immunometabolism may revolutionize the ongoing research by combining drugs and nutritional supplementation to boost the therapy response and to limit side effects at the same time. Another striking progress may be achieved by the discovery of new biomarkers as changes in metabolite levels whose determination is cheap and non-invasive.

The study by Nikolaus et al. (2017) has reported on lower serum Trp levels and an increased Kyn to Trp ratio in IBD patients which, together with the increased *IDO1* expression, indicates an increased Trp catabolism via the KP. Further studies on mice have shown that tryptophan malnutrition enhances the susceptibility to DSS colitis (Hashimoto et al., 2012); and Trp supplementation, in turn, has alleviated the DSS colitis phenotype in mice presumably via signaling through the AhR pathway (Islam et al., 2017). It has yet been insufficiently investigated how Trp can directly act on immune signaling in IECs, despite their importance as barrier keepers. To my knowledge, most research on intestinal inflammation has focused on the ability of Trp derivatives to activate AhR, and no investigation on the impact of Trp on the cGAS/STING pathway has been published as of 2023.

The mentioned reports raised the question whether decreased Trp levels affect the epithelial immune response and thereby contribute to the IBD disease phenotype. The overall aim of this project is to elucidate the importance of Trp for different immune pathways in IECs, and thus to provide an understanding whether the Trp pathway might serve as a target for IBD therapy. The project therefore addressed the following major questions:

I) Does Trp starvation affect the immune response of the intestinal epithelium?

The clinical finding of reduced serum Trp levels was translated into an *in vitro* research model of both intestinal epithelial cells and organoids. The immunocompetence was assessed by exposing the cultures to Trp starvation and subsequently to different inflammatory triggers.

II) How does Trp starvation affect the cGAS/STING pathway on the mechanistical level?

After initial data hinted at a connection between Trp and STING, the cause by which Trp starvation might impair the cGAS/STING response on the molecular level was investigated. In specific, the dependence on the induction of autophagy was tested as well as the possible involvement of oxidative stress and inhibition of protein translation.

2. Materials and Methods

A list of all materials used is given in the appendix section.

2.1 Cell biological methods

Cell culture

ModeK cells

Unless otherwise stated, all *in vitro* experiments were performed on ModeK cells. This epithelial cell line was derived from a murine SI and immortalized via SV40-6 retrovirus-mediated large T gene transfer. The resulting cell line closely resembles *in vivo* murine enterocytes with regard to both morphological and phenotypic characteristics and also expresses major histocompatibility complex (MHC) I molecules and, upon IFN- γ stimulation, also MHC II molecules (Vidal et al., 1993). Therefore, ModeK cells provide a suitable *in vitro* model to study the role of enterocytes in immunity.

The ModeK iXBP1 cell line was created by transfecting ModeK cells with an SFG Δ U3hygro iXBP-specific RNAi retroviral vector; and the KD efficacy was confirmed by qPCR. An empty control vector was used to generate the corresponding iCtrl ModeK cells (Kaser et al., 2008; Lee et al., 2003). To create the *Atg16l1* KO cell line, the gene was knocked out using the clustered regularly interspaced short palindromic repeats (CRISPR) / CRISPR-associated protein 9 (Cas) technique as described below.

ModeK cells were both grown and seeded in Dulbecco's Modified Eagle Medium (DMEM) GlutaMAX medium supplemented with 10 % fetal bovine serum (FBS), 1 % penicillin / streptomycin (P/S) [10,000 μ g/mL], 1% non-essential amino acids (NEAA) [100 X], and 1 % N-2-hydroxyethylpiperazine-N-2-ethane sulfonic acid (HEPES) buffer [1 M] and incubated at 37 °C with 5 % CO₂.

Customized starvation medium

For nutritional intervention studies, the cells were cultured in specific amino acid-free medium, which was prepared from customized DMEM powder (Cell Culture Technologies, Switzerland) to which the following components were added: sodium bicarbonate, glucose, L-glutamine, L-serine, L-tryptophan, glycine at concentrations resembling regular DMEM (listed in the appendix section). The corresponding starvation medium lacks the stated ingredient. This powder was dissolved in ddH₂O and sterile filtrated before use, only supplemented with 10 % dialyzed FBS, and does not contain sodium pyruvate. The FBS was purchased as dialyzed by tangential flow filtration with 10,000 mw cut-off to reduce the concentration of small molecules.

CRISPR/Cas

The *Atg16l1* gene was knocked out in ModeK cells using the GeneArt CRISPR kit with TOP10 competent cells and cluster of differentiation 4 (CD4) selection marker from Invitrogen with little modifications to its manual. In specific, the primers coding for *Atg16l1*-specific CRISPR RNA (crRNA) were annealed, and then cloned into the linearized Cas9 nuclease reporter vector using the T4 DNA ligase. The resulting vector was transformed into competent TOP10 *E. coli* and plated on agar containing ampicillin (Amp) allowing for selection of successfully transformed resistant bacteria. The next day, half a colony was scraped off and incubated in lysogeny broth (LB) -Amp medium and grown overnight. By means of the GeneJET Plasmid Miniprep Kit by ThermoScientific, the plasmid was isolated, amplified by polymerase chain reaction (PCR) and then Sanger sequenced for quality control. The plasmid containing the right *Atg16l1*-targeting crRNA was amplified by incubating the remaining other half of the corresponding *E. coli* colony in LB-Amp medium and let grown for two days. The plasmid was isolated by using the Midiprep kit from Invitrogen, and then transfected into ModeK cells. The successfully transfected cells were selected by means of CD4 beads and diluted accordingly to plate a single cell into each well of a 96-well plate in 100 μ L growth medium. The *Atg16l1* KO was confirmed by WB of different clones.

Table 1 Information on the primer used for the crRNA targeting the *Atg16l1* gene
Abbreviations used: PAM - protospacer adjacent motif, gRNA – guide RNA

Primer information		
Gene <i>Atg16l1</i> , chromosome 1; Targeted exons: 1, 3; Direction (+); PAM: AGG; Binding sites: 1		
	Orientation	Sequence
Atg16l1-gRNA-T1	Forward	GTCACATCGCGGAGGAACTGGTTTT
	reverse	CAGTTCCTCCGCGATGTGACCGGTG

Crypt isolation

A C57BL/6 mouse was sacrificed by cervical dislocation and the ileum was harvested. After the fat was removed, the ileum was cut open longitudinally, washed with phosphate buffered saline (PBS), and cut into small pieces of approximately 1 mm length. The pieces were transferred to a falcon containing 20 mL ice cold PBS and the falcon was shaken a couple of times. The supernatant was discarded, and new PBS was added. This washing step was repeated 3 times, and the tissue sections were subsequently transferred to a new falcon tube containing 30 mL of 15 mM ethylenediamine tetraacetic acid (EDTA) -PBS and incubated on ice for 40 min. All further steps were performed on ice. The supernatant was discarded, and the tissue sections were washed by pipetting up and down in 10 mL PBS. The supernatant was collected in another falcon, and this washing procedure was repeated 5 times. The fractions were filtered through a 100 μ m cell strainer and then centrifuged at 400 g for 3 min at 4 °C. After discarding the supernatant, the cell pellet was resuspended in Advanced DMEM/F12 (ADF) to

allow for seeding the organoids. For the first passage, Y-27632 [10 μ M] was added to the growth medium.

Organoid culture

The murine SI organoids were seeded in 40 μ L Matrigel diluted with ADF (1:2) in 24-well plates and cultured at 37 °C with 5 % CO₂. The 3D growth medium (ENR medium) consisted of ADF, 1 % P/S, 20 % R-Spondin conditional medium, 10 % Noggin conditional medium, 1 % HEPES buffer, 1 % GlutaMax, N-acetylcysteine (NAC) [1 mM], and human epidermal growth factor (hEGF) [50 ng/mL].

The organoids were passaged by mechanical breaking. Therefore, the medium was removed, and 500 μ L ice-cold PBS were added to the well. The Matrigel was broken by scraping and pipetting up and down rigorously a couple of times. The organoid wells of the same genotype were collected in one falcon and centrifuged at 400 rpm for 3 min. The supernatant was removed, and the pellet was resuspended in an adequate amount of ADF, and the cell clusters were broken to single cells by pipetting rigorously a couple of times. An adequate amount of Matrigel was added and the organoids were seeded. The growth medium was added after the gel had solidified.

All organoid experiments were performed in collaboration with Mrs. Guang Yang (UKSH, IKMB).

Customized starvation medium

ADF medium lacking all AAs and glucose was received from Dr. Felix Sommer (UKSH, IKMB) to which glucose and all AAs, except for the one indicated, were added at the same concentration as contained in regular ADF (listed in the appendix section). HEPES [20 mM] was added to reach a pH value of 7, and further rhNoggin [100 ng/mL], rhR-Spondin [1 μ g/mL], and rhEGF [50 ng/mL] were supplemented. The starvation group was compared to ENR medium with recombinant Noggin and R-Spondin supplementation, and to control starvation medium.

MTS assay

ModeK cells were seeded at 1.25×10^4 cells in 100 μ L/well in a 96-well plate and allowed to grow confluent for 48 h. The medium was changed to customized DMEM containing the indicated Trp concentrations and supplemented with 10 % dialyzed FBS. After 24 h, the cell viability assay was performed. Therefore, the medium was removed and 100 μ L of working solution containing 80 μ L PBS, 19 μ L (3-(4,5-dimethylthiazol-2-yl)-5-(3-carboxymethoxyphenyl)-2-(4-sulfophenyl)-2H-tetrazolium) (MTS), and 1 μ L phenazine methosulfate (PMS) (MTS CellTiter 96 Aqueous Proliferation Assay, Promega) was added to each well including blanks. After an incubation time of 3 h at 37 °C, the

absorbance was measured at 490 nm optical density (OD) in a plate reader. The percentage of viable cells was calculated using untreated (Trp-containing medium) cells as reference.

Transfections

siRNA

ModeK cells were plated in P/S-free growth medium at a density of 0.5×10^5 cells in 500 μ L/well (24-well plate) or at 2×10^5 cells in 2 mL/well (6-well plate) and allowed to adhere. The next day, small interfering RNA (siRNA) was transfected into the cells with Lipofectamine RNAiMAX reagent from Invitrogen for KD studies. For protein quantification, a total of 25 pmol siRNA was used per well of a 6-well plate complexed with 7.5 μ L Lipofectamine RNAiMAX; whereas 5 pmol siRNA with 1.5 μ L Lipofectamine RNAiMAX was used per well of a 24-well plate for transcriptome analysis. The siRNA-lipid complex was diluted with Opti-Mem to make up transfection volumes of 50 μ L or 250 μ L for the respective well format and was incubated for 24 h until additional stimulation or harvest. The knockdown (KD) efficiency of the target was determined by either quantitative PCR (qPCR) or Western blot (WB) with non-targeting control siRNA as reference.

dsDNA and cGAMP

The cGAS/STING pathway was activated by transfecting cGAMP (2'3' or 3'3') or *E. coli*-derived dsDNA into the cells using Lyovec. ModeK cells were plated in growth medium at a density of 0.5×10^5 cells in 500 μ L/well (24-well plate) or at 2×10^5 cells in 2 mL/well (6-well plate). When adherent, the cells were washed with PBS and incubated in either Trp-containing or -deficient DMEM for 24 h prior to transfection. The transfection volume containing either 1 μ g/mL dsDNA or 10 μ g/mL cGAMP was complexed with Lyovec equaled 1/20 of the volume ratio. After incubation for 9 h, the cells were harvested for protein lysates or RNA isolation.

2.2 Molecular biological methods

RNA isolation

ModeK cells

Using 24-well plates, the indicated ModeK cell line was seeded at 0.5×10^5 cells in 500 μ L/well for transfection experiments, or at 0.75×10^5 cells in 500 μ L/well for stimulation experiments, respectively. In order to analyze the transcriptome, the Monarch RNA extraction kit was used to isolate the RNA of ModeK cells. Therefore, the cells were washed with cold PBS and then frozen in DNA/RNA protection reagent at -80 °C until further proceeding.

The plate was thawed at room temperature (RT) and an equal volume of lysis buffer was added to each well containing the protection reagent. The samples were pipetted onto genomic DNA (gDNA) removal columns and spun down. An equal amount of pure EtOH was added to each flow-through and mixed by pipetting. The mixtures were then transferred onto RNA purification columns and spun down. The columns were washed with wash buffer prior to incubation with DNase, after which RNA priming buffer was added to each column and then spun down. Following two washing steps, the RNA was eluted by nuclease-free water and the concentrations were determined by measuring the absorbance.

cDNA synthesis

In order to allow for quantification, the RNA was reverse transcribed to synthesize complementary DNA (cDNA). Each sample was diluted with nuclease-free H₂O to obtain 10 µl of equally concentrated RNA. The first master mix containing oligo dTs (0.125 µL/sample), deoxynucleotide triphosphates (dNTPs) (0.5 µL/sample), and nuclease-free H₂O (2.375 µL/sample) was added to each sample after which they were vortexed and then centrifuged. Subsequently, the samples were incubated for 5 min at 65 °C in a PCR cycler. The second master mix of RT buffer (2 µL/sample) and reverse-transcriptase (0.5 µL/sample) was added to each sample which were then run at a PCR program (10 min at 25 °C, 15 min at 50 °C, 5 min at 85 °C, hold at 4 °C; 1 cycle) and afterwards diluted to 10 ng/µL with nuclease-free H₂O before frozen at -20 °C until required.

qPCR

The cDNA samples were analyzed for expression of the gene of interest and 18S ribosomal RNA (rRNA) as housekeeping control using TaqMan assays and StepOnePlus qPCR. The TaqMan master mix was added as 0.5 µL gene expression assay (20X) and 4.5 µL gene expression master mix (2X) to 10 ng cDNA sample. Thereby, each sample was run in duplicates (10 µL/well) on a 96-well plate (PCR stage (40 cycles): 10 sec at 95 °C, 1 min at 60 °C; followed by melting point curve analysis). Each independent experiment included three technical replicates.

Consumption release rate (CORE)/Analysis of Medium Exchange Rates

The metabolite measurements were performed in collaboration with Dr. Björn Becker (LIH, Luxembourg).

The metabolites were extracted by mixing 20 µl of the medium sample with 180 µl extraction solvent (80 % MeOH/20 % m_qH₂O) which contained the internal standards [U-13C]-ribitol (50 µg/ml) and pentanedioic-d₆ acid (20 µg/ml). The samples were vortexed for 10 s, incubated in a thermomixer at

4°C and shaken at 1350 rpm for 15 min, and then centrifuged for 5 min at max speed. Subsequently, 50 µl of the supernatant was transferred onto a GC-vial and dried overnight using SpeedVac. Metabolites were derivatized by means of a multi-purpose sample preparation robot (Gerstel). The dried medium extracts were dissolved in 30 µl pyridine that contained 20 mg/mL methoxyamine hydrochloride (Sigma-Aldrich), and the samples were shaken for 120 min at 45 °C. Subsequently, 30 µl N-methyl-N-trimethylsilyl-trifluoroacetamide (Macherey-Nagel) was added, and the samples were shaken for 30 min at 45 °C.

Gas chromatography–mass spectrometry (GC-MS) analysis was conducted using an Agilent 7890A GC coupled to an Agilent 5975C inert XL Mass Selective Detector (Agilent Technologies) as described in detail in Becker et al. (2023, Preprint). Absolute uptake and release rates were calculated as described in Hiller et al. (2009). A description of the medium quantification and exchange rate calculation can be found in Meiser et al. (2016).

Glucose tracing

The glucose tracing experiments were performed in collaboration with Dr. Björn Becker (LIH, Luxembourg).

Stable isotope tracing

In a 12-well plate, cells were seeded in triplicates at a density of 2×10^5 cells/well using 1 mL/well in regular cell culture medium. The following day, the medium was changed to customized DMEM with or without 78 µM Trp (Cell Culture Technologies, Switzerland), with 17 mM [U-¹³C]-glucose tracer (Cambridge Isotope Laboratories), and 10 % dialyzed FBS. After 24 h, the metabolites of one set of triplicates were extracted for subsequent liquid chromatography–mass spectrometry (LC-MS) analysis, and another parallel set of triplicates was used for normalization based on the packed cell volume (PCV) which takes both the cell count and cell volume into account.

LC-MS analysis of metabolite levels and mass isotopologue distribution

The cells in the 12-well plates were washed using 1 mL ice-cold PBS per well and then incubated with 400 µL extraction solvent (MeOH:acetonitrile:H₂O, 50:30:20) for 5 min at 4 °C under agitation. Then, the extracts were centrifuged at full speed for 10 min at 4 °C, and the supernatant was used for the LC-MS analysis. A description of the LC-MS instrumentation and analysis can be found in Green et al. (2023) and Meiser et al. (2016) with the exception that both an internal standard and the PCV were used for data normalization.

2.3 Biochemical methods

Quantification of protein expression was done by WB, prior to which the total protein concentration was determined by Lowry assay.

Protein lysates and total protein concentration determination

ModeK cell lysates

ModeK cells of the indicated genotype were seeded in a 6-well plate in 2 mL/well at either 2×10^5 cells for transfections, or at 3×10^5 cells for stimulations.

Initially, the cells were washed with ice-cold PBS and, subsequently, 60 μ L of lysis buffer (radioimmunoprecipitation assay (RIPA) buffer and 1 % phosphatase and protease inhibitor) was added per well. The cell lysates were scratched off with a cell scraper and transferred to an Eppendorf tube. The samples were incubated on ice and vortexed before they were sonicated for 10 sec each. After centrifugation for 15 min at max speed at 4 °C, a fixed amount of supernatant was transferred to a new Eppendorf tube.

Organoid lysates

The organoids were harvested using 500 μ L Cell Recovery Solution to collect three wells in one 15 mL falcon. After pipetting up and down to break the Matrigel, the organoids were incubated on ice for 1 h. The organoids were then centrifuged at 400 g for 3 min at 4 °C, and the supernatants were discarded. The pellets were resuspended in 500 μ L ice-cold PBS, transferred to Eppendorf tubes, and centrifuged again. Afterwards, the supernatant was discarded and the pellets were resuspended in 40 μ L lysis buffer (RIPA buffer and 1 % phosphatase and protease inhibitor). As for the ModeK cells, the samples were sonicated for 10 sec, centrifuged at max speed for 15 min at 4 °C, and finally, a fixed amount of supernatant was collected in a new Eppendorf tube.

Protein concentration

The total protein concentration was determined by means of Lowry assay. In a 96-well plate, 5 μ L of bovine serum albumin (BSA) standards at concentrations varying from 5 mg/mL to 0.078 mg/mL were added in duplicates, and the samples were, diluted 1:6, also loaded in duplicates. PBS served as blank. A total of 25 μ L of reagents S+A mix (0.5 μ L S/sample, and 24.5 μ L A/sample) and 200 μ L reagent B were added per well. After a short incubation at RT, the absorbance was measured at 750 nm.

The protein samples were diluted in PBS to reach the same concentrations and then diluted in Laemmli buffer (5x Laemmli buffer: 0.5 M Tris-HCL pH 6.8, glycerol, 0.25 g SDS dissolved in 1 ml Tris-HCL, 0.25

% bromophenol blue β -mercaptoethanol (β -ME)). The protein samples were incubated at 95 °C for 5 min and then either frozen at -20 °C or directly run by gel electrophoresis.

WB

SDS-PAGE and transfer

Unless otherwise stated, 12 % bis-acrylamide gels were used for the sodium dodecyl sulfate polyacrylamide gel electrophoresis (SDS-PAGE). When frozen, the protein samples were again heated up at 95 °C for 5 min prior to loading at 20 μ g per well onto the bis-acrylamide gel. The gels were immersed in Tris-glycine-SDS (TGS) buffer and proteins were separated at 80 V, which was increased to 120 V upon reaching the separation gel. The gels were transferred onto a 0.45 μ m polyvinylidene difluoride (PVDF) membrane by semi-dry transfer (for which the sandwich consisted of a bottom filter paper was soaked in anode buffer 2, another filter paper soaked in anode buffer 1 on top, PVDF membrane, gel, and a cathode buffer-soaked filter paper on the top; buffer recipes are given in the appendix section). The transfer was performed at 25 V and 0.3 A for 60 min. After blocking the membrane in 5 % skim milk dissolved in tris-buffered saline with tween (TBS-T) (0.1% Tween 20) for 1 h, the membranes were incubated with the specific primary antibodies (Table 13) dissolved in either 5 % skim milk or 5 % ovalbumin in TBS-T overnight in the cold room.

Immunodetection

The next day, the membranes were washed three times with TBS-T for 10 min, before they were incubated with the respective secondary antibody (Table 13) for 1 h at RT. The membranes were washed again three times with TBS-T, before chemiluminescent detection with enhanced chemiluminescence (ECL) substrate using the Chemidoc. If necessary, blots were stripped in ThermoFisher stripping buffer for 20 min, briefly washed with TBS-T, blocked, and re-probed with primary antibody.

2.4 Cohorts and bioinformatical analysis

The bioinformatical analysis performed in collaboration with Dr. Jan Taubenheim (CAU, IEM) was based on patient samples of the two cohorts eMED and FUTURE. All timepoints and patient activities of the respective cohort were combined. The WARS1 expression in the gut was associated with the tryptophan serum levels by using linear mixed effect models with following formula ``WARS1_expression ~ Cohort+ Diagnosis*Trp_concentration + (1|Patient)``. The modeling was performed using the lme4 package (v1.1-29) in R (v4.2.1). The model was tested against a null model and a simplified version with only Trp_concentration in the fixed term using log-likelihood ratio test

using the R package car (v3.0-13). The WARS1 expression was measured as transcript per million (TPM) and was log₂ transform to fulfill the assumption of normally distributed residuals of the model. Diagnostic plotting was performed to check normality and homoscedasticity of residuals. Plotting was performed with the R package ggplot2 (v3.3.6).

eMED cohort

The eMED cohort, as published in Zeissig et al. (2019), recruited 18 active IBD patients (CD $n = 9$, UC $n = 9$) who received the anti-integrin $\alpha 4\beta 7$ -antibody vedolizumab treatment, and 20 active IBD patients (CD $n = 8$, UC $n = 12$) who were administered the anti-TNF α antibody infliximab as a control for longitudinal investigation. The blood samples and sigmoidal colon biopsies were taken at baseline, and right before the treatments at weeks 2, 6, and 14.

FUTURE cohort

The FUTURE cohort refers to a 12-week, open-label, prospective phase 2a clinical trial that was conducted at both the University Medical Center Schleswig-Holstein in Kiel, Germany, and at the Asklepios Westklinikum in Hamburg, Germany for a period of 21 months in 2016 to 2019. It recruited 16 active IBD patients at the age of 21 - 66 who were treated with the trans-signaling inhibitor olamkicept (sgp130Fc) biweekly for 12 weeks. Blood as well as sigmoid mucosal biopsies were taken at both 4 h and 24 h after therapy. The clinical disease activity was determined at baseline, 2 w, 6 w, and 14 w. A more detailed description can be found in Schreiber et al. (2021).

2.5 Statistical analysis

All statistical analysis was performed using GraphPad Prism software version 5.03. The student's paired t-test was used for comparisons between two groups of the same genotype, whereas the student's unpaired t-test was used to compare two different genotypes. Each independent experiment consisted of three technical replicates which were averaged, and the statistical analysis was performed on at least three biological replicates. All data are expressed as mean \pm standard error of the mean (SEM). The statistical significance is indicated with asterisks, expressed as $*p \leq 0.05$, $**p \leq 0.01$, $***p \leq 0.001$, $****p \leq 0.0001$.

3. Results

Considering the association between Trp metabolism and inflammation, the aim of this project was to investigate how a drop in Trp levels influences the cellular response to different immunologic stimuli *in vitro*.

3.1 The intestinal mucosa of IBD patients exhibits shortage of Trp

Taking the findings by Nikolaus et al. (2017) as a basis, who described that IBD patients feature lower Trp serum levels, it remained to be investigated whether the intestine as a nutrient rich environment experiences a shortage of Trp levels in the first place. Therefore, a bioinformatics approach was used to estimate whether the intestinal mucosa of IBD patients experiences Trp shortage. The serum Trp levels were correlated with mucosal WARS1 expression in the patients of two cohorts (Figure 3.1). A description of the cohorts can be found in the methods section. As WARS1 is upregulated in response to Trp reduction (Adam et al., 2018), its over-expression can be used as an indication of Trp shortage.

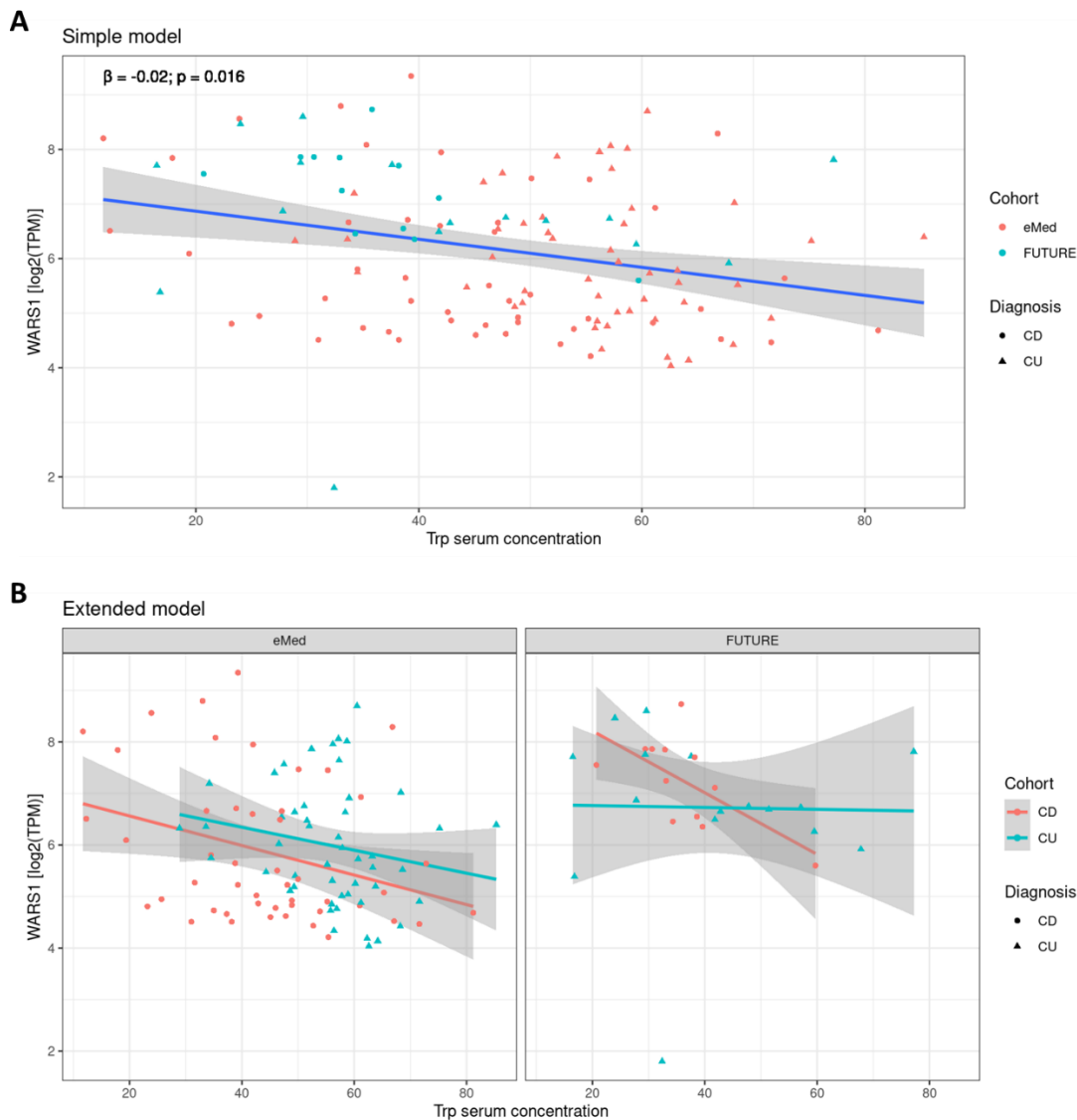


Figure 3.1 IBD patients have reduced mucosal Trp levels

Serum Trp levels and mucosal WARS1 expression was correlated in IBD patients of the two cohorts eMED ($n = 38$) and FUTURE ($n = 16$). The bioinformatical analysis was done in collaboration with Dr. Jan Taubenheim (CAU, IEM).

All timepoints and patient activities of the two IBD cohorts eMED (published in Zeissig et al., 2019) and FUTURE (published in Schreiber et al., 2021) were combined for this analysis. As expected, the mucosal WARS1 expression negatively correlated with the serum Trp levels. As for the eMED cohort, both CD and UC featured the same association. The FUTURE cohort, however, only showed this correlation in CD patients. Caution must be taken with this interpretation because the FUTURE cohort included only a few patients (Figure 3.1). Thus, it can be concluded that IBD patients not only have reduced serum Trp levels but are likely to exhibit a reduction of Trp in the intestinal mucosa as well.

3.2 Trp starvation decreases the cell viability *in vitro*

Based on this, the investigation was continued using the murine SI cell line ModeK to decipher the impact of Trp starvation on the cellular level. The ModeK cell line was cultured in customized DMEM medium either containing 78.4 μM (matches Trp concentration in regular DMEM) or 0 μM Trp for 24 h, supplemented with dialyzed FBS to ensure that only a minimal amount of Trp was included. The cell condition was analyzed with MTS assay and the phenotype was checked under the microscope, while *Wars* induction served as a marker for successful Trp starvation (Figure 3.2).

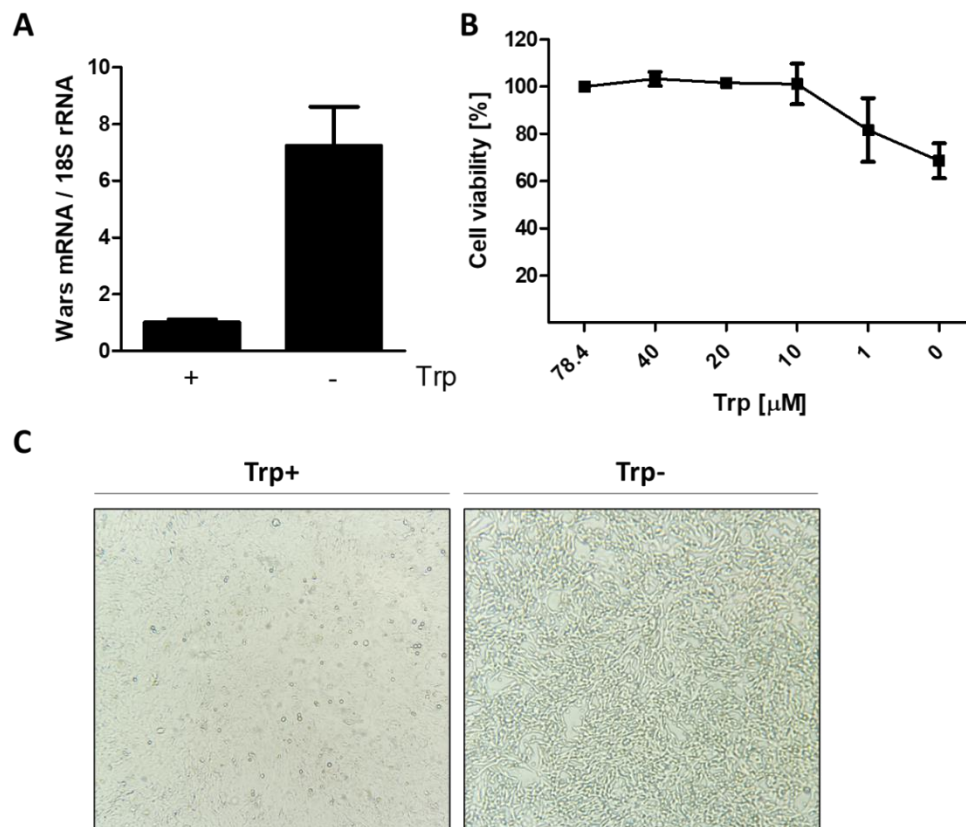


Figure 3.2 Trp starvation for 24 h induces *Wars* expression and decreases cell viability

(A) ModeK WT cells were cultured in the presence or absence of Trp for 24 h, and then analyzed for *Wars* expression by qPCR. Data are presented as mean \pm SEM normalized to Trp+ of three independent experiments ($n = 3$).

(B) MTS assay was performed of iCtrl cells cultured in media containing different Trp concentrations. Data are presented as mean \pm SEM normalized to 78 μM Trp of three independent experiments ($n = 3$).

(C) The phenotype of ModeK WT cells was observed under the microscope after 24 h culture in the presence or absence of Trp. Pictures were taken with a light microscope at 100x magnification.

Although not significantly, Trp starvation markedly induced *Wars* mRNA expression as compared to controls, meaning that the starvation was successful. As observed under the microscope, Trp starvation induced cell death which was further determined by MTS assay. At Trp concentrations of 10 μM or lower, the cell viability seemed unaffected, whereas the cell viability was reduced to approximately 70 % when Trp was omitted completely (Figure 3.2).

3.3 Trp starvation sensitizes cells to NF- κ B activation

Based on the finding that inflammation negatively correlates with serum Trp levels, the consequences of Trp starvation were investigated in an *in vitro* model. Therefore, the murine SI cell line ModeK was cultured for 24 h with customized medium deprived of Trp before stimulation with either LPS or IL-1 β (Figure 3.3), both of which are well established models of *in vitro* inflammation and known to activate NF- κ B.

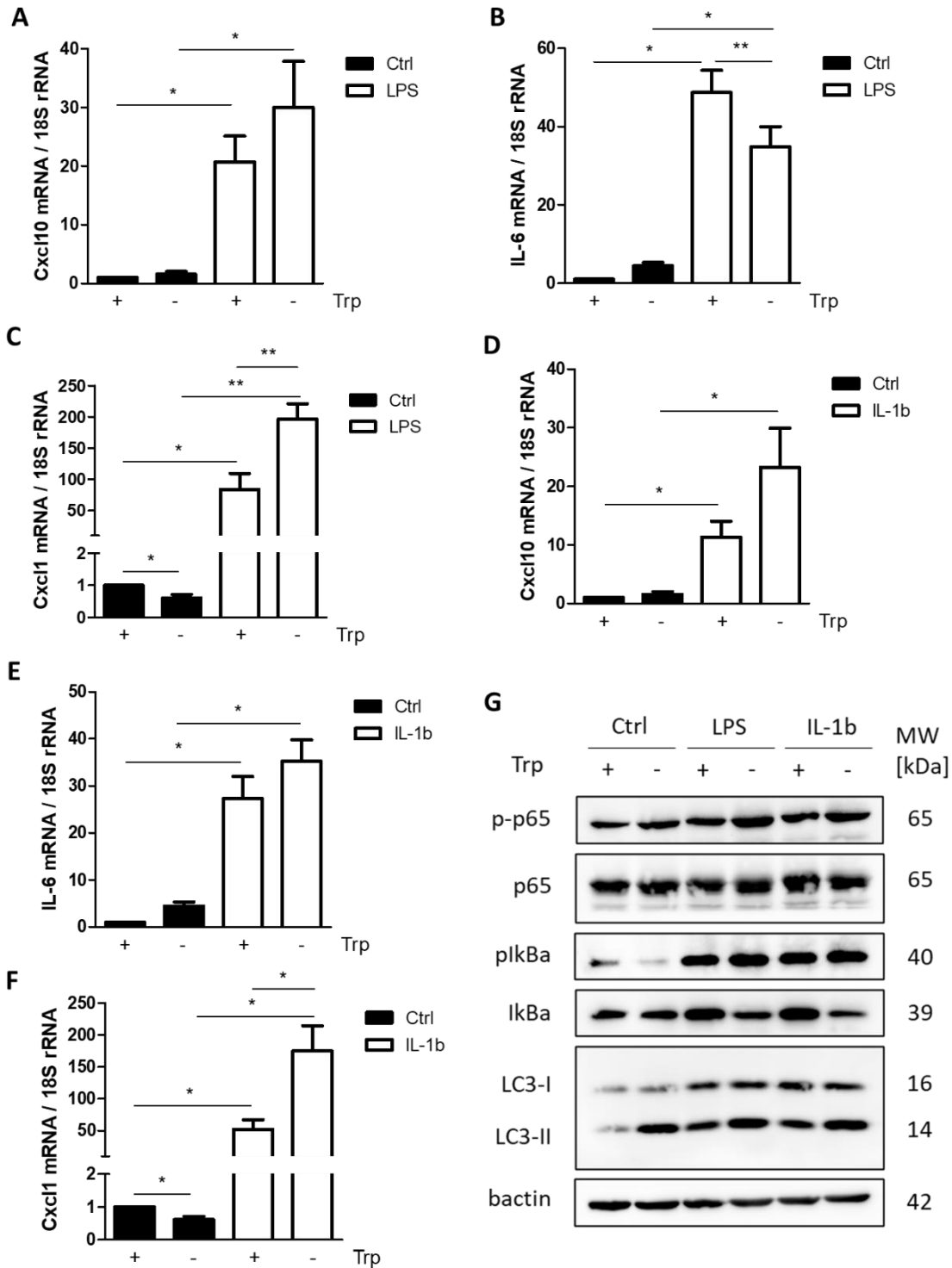


Figure 3.3 Trp starvation potentiates NF-κB activation

ModeK cells were cultured with [78.4 μM] or without [0 μM] Trp for 24 h and then stimulated with either LPS [100 ng/mL] or IL-1β [50 ng/mL].

(A-F) Target mRNA levels were determined by means of qPCR after a stimulation time of 3 h.

(A,C,D,F) Data are presented as mean ± SEM normalized to Trp+ Ctrl of five independent experiments ($n = 5$). $*p \leq 0.05$; $**p \leq 0.01$.

(B,E) Data are presented as mean ± SEM normalized to Trp+ Ctrl of three independent experiments ($n = 3$). $*p \leq 0.05$; $**p \leq 0.01$.

(G) WB of target proteins after a stimulation time of 2 h. Image is representative of two independent experiments ($n = 2$).

Stimulation with LPS or IL-1 β successfully induced the expression of the inflammatory cytokines C-X-C motif chemokine ligand (Cxcl)10, Cxcl1, and IL-6 as measured with qPCR. Strikingly, the inflammatory response to both LPS and IL-1 β stimulation of Trp-deprived cells was even higher than that of cells cultured with Trp, except IL-6 levels induced by LPS (Figure 3.3). Activation of the NF- κ B pathway was confirmed by WB analysis and showed a strong phosphorylation of I κ B α upon LPS or IL-1 β challenge. Blotting of the autophagy marker LC3 serves as control for Trp starvation (Figure 3.3): LC3-I is the cytosolic form of LC3 and LC3-II is conjugated with PE which is why increasing LC3-II indicates autophagosome formation (Mizushima and Yoshimori, 2007).

3.4 Trp starvation lowers STING protein levels

Next, the stimulation was extended to IFNs in order to assess whether Trp starvation influences other inflammatory pathways as well. ModeK cells were starved of Trp for 24 h and subsequently treated with either Ifn β [100 ng/mL] or Ifn γ [100 ng/mL] to determine the induced expression of Cxcl10, Cxcl1, and IL-6 by qPCR (Figure 3.4).

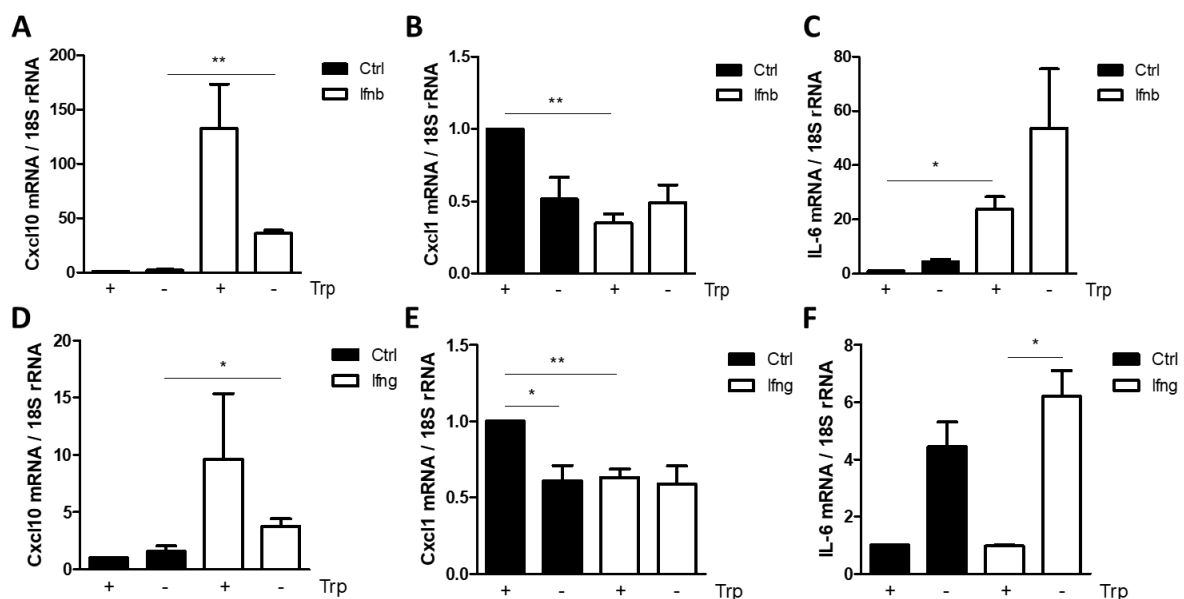


Figure 3.4 Trp starvation impairs Cxcl10 induction after IFN treatment

After 24 h Trp starvation, ModeK cells were treated with either Ifn β [100 ng/mL] or Ifn γ [100 ng/mL] for 3 h and the expression of target mRNAs was measured with qPCR.

(A-C,F) Data are presented as mean normalized to Trp+ Ctrl of three independent experiments ($n = 3$). * $p \leq 0.05$; ** $p \leq 0.01$.

(D,E) Data are presented as mean \pm SEM normalized to Trp+ Ctrl of five independent experiments ($n = 5$). * $p \leq 0.05$; ** $p \leq 0.01$.

As previously observed with IL-1 β stimulation, both Ifn γ and Ifn β induced stronger IL-6 expression in Trp-starved cells as compared to controls. Cxcl10 induction by either Ifn γ or Ifn β , however, was reduced in cells cultured without Trp (Figure 3.4).

The impaired Cxcl10 response to IFN stimulation led to the hypothesis that Trp may impact on the cGAS/STING pathway. To investigate an association between Trp and STING, ModeK cells were cultured with different Trp concentrations [0, 1, 10, 20, 40, 78 μ M] for 24 h and then analyzed for STING expression by WB. Additionally, murine SI organoids were starved of Trp (Figure 3.5).

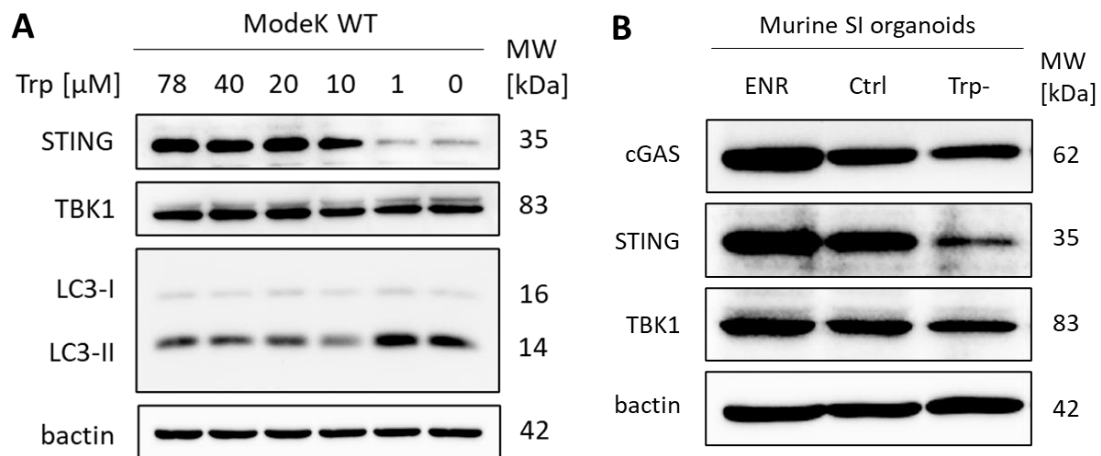


Figure 3.5 Trp starvation reduces STING expression in ModeK cells and murine SI organoids

(A) ModeK cells were cultured in medium containing different Trp concentrations for 24 h and then analyzed by means of WB. Image is representative of six independent experiments ($n = 6$).

(B) Control murine SI organoids were cultivated in normal organoid medium (ENR), or customized control 3D medium (Ctrl). The organoids were starved by cultivation in customized medium lacking Trp. After 48 h, protein lysates were prepared and analyzed with WB. Image is representative of three independent experiments ($n = 3$). The organoid experiments were performed in collaboration with Mrs. Guang Yang (IKMB).

The autophagy marker LC3 indicates successful induction of autophagy upon Trp starvation to validate the Trp titration. Whereas Trp deprivation did not have an impact on TBK1 protein levels, ModeK cells exhibited a striking reduction in STING protein levels when cultured with 1 μ M Trp or less (Figure 3.5A). The finding was validated in murine SI organoids who also showed markedly reduced STING levels under conditions of Trp deprivation (Figure 3.5).

STING is quickly degraded after its activation, and both its activation and subsequent degradation depend on its phosphorylation by TBK1 (Chen et al., 2016). In order to test whether the loss of STING is due to its previous activation, the cytokine levels were measured after 24 h of Trp starvation (Figure 3.6A-B). Further, TBK1 was knocked down by siRNA to prevent the phosphorylation of STING, and the protein levels were analyzed with WB (Figure 3.6D).

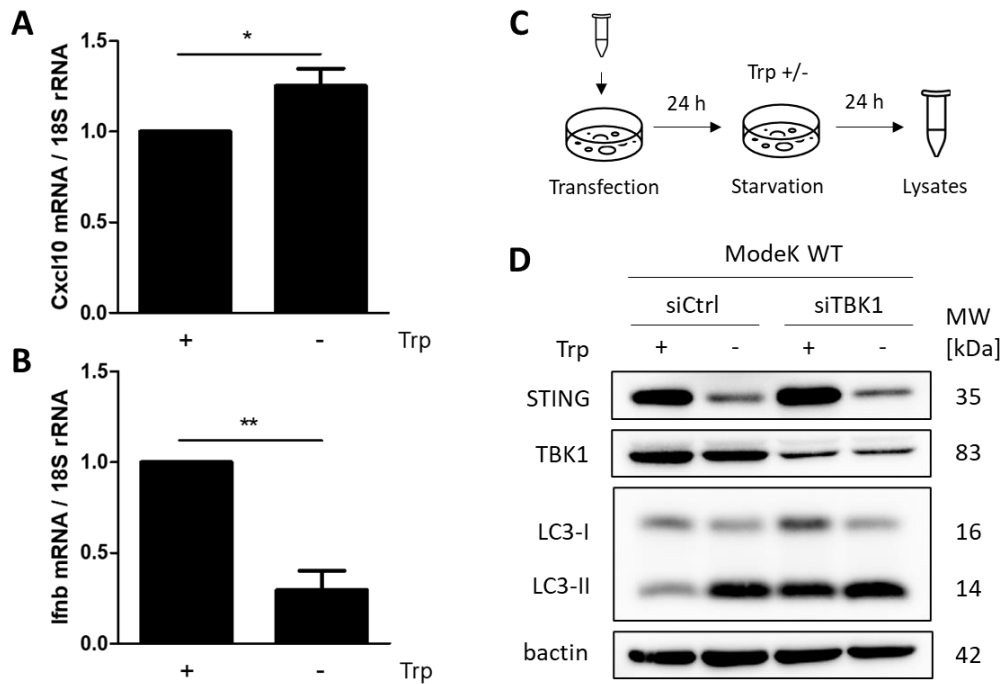


Figure 3.6 Trp starvation-induced STING loss does not depend on TBK1

(A-B) ModeK cells were cultured without Trp for 24 h and then analyzed for cytokine expression by qPCR.

(A) Data are presented as mean \pm SEM normalized to Trp+ of seven independent experiments ($n = 7$). $*p \leq 0.05$; $**p \leq 0.01$.

(B) Data are presented as mean \pm SEM normalized to Trp+ of five independent experiments ($Ifnb$: $n = 5$). $*p \leq 0.05$; $**p \leq 0.01$.

(C-D) ModeK cells were transfected with siRNA against TBK1. After 24 h, the medium was changed to Trp starvation medium or control, and cells were lysed after another 24 h. Image is representative of three independent experiments ($n = 3$).

Trp starvation for 24 h elicited neither Cxcl10 nor Ifn β expression in ModeK cells (Figure 3.6A+B).

Likewise, a KD of TBK1 did not rescue STING levels in Trp-starved cells (Figure 3.6D).

3.5 Trp starvation impairs the cGAS/STING response

Owing to the reduction of STING, it was hypothesized that Trp starvation renders the cell in an immunocompromised state by impairing the cGAS/STING response. The ability of Trp-deprived cells to mount a STING response was tested by using the direct STING agonist 5,6-dimethylxanthenone-4-acetic acid (DMXAA) after 24 h of Trp starvation. The activation was read out by phosphorylation of both STING and TBK1 and the induction of cytokine expression (Figure 3.7).

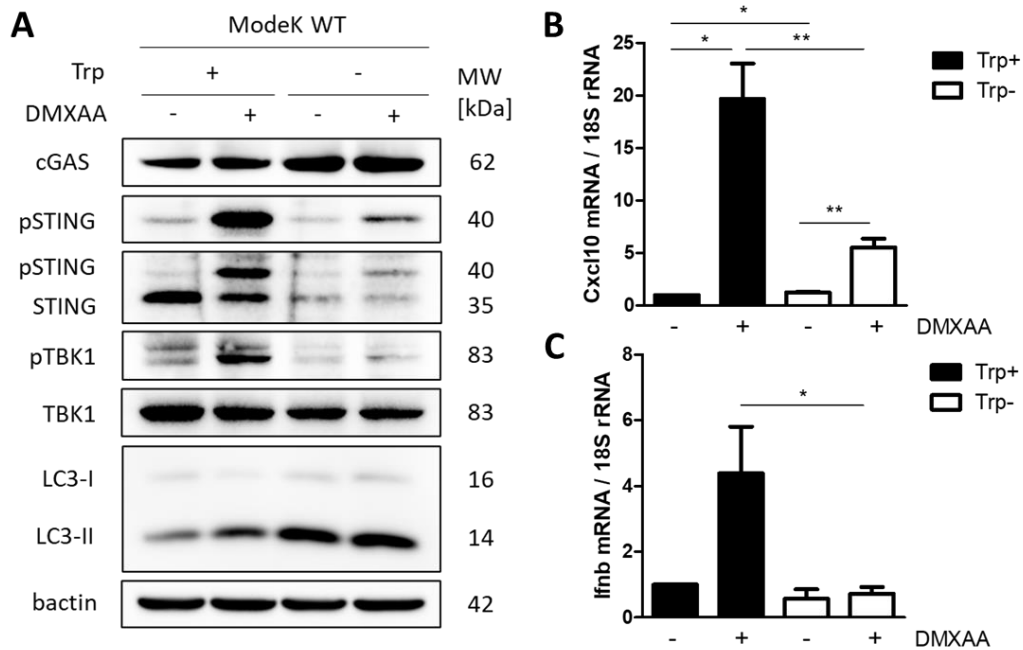


Figure 3.7 Trp-starved cells scarcely respond to DMXAA

ModeK cells were cultured with or without Trp for 24 h before stimulation with DMXAA [100 µg/mL] for (A) 2 h or (B-C) 3 h, respectively.

(A) Image is representative of four independent experiments ($n = 4$).

(B) Data are presented as mean \pm SEM normalized to Trp+ Ctrl of seven independent experiments ($n = 7$). $*p \leq 0.05$; $**p \leq 0.01$.

(C) Data are presented as mean \pm SEM normalized to Trp+ Ctrl of six independent experiments ($n = 6$). $*p \leq 0.05$; $**p \leq 0.01$.

Cells cultured under normal conditions responded well to DMXAA stimulation as shown by phosphorylation of both STING and TBK1, and upregulated Cxcl10 and Ifn β levels. On the contrary, cells deprived for Trp had significantly lower STING levels and in this way reduced STING and TBK1 phosphorylation compared to controls. They further showed impaired expression of Cxcl10 and Ifn β relative to controls (Figure 3.7).

The functional response was further validated by transfecting the cells with 2'3' cGAMP and 3'3' cGAMP. Additional transfection with dsDNA enabled testing the functionality of the whole cGAS/STING pathway since DMXAA does not involve cGAS activation (Figure 3.8).

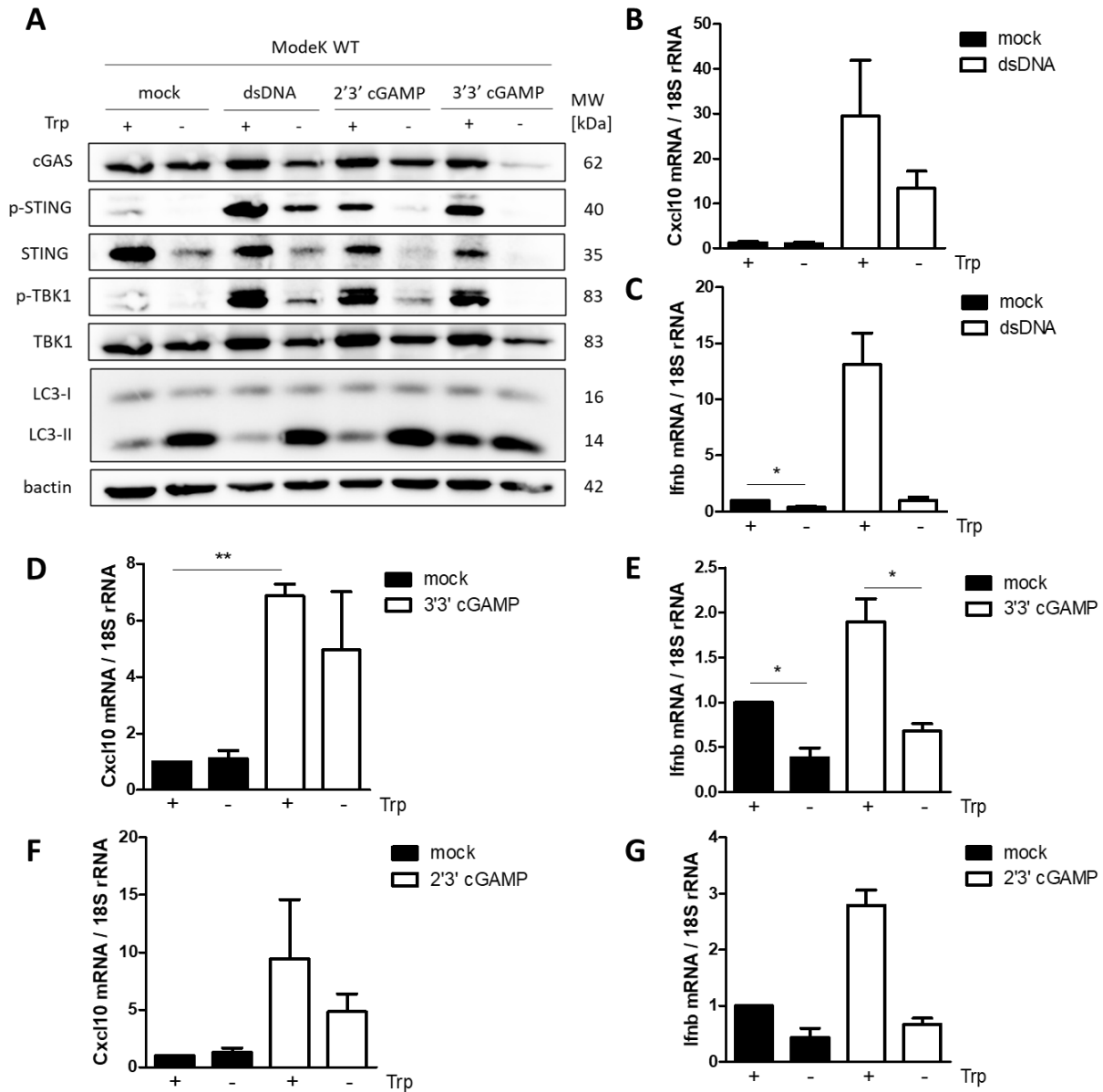


Figure 3.8 Trp starvation impairs the cGAS/STING response

After starving ModeK cells for Trp for 24 h, they were transfected with dsDNA [1 µg/mL], 2'3' cGAMP [10 µg/mL], or 3'3' cGAMP [10 µg/mL] for 9 h.

(A) Image is representative of four independent experiments ($n = 4$) with the exception of 2'3' cGAMP stimulation representing two independent experiments ($n = 2$).

(B-E) Data are presented as mean \pm SEM normalized to Trp+ Ctrl of three independent experiments ($n = 3$). * $p \leq 0.05$; ** $p \leq 0.01$.

(F-G) Data are presented as mean \pm SEM normalized to Trp+ Ctrl of two independent experiments ($n = 2$). * $p \leq 0.05$; ** $p \leq 0.01$.

Stimulation of 2'3' cGAMP or 3'3' cGAMP validated the results obtained for DMXAA. Accordingly, STING and TBK1 phosphorylation in response to dsDNA was drastically reduced in Trp-starved cells compared to controls, as well as induction of Cxcl10 and Ifn β (Figure 3.8), meaning that Trp-deprived cells feature an impaired cGAS/STING pathway.

3.6 Replenishing Trp restores STING expression

In order to test whether Trp starvation leaves a stable imprint, ModeK cells were deprived of Trp for 48 h, and then cultured in Trp-containing medium for 24 h to analyze STING levels by WB (Figure 3.9).

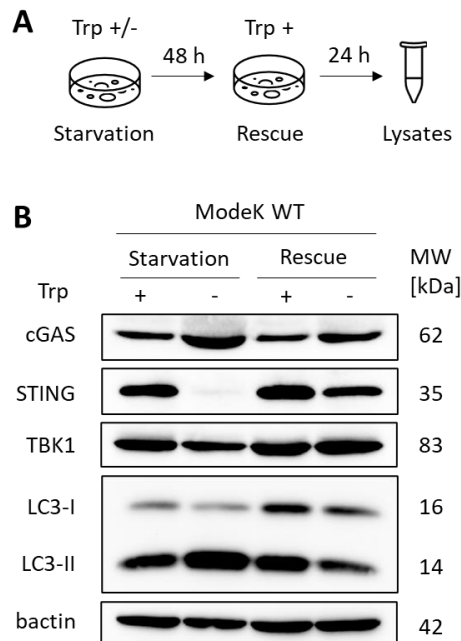


Figure 3.9 Replenishing Trp levels rescues the phenotype

After ModeK cells were cultured with or without Trp for 48 h, the medium was changed to Trp-containing medium and cells were lysed 24 h to be analyzed by WB.

(A) Experimental setup.

(B) Image is representative of three independent WB experiment ($n = 3$).

STING expression was lost in the cells that were starved of Trp for 2 d. When the starved cells were then cultured with Trp for 1 d as a rescue approach, STING expression was restored although not yet equal to control levels (Figure 3.9). This indicates that the phenotype is reversible.

3.7 Starvation-induced STING decrease is specific to Trp

In enterocytes, Trp can be metabolized along the KP. Although boosted under inflammatory conditions, it is important to exclude that the observed phenotype stems from a lack of a Trp metabolite rather than from a lack of Trp itself. The importance of a KP metabolite for STING expression was tested by supplementing L-Kyn to Trp-starved ModeK cells (Figure 3.10).

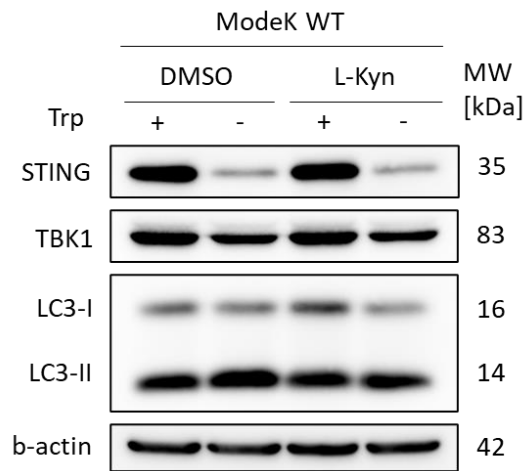


Figure 3.10 Starvation-induced STING decrease is specific to Trp

ModeK cells were cultured with or without Trp and additionally supplemented with L-Kyn [50 μ M] for 24 h. (A) Image is representative of three independent WB experiments ($n = 3$).

The addition of L-Kyn did not influence STING protein levels in either control or Trp-lacking ModeK cells (Figure 3.12).

3.8 Trp starvation does not affect the cellular ATP levels

Starvation in general often is associated with a state of energy deficiency. Hence, the hypothesis was raised that a reduction in Trp leads to an energy deficient state and thereby decreases STING expression. This was tested by means of a U-¹³C-labeled glucose tracing and simultaneous Trp starvation in ModeK cells (Figures 3.11-3.13). First, the glycolysis pathway activity was compared between cells cultured in Trp-containing and non-containing medium (Figure 3.11).

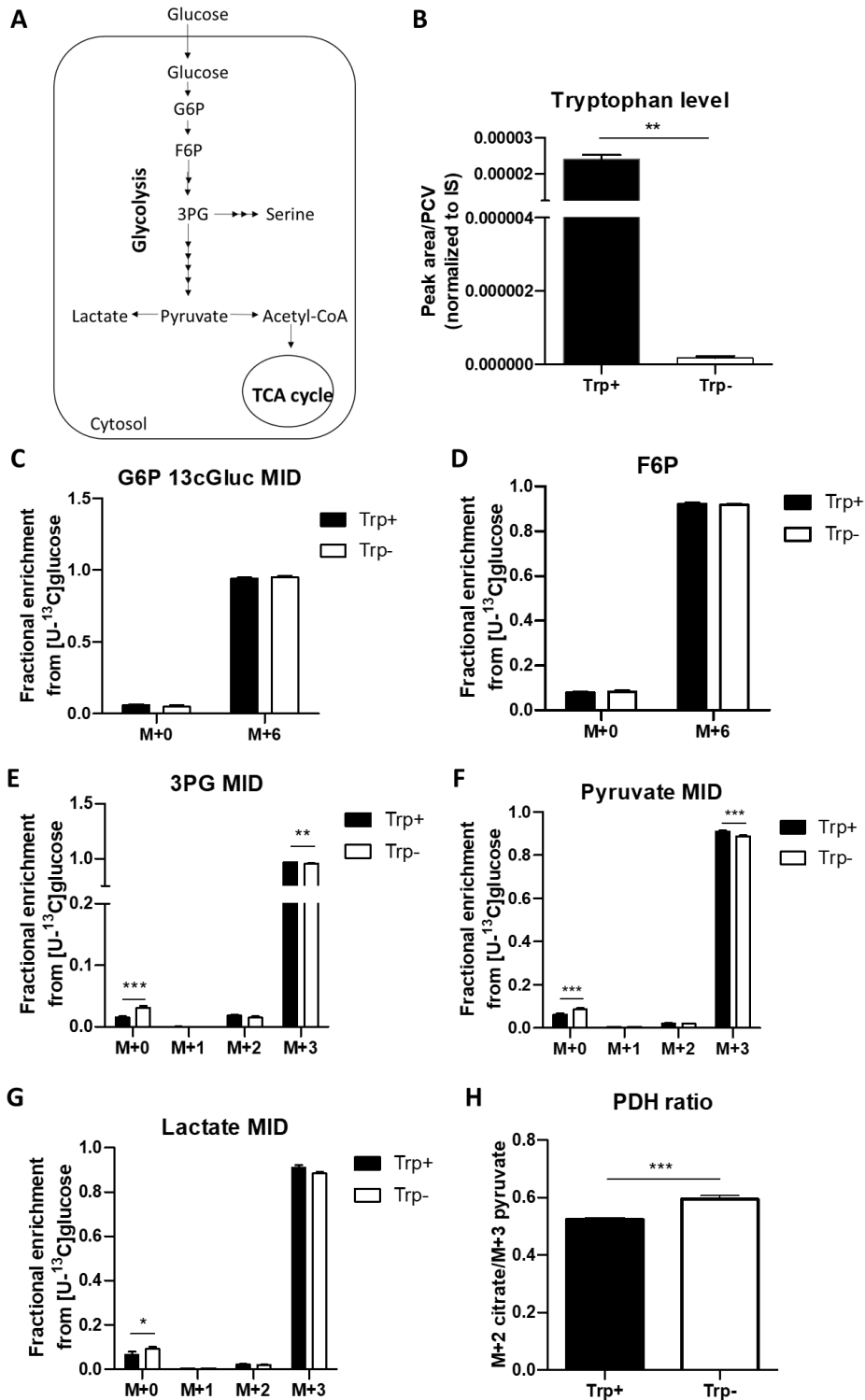


Figure 3.11 Trp starvation does not affect the glycolytic activity in ModeK cells

(A) Glycolysis pathway overview.

(B-H) Simultaneous Trp starvation and glucose [U-13C] tracing for 24 h in ModeK cells.

(B) Intracellular Trp levels determined by Peak area/PCV.

(C-G) Intracellular labeling of the indicated metabolites of the glycolytic pathway.

(H) The PDH ratio calculated by citrate levels/pyruvate levels.

Data are presented as mean \pm SEM of three independent experiments ($n = 3$). * $p \leq 0.05$, ** $p \leq 0.01$, *** $p \leq 0.001$.

Data were obtained in collaboration with Dr. Björn Becker (LIH Luxembourg).

The successful Trp starvation was verified as intracellular Trp was hardly detectable in Trp-starved cells (Figure 3.11B). The lactate labeling differed only slightly between the two groups. Albeit significant, the labeling of the M+3 fraction of pyruvate scarcely decreased in Trp-deprived cells, and likewise, pyruvate dehydrogenase (PDH) activity rose (Figure 3.11C+H). This scarce difference suggests that the glycolytic activity is not affected by Trp starvation. Next, the metabolite labeling involved in the tricarboxylic acid cycle (TCA) cycle was determined (Figure 3.12).

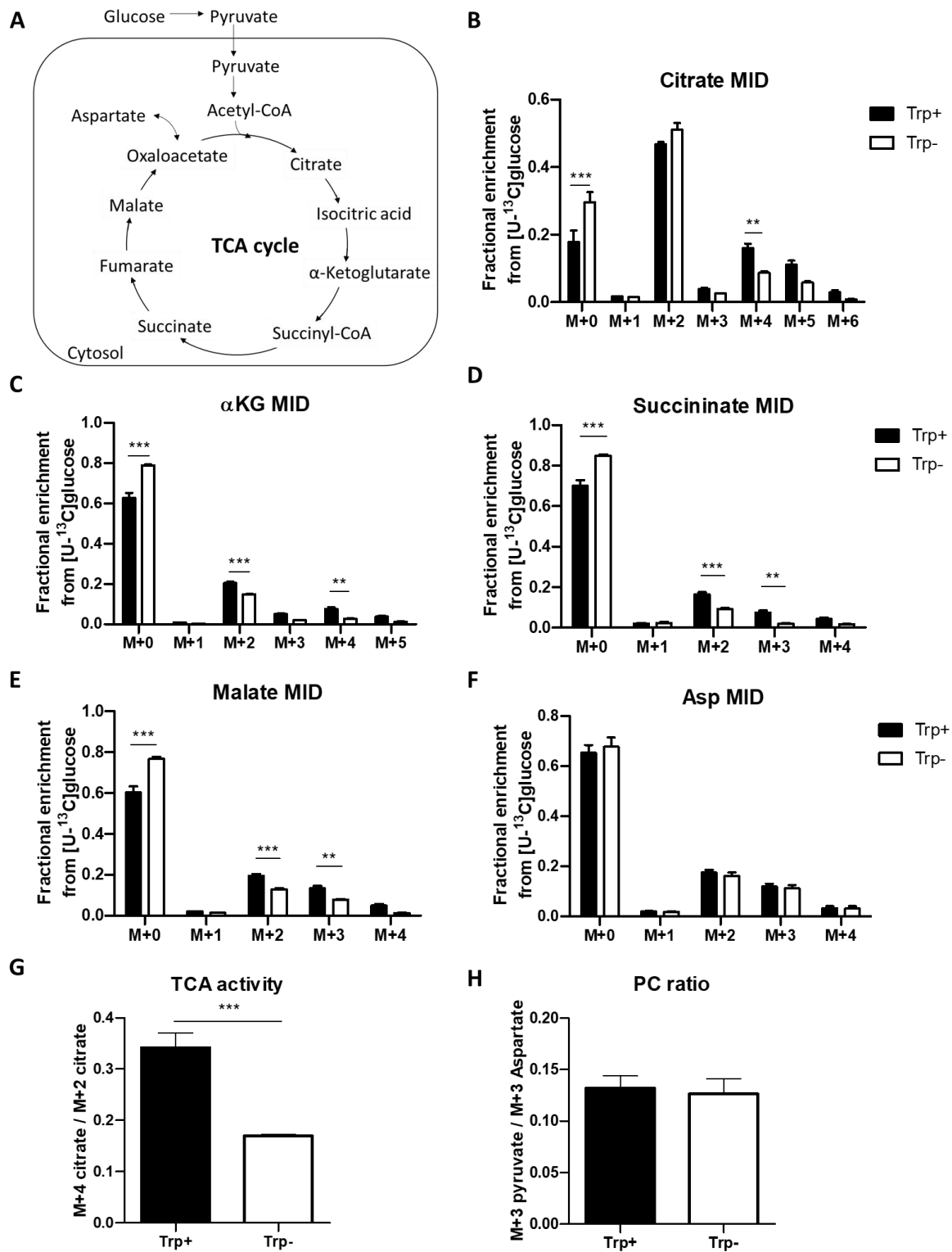


Figure 3.12 TCA cycle activity is reduced under Trp starvation

(A) Overview of TCA cycle metabolites.

(B-H) Simultaneous Trp starvation and glucose [U-13C] tracing for 24 h in ModeK cells.

(B-F) Intracellular labeling of the indicated metabolites of the TCA cycle.

(G) TCA activity determined by the ratio between labeled fractions of citrate.

(H) The PC ratio calculated by pyruvate levels/aspartate labeling.

Data are presented as mean \pm SEM of three independent experiments ($n = 3$). $*p \leq 0.05$, $**p \leq 0.01$, $***p \leq 0.001$.

Data were obtained in collaboration with Dr. Björn Becker (LIH Luxembourg).

In contrast to glycolysis, TCA cycle activity was strongly decreased in cells lacking Trp (Figure 3.12G). The labeling of the four metabolites citrate, α -ketoglutarate (α -KG), succinate, and malate were reduced in Trp-starved cells compared controls, especially in the fractions M+2, and M+3 or M+4, respectively (Figure 3.12B-E). The pyruvate carboxylase (PC) activity, however, as well as aspartate (Asp) labeling were unaltered between Trp-containing and non-containing cells (Figure 12F,H).

The actual cellular energy state can only be recorded by measuring the overall ATP levels as a consequence of the ATP generation and consumption (Figure 3.13).

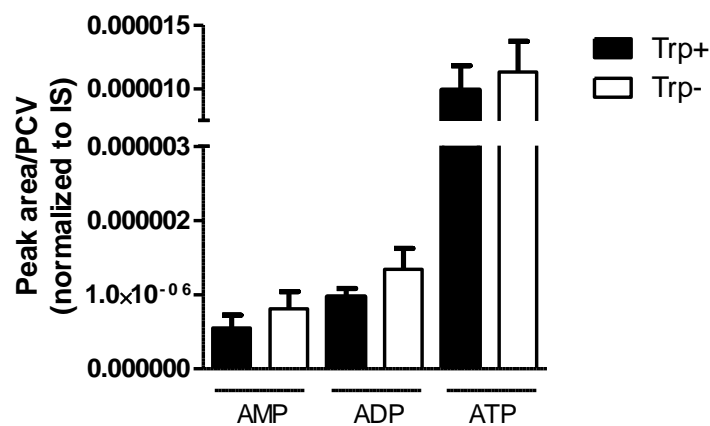


Figure 3.13 Intracellular ATP levels are not affected by Trp starvation

Intracellular labeling of AMP, ADP, and ATP after simultaneous Trp starvation and glucose [U-13C] tracing for 24 h in ModeK cells. Data are presented as mean \pm SEM of three independent experiments ($n = 3$). * $p \leq 0.05$, ** $p \leq 0.01$, *** $p \leq 0.001$.

Data were obtained in collaboration with Dr. Björn Becker (LIH Luxembourg).

There was no significant difference in either adenosine monophosphate (AMP), adenosine diphosphate (ADP), or ATP labeling between cells cultured in the presence or absence of Trp (Figure 3.13). It can thus be assumed that Trp-starvation does not render cells in an energy-deficient state.

The energy dependency was further investigated by adding nicotinamide (NAM) to the cell culture as a rescue approach (Figure 3.14). NAM represents the final metabolite of the KP and can serve as an energy source for the cell (Badawy, 2015; Navarro et al., 2021). The work on T cells by Murray and Srinivasan (1995) was taken as inspiration for the concentrations of NAM supplementation in cell culture.

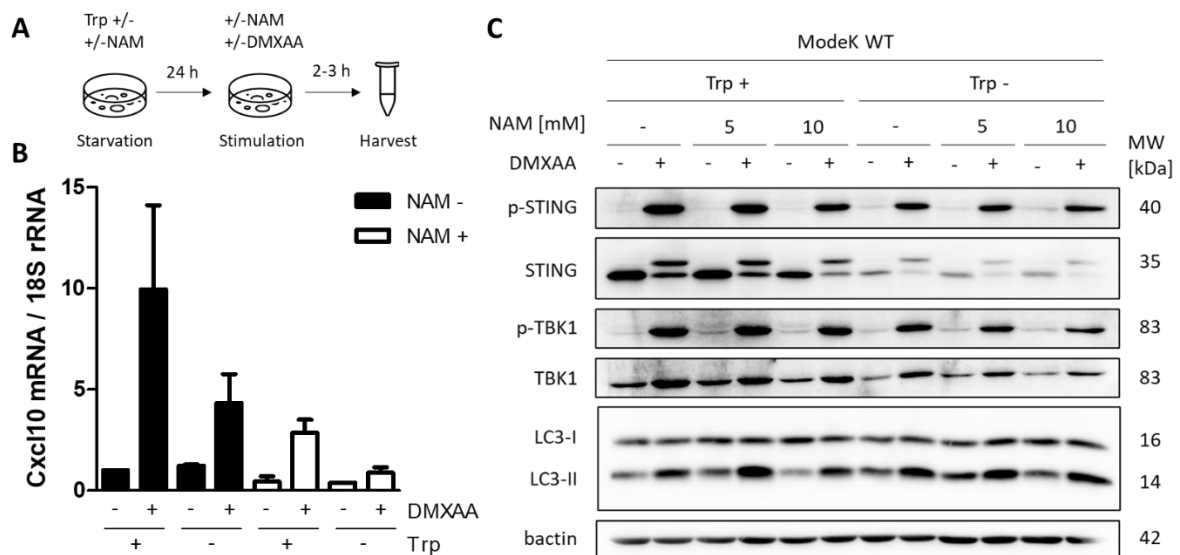


Figure 3.14 Supplementation of the Trp derivative NAM does not restore STING levels

ModeK WT cells were cultured with or without Trp and additionally supplemented with NAM.

(A) Experimental setup.

(B) Cells were treated as depicted in (A) with 10 mM NAM and 100 $\mu\text{g}/\text{mL}$ DMXAA for 3 h before RNA was extracted for qPCR analysis. Data are presented as mean \pm SEM normalized to Trp+ Ctrl of two independent experiments, respectively ($n = 2$).

(C) Cells were treated as depicted in (A) with 10 mM NAM and 100 $\mu\text{g}/\text{mL}$ DMXAA for 2 h and then lysed for WB analysis. Image is representative of one independent experiment ($n = 1$).

The qPCR analysis revealed an even lower Cxcl10 response to DMXAA stimulation in cells supplemented with NAM although less obvious in WB. In line with the ATP measurement, supplementation with NAM as an energy source rescued neither STING levels nor STING response in Trp-starved cells (Figure 3.14). Hence, the energy state does not appear as the underlying mechanism by which Trp starvation impacts on STING.

3.9 Autophagy inhibition does not rescue STING levels

As starvation induces autophagy, and STING is degraded via autophagy under homeostatic conditions, it can be speculated that autophagy represents the underlying mechanism by which STING is decreased under conditions of Trp starvation. First, different autophagy inducers were compared for their influence on STING (Figure 3.15).

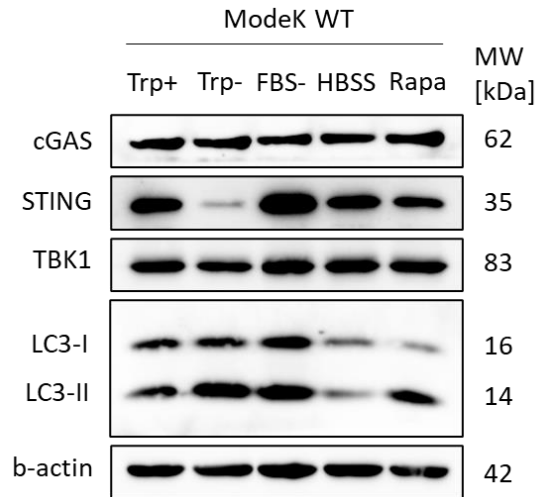


Figure 3.15 General autophagy inducers do not lead to a decrease in STING

ModeK cells were cultured with Trp (control), without Trp (Trp-), or without FBS (FBS-) for 24 h, or cultured in HBSS for 2 h, or stimulated with rapamycin (Rapa) [1 μ M] for 6 h, before lysed and analyzed by WB.

Image is representative of three independent experiments ($n = 3$), with the exception of HBSS stimulation representing two replicates ($n = 2$).

Unlike cells lacking Trp, cells in which autophagy was induced either by omitting FBS supplementation, by incubation in Hanks' balanced salt solution (HBSS), or by rapamycin stimulation, did not show a decrease in STING (Figure 3.15).

Thus, the association between autophagy and STING may be specific to Trp starvation rather than a general phenomenon of starvation or autophagy induction. The specific role of autophagy in lowering STING levels was tested by titrating Trp in autophagy-deficient ModeK cells (Figure 3.16). The *Atg16l1* gene was therefore knocked out using the CRISPR/Cas9 system and confirmed by WB (Figure 3.16). Out of all genes crucial for a functional autophagic machinery, the *ATG16L1* T300A variant has been confirmed as a CD risk gene (Hampe et al., 2007) and was thus chosen to enable translational IBD research.

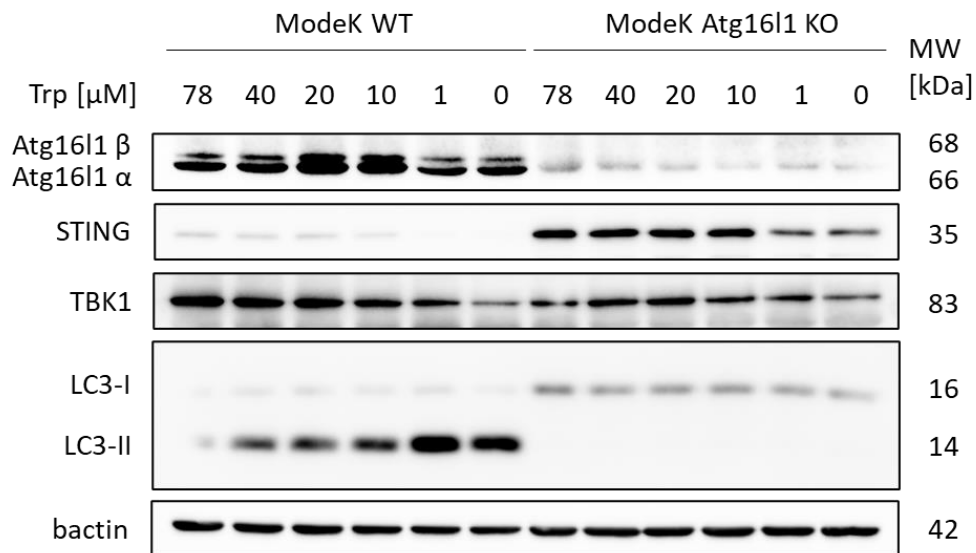


Figure 3.16 STING is reduced in autophagy-deficient cells upon Trp starvation

ModeK WT and *Atg16l1* KO cells were cultured with various Trp concentrations [78 – 0 μ M] for 24 h and then analyzed by WB.

Image is representative of three independent experiments ($n = 3$).

ModeK *Atg16l1* KO cells, unable to induce autophagy as validated by the lack of LC3-II, featured strikingly elevated STING levels under baseline conditions compared to WT controls. However, reducing the Trp content in the medium also lowered STING detection in these KO cells (Figure 3.16).

Next, the response to DMXAA was assessed in *Atg16l1* KO cells to investigate whether the accumulation of STING owing to the defective autophagic machinery is functional (Figure 3.17). Since their STING levels even under Trp deprivation seemed to be higher than those of WT cells, one might speculate that the decrease does not result in an immunocompromised state and therefore can be neglected.

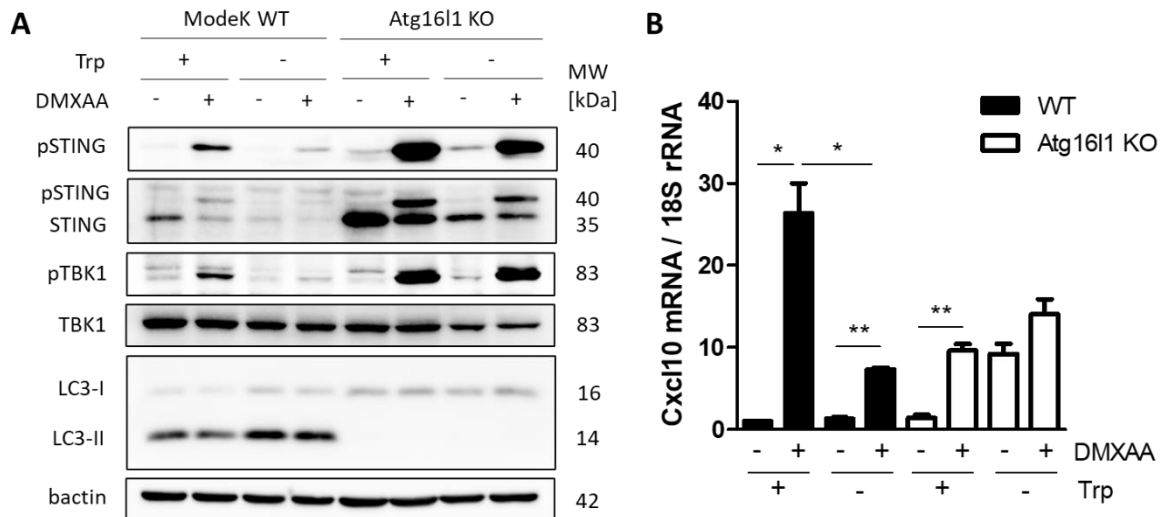


Figure 3.17 Trp starvation-induced STING decrease does not depend on Atg16l1-mediated autophagy

After depriving ModeK WT and *Atg16l1* KO cells of Trp for 24, they were stimulated with DMXAA [100 µg/mL].

(A) After a stimulation time of 2 h, cells were lysed and analyzed by WB. Image is representative of three independent experiments ($n = 3$).

(B) Cells were stimulated for 3 h before RNA extraction and investigation by qPCR. Data are presented as mean \pm SEM normalized to WT Trp+ Ctrl of three independent experiments, respectively ($n = 3$). * $p \leq 0.05$; ** $p \leq 0.01$

As expected, DMXAA-stimulated *Atg16l1* KO cells exhibited an increase in both pSTING and pTBK1 compared to WT controls even under Trp starvation conditions (Figure 3.17A). This, however, is not reflected by increased Cxcl10 expression. Interestingly, even *Atg16l1* KO cells cultured with Trp had a decreased Cxcl10 response compared to WT cells (Figure 3.17B).

The dependence of Trp starvation-mediated STING decrease on autophagy was further investigated by inhibiting the GCN2 pathway to prevent sensing of the Trp shortage. Therefore, cells were transfected with siRNA against Eif2αk4 (gene encoding GCN2) and 24 h later starved of Trp. Additional 24 h later, cells were stimulated with DMXAA (Figure 3.18).

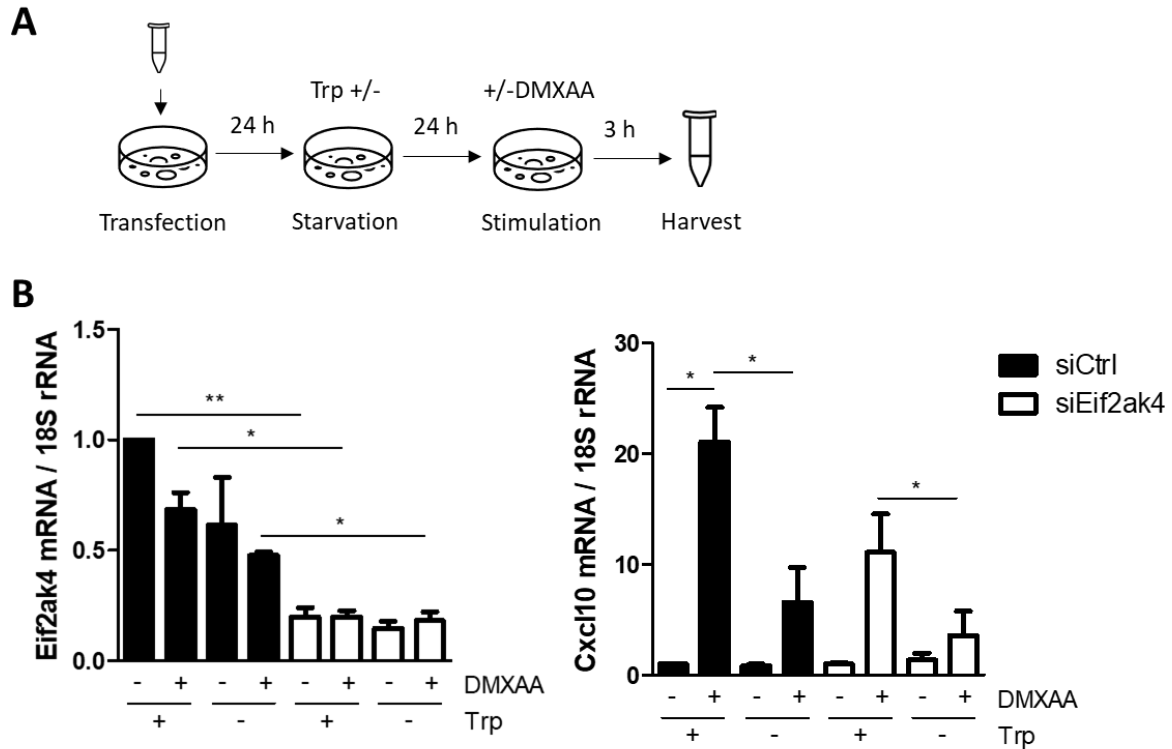


Figure 3.18 Trp starvation-induced STING loss is independent of Gcn2-mediated autophagy

(A) ModeK WT cells were transfected with siRNA against Eif2ak4 for 24 h. The medium was changed to +/- Trp and 24 h later, cells were stimulated with DMXAA [100 µg/mL] for 3 h and then harvested for RNA extraction. (B) Cells were treated as depicted in (A) and analyzed by qPCR for target gene expression. Data are presented as mean ± SEM normalized to Trp+ Ctrl of three independent experiments ($n = 3$). $*p \leq 0.05$; $**p \leq 0.01$

The successful KD of *Eif2ak4* was confirmed by qPCR analysis. The abrogated GCN2 pathway did not rescue Cxcl10 induction upon DMXAA treatment in cells cultured without Trp (Figure 3.18).

3.10 Trp starvation does not affect STING via ER stress

Several publications have reported on an effect of oxidative stress on STING that includes post-translational modifications rendering STING unfunctional (Jia et al., 2020; Zamorano Cuervo et al., 2021). It was thus speculated that Trp starvation may induce cellular stress that impacts on STING. First, the potential upregulation of stress markers upon Trp starvation was determined by qPCR. The impact of stress on the Trp pathway was further investigated by using iXBP1 cells as a model of chronic ER stress that further enables translational research given that *XBP1* variants have been associated with human IBD (Kaser et al., 2008). The demand for Trp by stressed cells was assessed by measuring the Trp consumption rate in cell supernatants (Figure 3.19).

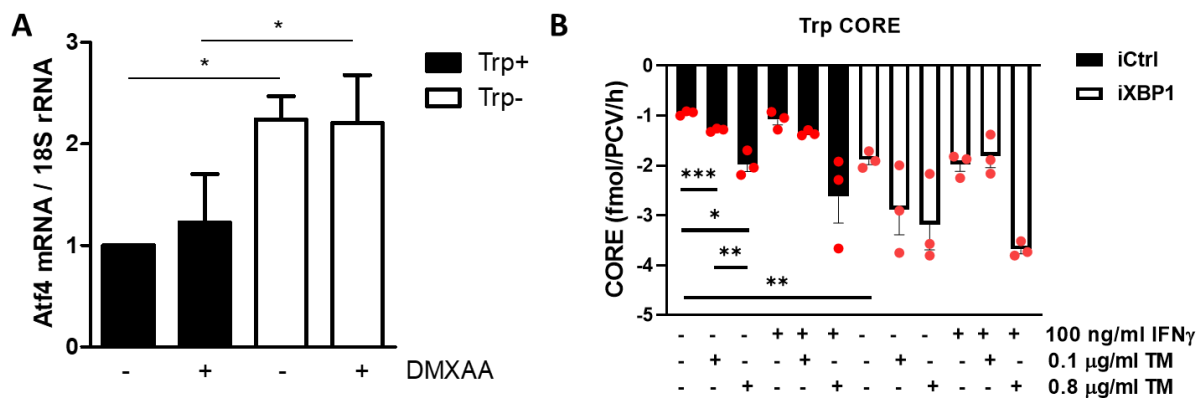


Figure 3.19 Cellular stress and Trp starvation positively correlate

(A) ModeK WT cells were cultured without Trp for 24 h and then analyzed by qPCR. Data are presented as mean \pm SEM normalized to Trp+ Ctrl of four independent experiments, respectively ($n = 4$). $*p \leq 0.05$; $**p \leq 0.01$.

(B) ModeK iCtrl and iXBP1 cells were treated with tunicamycin (TM) or IFN γ for 24 h. The Trp CORE in the cell culture supernatants were determined by GC-MS. Data are presented as mean \pm SEM of three independent experiments ($n = 3$). $*p \leq 0.05$, $**p \leq 0.01$, $***p \leq 0.001$. Data were obtained in collaboration with Dr. Björn Becker (LIH, Luxembourg).

Trp starvation led to an increase in the stress marker Atf4 in WT cells (Figure 3.19A). Induction of cellular stress by tunicamycin (TM) treatment or *XBP1* deficiency led to an increased Trp consumption rate (Figure 3.19B).

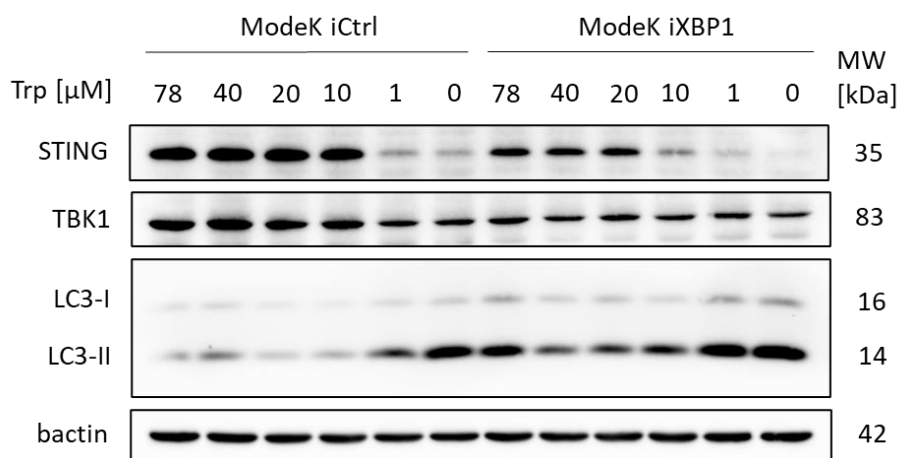


Figure 3.20 ER-stressed cells are more sensitive to Trp reduction

ModeK iCtrl and iXBP1 cells were cultured with various Trp concentrations [78 – 0 μ M] for 24 h and then analyzed by WB.

Image is representative of three independent experiments ($n = 3$).

Chronically stressed iXBP1 cells had reduced STING protein levels compared to iCtrl cells under baseline conditions. They also seemed to be more sensitive to Trp reduction as they started to lose STING when Trp was reduced to 10 μ M, whereas the decrease in control cells is only visible when cultured with 1 μ M Trp or lower (Figure 3.20).

The functional response of the STING pathway to DMXAA stimulation was assessed in both iCtrl and iXBP1 cells cultured with or without Trp (Figure 3.21)

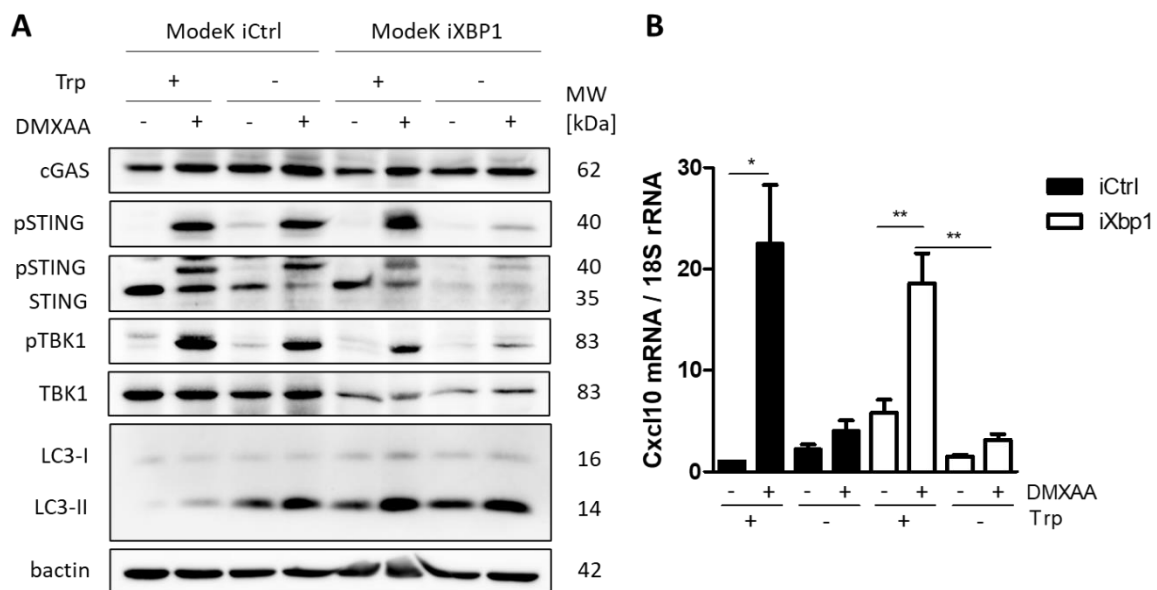


Figure 3.21 ER-stressed cells are more sensitive to Trp starvation

After depriving ModeK iCtrl and iXBP1 cells for Trp for 24, they were stimulated with DMXAA [100 µg/mL]. (A) After a stimulation time of 2 h, cells were lysed and analyzed by WB. Image is representative of three independent experiments ($n = 3$).

(B) Cells were stimulated for 3 h before RNA extraction and investigation by qPCR. Data are presented as mean \pm SEM normalized to iCtrl Trp+ of three independent experiments ($n = 3$).

ModeK iXBP1 cells had lower STING levels than iCtrl cells under Trp-containing conditions, and even lower under Trp starvation conditions. Likewise, their ability to phosphorylate TBK1 was reduced as well. However, Cxcl10 expression in iXBP1 cells in response to DMXAA treatment differed only slightly from controls (Figure 3.21).

Since there is an association between Trp and intracellular stress, it was speculated that Trp starvation may lead to an increase in reactive oxygen species (ROS) which then impairs STING response. Therefore, the ROS scavenger NAC was used to rescue a potential induction of oxidative stress (Figure 3.22).

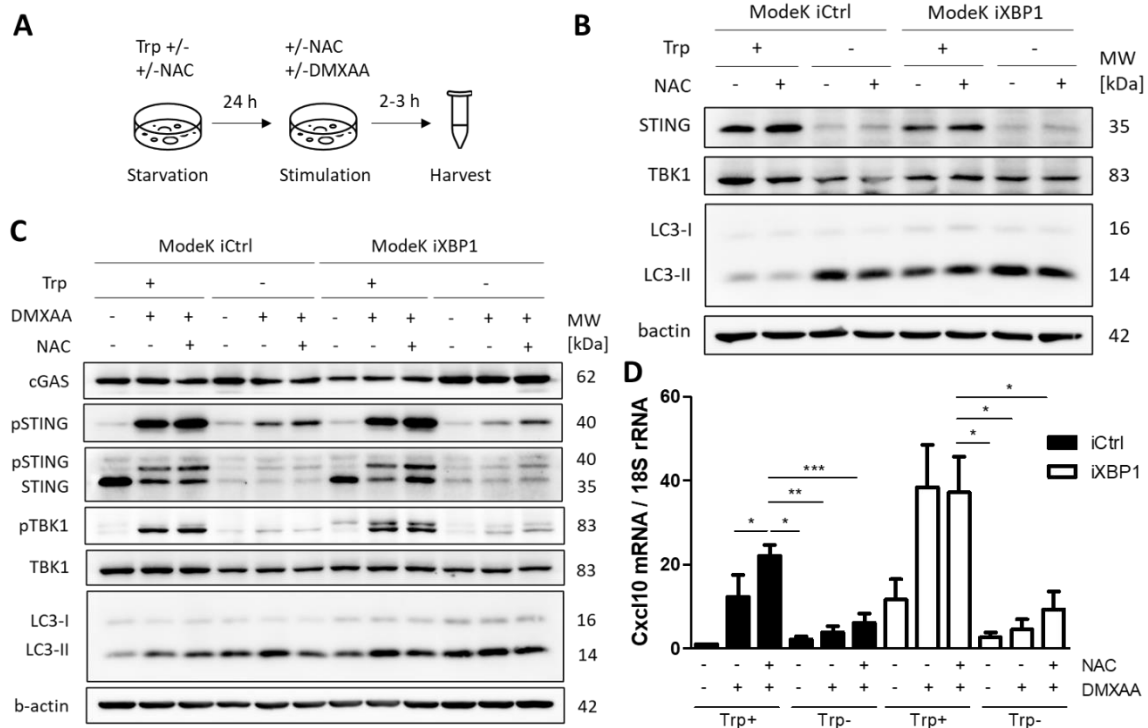


Figure 3.22 The impaired STING response under Trp starvation is independent of oxidative stress

ModeK iCtrl and iXBP1 cells were cultured with or without Trp and supplemented with 5 mM NAC for 24 h. Cells were then stimulated with 100 μ g/mL DMXAA and additional 5 mM NAC for (C) 2 h or (D) 3 h.

(A) Experimental setup.

(B) Image is representative of two independent experiments ($n = 2$).

(C) Image is representative of three independent experiments ($n = 3$).

(D) Data are presented as mean \pm SEM normalized to iCtrl Trp+ of three independent experiment with three technical replicates ($n = 3$).

NAC addition to either Trp-containing or non-containing medium influenced STING in neither iCtrl nor iXBP1 cell lines (Figure 3.22B). Neither was NAC supplementation able to significantly change DMXAA-induced STING response as shown by both WB and qPCR analysis (Figure 3.22C+D).

It is important to mention that NAC supplementation led to a drastically increased cell death in iXBP1 cells as observed under the microscope (Figure 3.23).

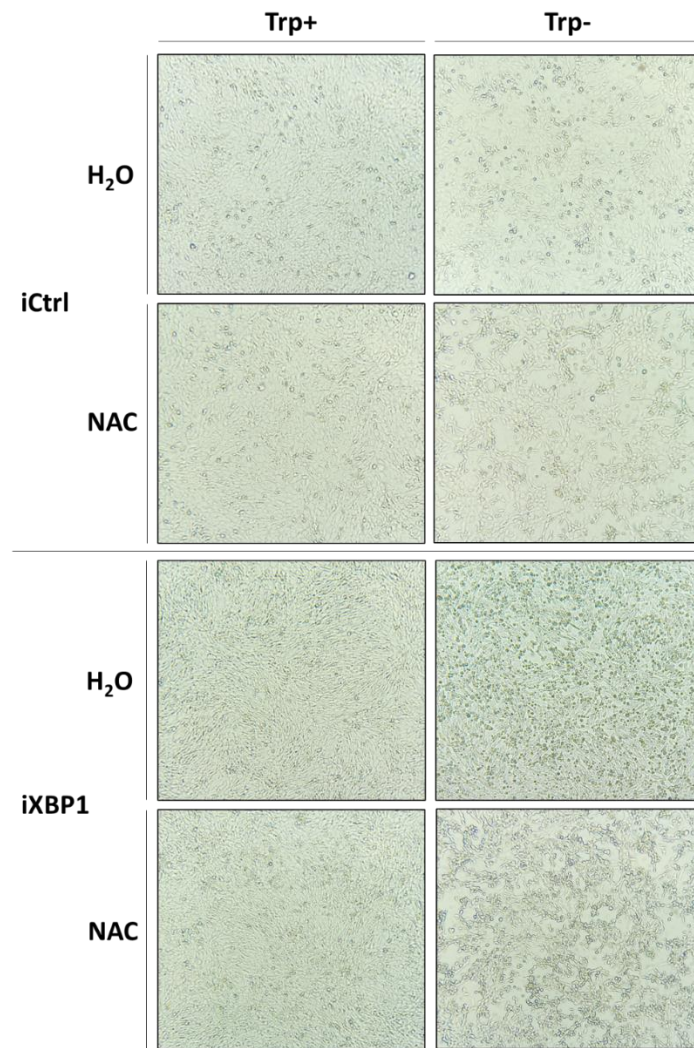


Figure 3.23 NAC supplementation increased the cell death in Trp-starved iXBP1 cells

ModeK iCtrl and iXBP1 cells were supplemented with 5 mM NAC at the onset of Trp starvation, and once more after 24 h together with DMXAA treatment as shown in Fig. 3.22A. Only DMXAA-negative controls are shown. Pictures were taken with a light microscope at 100x magnification.

This indicates that NAC supplementation does not provide benefit to stressed, Trp-starved cells.

3.11 Trp starvation decreases Tmem173 mRNA levels

It remains to be investigated whether Trp starvation influences STING on the transcriptional, translational, or post-translational level. Therefore, the Tmem173 mRNA expression pattern was analyzed under Trp starvation compared to the control condition.

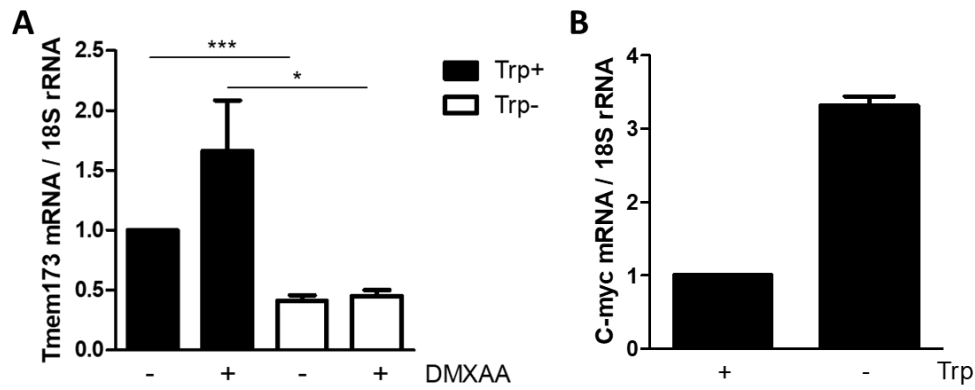


Figure 3.24 Trp starvation impacts on Tmem173 mRNA levels

(A) Tmem173 mRNA expression was determined in ModeK WT cells cultured with or without Trp for 24 h and subsequently stimulated with DMXAA for 3 h [100 μ g/mL]. Data are presented as mean \pm SEM normalized to Trp+ Ctrl of five independent experiments ($n = 5$).

(B) ModeK WT cells were starved of Trp for 24 h and then analyzed by qPCR for c-myc expression. Data are presented as mean \pm SEM normalized to Trp+ Ctrl of two independent experiments ($n = 2$).

Trp deprivation significantly decreased Tmem173 mRNA levels compared to the control (Figure 3.24). It has been reported that cellular Myc (c-myc) overexpression can increase STING (Wang et al., 2016), thus, c-myc expression was analyzed under Trp starvation. However, cells starved of Trp increased c-myc expression and yet decreased STING at both mRNA and protein level (Figure 3.24).

Another factor known to negatively influence Tmem173 RNA is the nuclear factor erythroid 2-related factor 2 (Nrf2) (Olagnier et al., 2018), which is a transcription factor with utmost importance in regulating the oxidative stress response (Olagnier et al., 2018; Sun et al., 2020). Since the oxidative stress comprises many pathways and molecules, NAC as added in previous experiments may only provide rescue under specific conditions. Thus, the Nrf2 pathway was investigated to test whether Trp starvation induces STING decrease by influencing Tmem173 mRNA stability via Nrf2. To do so, WT cells were first transfected with siRNA against Nfe2l2 (gene encoding Nrf2) and 24 h later starved of Trp. After another 24 h, cells were stimulated with DMXAA and then analyzed by qPCR (Figure 3.25).

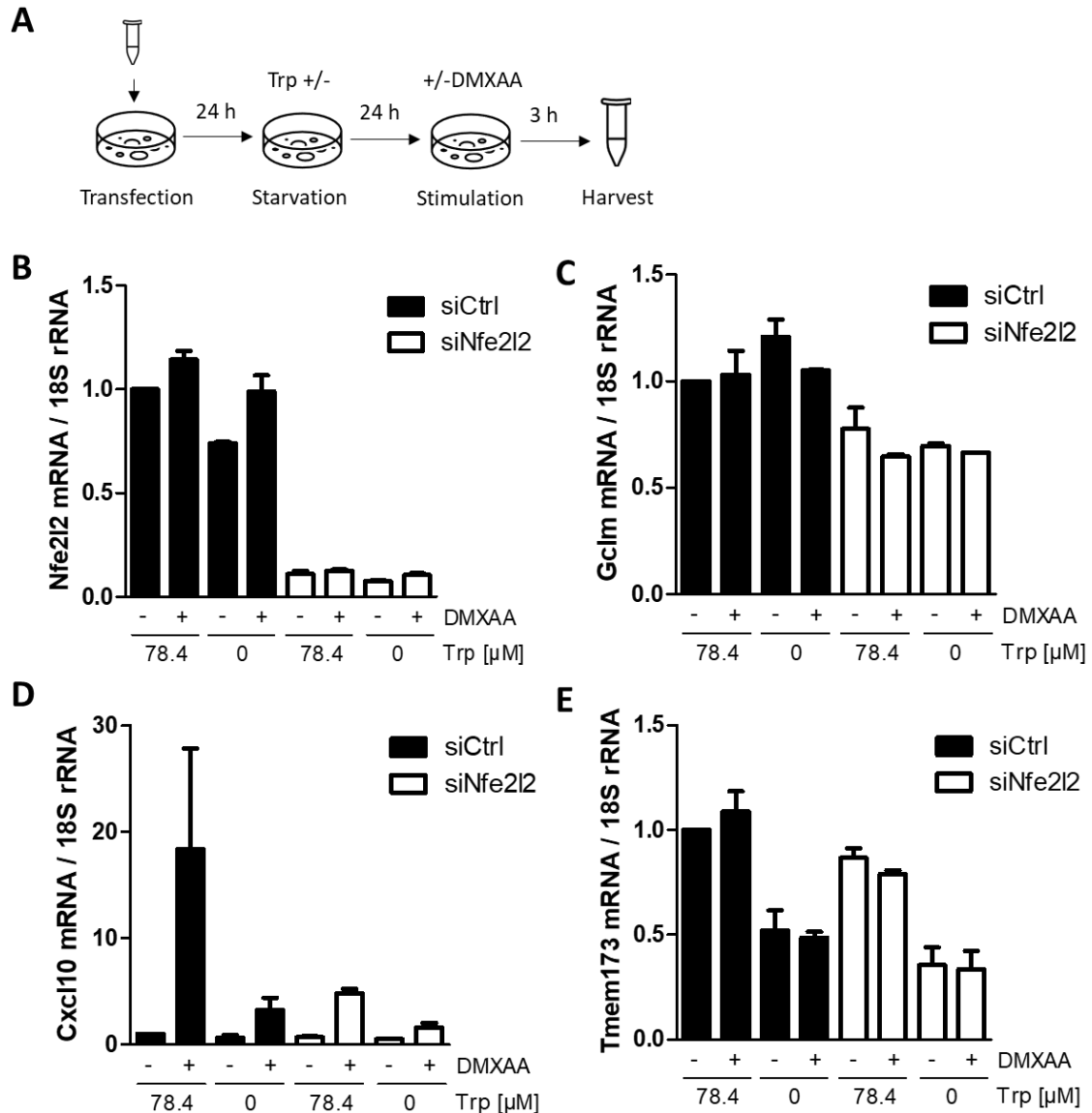


Figure 3.25 Trp starvation does not impair STING response via engaging Nrf2 pathway

ModeK WT cells were first transfected with Nfe2l2 siRNA for 24 h, then starved of Trp for 24 h, and subsequently stimulated with DMXAA for 3 h to then be analyzed for gene expression.

(A) Experimental setup.

(B) qPCR data are represented as mean \pm SEM normalized to Ctrl Trp+ of two independent experiments, each with three technical replicates ($n = 2$).

The successful KD of Nrf2 was confirmed by gene expression analysis of both *Nfe2l2* and the Nrf2-responsive gene glutamate-cysteine ligase modifier subunit (*Gclm*). Unexpectedly, abrogation of Nrf2 pathway also impaired Cxcl10 induction upon DMXAA treatment in Trp-containing cells and in this way also abolished the STING response in Trp-lacking cells (Figure 3.25). It will be intriguing to investigate the influence of other transcription factors on *Tmem173* under Trp starvation.

3.12 Trp starvation requires protein translation for STING degradation

Next, cycloheximide (CHX) treatment was used, which blocks the translation of proteins, to further shed light on the level at which Trp starvation affects STING (Figure 3.26).

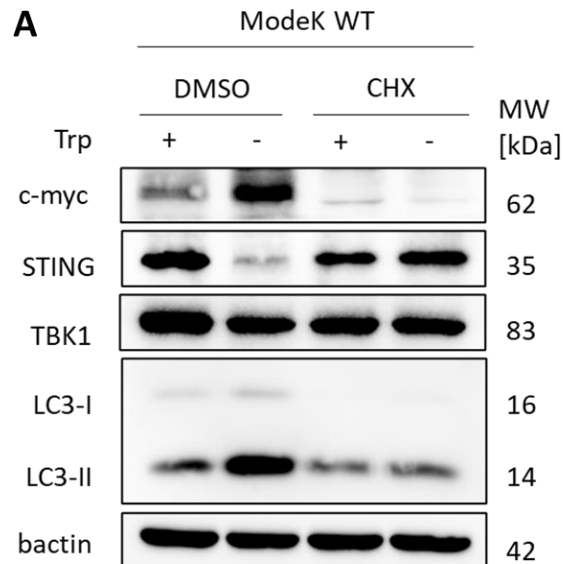


Figure 3.26 Trp starvation requires protein translation for STING degradation

(A) ModeK WT cells were cultured in either Trp-containing or non-containing medium and simultaneously treated with 50 $\mu\text{g}/\text{mL}$ CHX for 24 h. Image is representative of three independent experiments ($n = 3$).

CHX treatment successfully blocked protein translation as indicated by the loss of c-myc and LC3-I. STING was still detectable after 24 h treatment with CHX indicating that STING features a long half-life time. Interestingly, CHX reversed the Trp starvation-induced loss of STING (Figure 3.26). Together, these findings strongly support the idea that Trp starvation leads to the synthesis of a factor which is required for STING degradation.

4. Discussion

4.1 Trp levels are decreased in the inflamed intestinal epithelium

The study by Nikolaus et al. (2017) found that serum Trp levels negatively correlated with both the inflammatory status and disease activity of IBD patients, and low serum Trp seemed to be a potential biomarker to indicate the need for surgery. The Kyn/Trp ratio is increased in IBD compared to the control, and line with this, the expression of *IDO1* was upregulated in biopsies of active disease patients compared to healthy controls and points towards an increased Trp catabolism. Further downstream, the metabolite QA was increased in both UC and CD, whereas both picolinic acid (PIC) and kynurenic acid (KYA) were diminished in CD only. Significant differences in the dietary intake of Trp between inactive and active disease patients were excluded, but the reduced expression of the transporter solute carrier family 6 member 19/system B(0) neutral amino acid transporter 1 (*SLC6A19/BOAT1*) may hint at an impaired intestinal absorption of Trp (Nikolaus et al., 2017).

The fecal metabolite composition was investigated by Bosch et al. (2018) who have analyzed the AA contents of pediatric IBD patients compared to healthy controls regarding their informative value as diagnostic biomarkers. The IBD patients featured elevated levels of Trp, Phe, leucine, Tyr, valine, and histidine. These AAs correlated with IBD diagnosis to some extent, but not with disease activity. Their observation that UC patients had higher fecal AA levels than CD patients, made it possible to hypothesize that colonic leakage may play a bigger role in the AA loss than an impaired uptake in the SI (Bosch et al., 2018).

While the previously mentioned reports have focused on measuring serum or stool Trp levels, it remained unclear whether the availability of Trp is also altered in the intestinal mucosa itself. This question was addressed by an analysis of transcriptomic data from two different cohorts of IBD patients and controls (Zeissig et al., 2019; Schreiber et al., 2021). Upregulation of *WARS1* transcription, the gene encoding tryptophanyl-tRNA synthase, was taken as a proxy for low mucosal Trp levels. Indeed, *WARS1* expression of the intestinal mucosa was upregulated in active IBD patients and also negatively correlated with serum Trp levels, indicating that the intestinal mucosa experiences a drop in Trp as well (Figure 3.1).

4.2 Trp starvation sensitizes cells to NF- κ B activation

The hypothesis was raised that a reduction in mucosal Trp leads to an immunocompromised state in which the increased microbial burden cannot be cleared and thus resolution of inflammation cannot be initiated. In order to get an insight into the underlying mechanisms, it is necessary to translate the clinical findings into an *in vitro* model. Therefore, a cell culture model was established in which the murine SI cell line ModeK was cultured in specific Trp-lacking or Trp-containing control medium (Figure 3.2).

The general correlation of reduced Trp levels and an increased inflammatory state tempted to screen the cellular response to different immunologic stimuli after Trp starvation. The cells cultured without Trp for 24 h showed a markedly increased response to both LPS and IL-1 β compared to control cells as Cxcl10, Cxcl1, and IL-6 mRNA expressions increased (Figure 3.3). WB analysis of pI κ B α confirmed the activation of NF- κ B (Figure 3.3G).

Trp starvation significantly upregulated IL-6 transcripts in response to IL-1 β and, although not significant, did so even without additional stimulation (Figure 3.3). A relationship between Trp and IL-6 was already observed in 1993 when Maes and colleagues described that patients with major depressions were found to have reduced Trp plasma levels compared to healthy control subjects, similar to the aforementioned negative correlation of serum Trp to IBD disease activity, and Trp further negatively correlated with IL-6 levels. IL-6, which is increased upon NF- κ B activation, can induce IDO1 via the JAK/STAT pathway to catabolize Trp to Kyn and in this way may also reduce 5-HT levels. Kyn, in turn, can cross the blood-brain barrier (BBB) where it can be further metabolized to KYA and QA both of which are known for their neuroregulatory functions. Thus, it is tempting to speculate that the reduction in Trp stems from an increased Trp turnover under this inflammatory condition (Maes et al., 1993; Anderson et al., 2013). However, a diet containing half of the Trp concentration than recommended led to an upregulation of both IL-6 and IL-1 α in aged mice (Yusufu et al., 2021). This challenges the hypothesis of an overactivated Trp metabolism and again fuels the discussion whether Trp deprivation is a cause or consequence of inflammation.

Current research mainly focuses on Trp supplementation rather than starvation, which may be compared to the present study as a logical reverse. While the results presented here show a potentiated NF- κ B activation upon Trp deprivation, other studies reported that Trp supplementation alleviated LPS-induced inflammation. In an investigation, rats were fed a diet supplemented with either 0 %, 0.2 %, or 0.4 % Trp for 35 days and were then intraperitoneally injected with 100 μ g/kg LPS and slaughtered 4 h later. Analysis of the ileal tissue revealed that 0.2 % or 0.4 % Trp supplementation was able to decrease the concentrations of the LPS-induced inflammatory cytokines TNF- α , IL-1 β , IL-6, and IL-8, and increased IL-10 concentration. As Trp and some of its derivatives have been attributed with

antioxidant properties, they further investigated the expression of ER stress markers and apoptosis-related genes. Trp supplementation led to a decrease of GRP78, ATF6, caspase-1 and -3, and NLR family pyrin domain containing 3 (NLRP3) expression in response to LPS challenge compared to LPS-injected without additional Trp (Liu et al., 2022). In another study, mice were fed 200 mg/kg Trp for a period of 14 days and were subsequently intraperitoneally injected with 10 mg/kg LPS for 6 h. Both the inflammation and its associated damage was alleviated in the Trp-receiving group compared to the control. Mechanistically, cells isolated from a pig's jejunum required functional calcium-sensing receptor (CaSR) activation to induce β -defensin expression in response to Trp supplementation. This regulation was mediated via the AMP-activated protein kinase (AMPK) and JNK pathways by the Trp metabolites Kyn and 5-HT; and Trp supplementation also led to a decrease in NF- κ B pathway activity (Gao et al., 2021). This is in agreement with a previous investigation that used a Caco2 cell monolayer model incubated with different Trp concentrations and also induced epithelial damage via LPS treatment. LPS downregulated the expression of the tight junction proteins claudin-1, occludin, and zonula occludens-1 (ZO-1), but upregulated NF- κ B expression. While the high Trp concentration [80 μ M] could not rescue LPS-mediated inflammatory damage, low [20 μ M] and medium [40 μ M] concentrations of Trp successfully ameliorated the barrier integrity as they inhibited the NF- κ B pathway but activated the ERK1/2-MAP pathway. All Trp concentrations tested restored claudin-1 expression levels (Chen et al., 2019).

Further research is required to determine whether the elevated NF- κ B response under Trp starvation would alleviate or exacerbate colitis since the activation of NF- κ B plays a dual role in inflammation. A study on murine colitis demonstrated that the effect of NF- κ B activation is dependent on the timing and cell type. Whereas the inhibition of epithelial NF- κ B activation did not influence the severity of chronic inflammation, it was detrimental in acute DSS-mediated inflammation (Eckmann et al., 2008). Moreover, the occurrence of spontaneous colitis in *IL-10* KO mice as a model of chronic colitis showed opposing roles of NF- κ B in myeloid cells and in IECs: the deletion of IKK β in myeloid cells, but not in IECs, alleviated inflammation. NF- κ B might mediate its protective effects via protection against apoptosis and presumably via increasing the amount of infiltrating immune cells and the consequent secretion of mediators of barrier protection and tissue healing (Eckmann et al., 2008). These results highlight the dual function of the NF- κ B pathway in the gut mucosa where it contributes to both inflammation and mucosal healing. Therefore, careful evaluation of the circumstances is necessary prior to targeting the NF- κ B pathway in the treatment of IBD.

4.3 Trp starvation impairs the cGAS/STING response

The immunocompetence of Trp-starved cells was assessed by IFN stimulation, which showed that, compared to controls, the response of Trp-starved cells to IFNs is compromised as Cxcl10 levels were reduced (Figure 3.4). A pathway that leads to the production of IFN I is the cGAS/STING pathway, thus, it was tempting to specifically investigate the impact of Trp starvation on STING. Moreover, while it is known that activation of the cGAS/STING pathway can engage IDO to promote tolerance to the commensals (Chen et al., 2016), information on how Trp, in turn, influences the STING pathway is scarce.

ModeK WT cells and murine SI organoids both experienced a striking reduction in STING levels when cultured with either low or no Trp, whereas TBK1 levels remained unchanged (Figure 3.5). The advantage of intestinal organoids is that they provide a tool to investigate the mixture of differentiated cell types including enterocytes, goblet cells, Paneth cells, and enteroendocrine cells (Bartfeld, 2016). In future experiments, it may be interesting to differentiate organoids towards a specific cell type to allow for a more detailed investigation of the significance of Trp for the STING pathway. Since both ModeK cells and organoids exhibited the same phenotype, the mechanism by which Trp starvation affects STING is likely to be rather generally valid in the murine intestinal tissue. Possible mechanisms may comprise an activation of STING together with the failure to replenish its levels, degradation of STING as a recycling approach to generate energy and protein building blocks, or a rather direct inhibition of STING by either acting on the transcriptional or translational level.

For instance, starvation of arginine has been shown to trigger cGAS/STING activation in a prostate cancer cell line. Here, arginine starvation induced a leakage of nuclear DNA into the cytosol because of impaired OXPHOS, which led to increased ROS levels and genomic damage. Arginine starvation suppressed DNA repair enzymes and triggered excessive autophagy. Increased removal of broken nuclear membranes and elevated leakage of nuclear DNA led to an activation of the cGAS/STING pathway (Hsu et al., 2021). It was thus hypothesized that Trp starvation may activate STING by a similar mechanism. The enzyme TBK1 is responsible for STING phosphorylation leading to STING activation and its degradation soon after (Chen et al., 2016). The reduction of STING in response to Trp starvation, however, was independent of TBK1 (Figure 3.6). The functional response under Trp starvation will be discussed next to determine the relevance of the STING decrease.

The loss of STING raises the hypothesis that cells lacking Trp are immunocompromised. Therefore, the functional response of STING to DMXAA was assessed next. The flavonoid DMXAA is a direct agonist of murine STING only (Wu et al., 2020). Indeed, the ability of Trp-deprived cells to phosphorylate both STING and TBK1, and to mount a Cxcl10 or $I\text{fn}\beta$ response upon DMXAA stimulation was compromised (Figure 3.7). The effect of DMXAA was validated by activating STING with cGAMP transfection, whereby

2'3'-cGAMP represents the second messenger endogenously generated by cGAS and 3'3'-cGAMP is of exogenous source such as bacteria (Wu et al., 2020). Additionally, cells were transfected with dsDNA that will be processed by cGAS and is thus suitable to investigate the whole cGAS/STING pathway (Wu et al., 2020). Consistently, Trp starvation led to an impaired STING response when stimulated with either dsDNA, 2'3' cGAMP, or 3'3' cGAMP (Figure 3.8).

It remains to be investigated whether a reduction in both Trp and STING correlate in a multicellular organism. As opposed to our experimental setup, the supplementation of Trp or its metabolites has been investigated in murine colitis models. The administration of Trp was shown to alleviate DSS colitis in mice via signaling through AhR (Islam et al., 2017), and administration of Kyn to 2,4,6-trinitrobenzene sulfonic acid (TNBS)-challenged mice upregulated the Treg population and thereby repressed inflammation (Tashita et al., 2020). In DSS-challenged piglets, Trp supplementation has markedly reduced the induction of the pro-inflammatory cytokines IFN- γ , TNF- α , IL-1 β , and IL-6 and thereby reduced inflammation (Kim et al., 2010). It is thus tempting to speculate that Trp starvation in turn would exacerbate colitis. In line with this, Hashimoto et al. (2012) have shown that a Trp-free diet fed to mice led to an enhanced susceptibility to DSS colitis without elucidating the exact mechanism. On the one hand, the loss of STING may be harmful as *Tmem173* KO in mice resulted in enhanced susceptibility to DSS colitis. On the other hand, *Tmem173* and *IL-10* double KO resulted in protection against exacerbated inflammation (Ahn et al., 2017). Considering the augmented NF- κ B response of Trp-deprived cells, it will be intriguing to perform infection experiments with different types of pathogens in order to understand the impact of Trp starvation on the immunocompetence. The comparison of Trp-starved mice to STING ^{Δ IEC} mice could reveal whether Trp starvation mediates its effects mainly via impairing STING. Little is known about the crosstalk between the TLR4 and cGAS/STING pathways, but it was reported that STING activation primed bone marrow-derived dendritic cells (BMDCs) to enhance IFN response after LPS treatment (Tesser et al., 2021). In contrast, STING inhibition in BMDCs or *Tmem173* KO in bone marrow-derived macrophages (BMDMs) did not affect the response to LPS, suggesting that the two pathways synergize on the TBK1 level which, however, does not depend on STING (Ishikawa and Barber, 2008; Tesser et al., 2021).

Some bacteria are Trp auxotrophs (Agus et al., 2018; Palego et al., 2016) and in this way will not be affected by Trp shortage itself, but rather by the metabolites arising from an increased Trp catabolism. As such, augmented IDO activity was found to inhibit the growth of *Toxoplasma gondii* via Kyn-induced apoptosis (Pfefferkorn, 1984; Majumdar et al., 2019). On the other hand, IDO induction via cGAS/STING in dendritic cells (DCs) can also promote tolerogenic responses of Tregs depending on the circumstances (Huang et al., 2013). Moreover, the intracellular pathogen *Listeria monocytogenes* even uses the IFN response to favor its growth. Mice with an abrogated IFN response were less susceptible

to *L. monocytogenes* infection (Auerbuch et al., 2004; O`Connell et al., 2004), whereas IFNs are known to be essential to fight viral infections (Decker et al., 2002). Thus, the concrete consequence elicited by Trp starvation is likely dependent on the type of prevailing pathogen as well as the duration of the infection. Given this importance of both Trp and cGAS/STING in IBD, further experiments were conducted to shed light on the underlying mechanism by which Trp affects STING.

4.4 Replenishing Trp restores STING after starvation

With regard to a clinical phenotype, it was important to assess whether the effect of Trp starvation on STING was reversible or irreversible. Restoring Trp availability for uptake after its starvation reconstituted the STING expression (Figure 3.9), indicating that the phenotype is reversible.

Next, the contribution of Trp versus its derivatives on STING protein levels was assessed. Trp metabolites have become a great focus of attention in different settings. The commonly accepted depletion hypothesis during infection had to be revised since prokaryotes are capable of Trp synthesis, therefore Trp depletion alone is unlikely to protect against pathogens. Indeed, it is more likely that the formed Kyn metabolites and NAD⁺ confer protection against pathogens (Badawy, 2017). Although the classification of metabolites into either protective or toxic for the cell is not straight-forward but rather depends on the dose, general associations have been made. Particularly the AhR ligands, including Kyn, KYA, xanthurenic acid, and cinnabarinic acid, are known to modulate inflammatory reactions towards induction of resolution or immune tolerance. KYA further exerts antioxidant functions and PIC as well features immunomodulatory properties via chelating metals such as Cu, Ni, and Pb. On the contrary, the metabolites 3-HK, 3-hydroxyanthranilic acid (3-HAA), and QA can generate ROS and thus have been attributed to elicit damaging effects. The final metabolite NAD⁺ is key to mitochondrial ATP production and thus cell viability (Török et al., 2020; Tanaka et al., 2021).

The addition of L-Kyn [50 µM] to Trp-depleted medium did not maintain STING levels as compared to dimethyl sulfoxide (DMSO) controls, and supplementation of L-Kyn to Trp-containing control medium also did not affect STING protein levels as detected with WB (Figure 3.10). This leads to the conclusion that Trp itself rather than its Kyn derivatives is required for the cell to maintain STING expression. These results match the expectation because enterocytes do not metabolize Trp along the KP under basal conditions as IDO only is induced in inflammatory settings (Badawy, 2017). Nevertheless, it was important to exclude the contribution of Kyn in this setting to keep the focus on Trp.

4.5 Trp starvation does not affect cellular ATP levels

Metabolic remodeling has been extensively investigated in the field of cancer research (Eleftheriadis et al., 2014). With regard to starvation studies, cancer cells deprived of serine were found to have suppressed aerobic glycolysis activity along with an increased flux to the TCA cycle and consequently reduced ATP levels. Nevertheless, cell survival was assured by activation of tumor protein (p53) and arrest in the G1 cell cycle (Maddocks et al., 2013). Therefore, when studying immunocompromised settings and/or starvation, it is of utmost importance to assess the metabolic state and in particular the energy state of the cell to exclude indirect effects arising from a general lack of energy. The metabolic activity and the energy levels of Trp-starved cells compared to the control were measured by means of a [U-¹³C] glucose tracing (Figures 3.11-3.13). When interpreting the tracing data, it is important to keep in mind that the starvation and tracing was performed simultaneously for a duration of 24 h, whereas in most other applications a pre-starvation of 24 h was performed. Trp-deprived cells did not show elevated lactate labeling (Figure 3.11G) which means that Trp starvation does not lead to a Warburg effect. The labeling of pyruvate was slightly reduced in Trp-deprived cells compared to controls, as well as of the TCA cycle intermediates citrate, α -KG, succinate, and malate. Consequently, TCA cycle activity was found to be reduced under Trp starvation (Figure 3.12), which indicates that the cell may exhibit less recourses to generate ATP. Thus, the relative ATP labeling was measured to assess the overall energy state of the cell, showing that cells lacking Trp did not exhibit reduced AMP, ADP, or ATP labeling (Figure 3.13). MTS assay results indicated that both the mitochondrial activity and cell proliferation were reduced under Trp starvation (Figure 3.2B). Taken together, it is plausible that ModeK cells lacking Trp enter the quiescent cell cycle state and therefore require less ATP, whereas cells with Trp available for uptake keep on proliferating. This leads to the assumption that decreased ATP consumption balances out a possibly decreased ATP synthesis so that the overall energy state may remain equal between the two groups.

The role of Trp in metabolism has so far been addressed indirectly by focusing on the effect of IDO. In mixed-lymphocyte reactions of T cells, activated IDO engaged GCN2 and p53 to decrease glycolysis and further led to a cell cycle arrest mediated by p21. This may ensure optimal ATP generation despite the lack of Trp as the reduced levels of pyruvate are shuttled into the TCA cycle rather than being converted to lactate. IDO further blocked the synthesis of lipids and AAs, and thus inhibited the synthesis of molecules important for cell proliferation to save energy (Eleftheriadis et al., 2014). Nevertheless, the IDO-induced Trp deprivation is not directly comparable to the model presented in this project that uses Trp-free cell culture medium in which IDO is not activated. Despite the differences in cell types and methods, this study agrees with our hypothesis that Trp starvation leads to a proliferation arrest and the therefore reduced energy demand balances out a possibly decreased energy generation. It will

nevertheless be worthwhile to determine mitochondrial ATP production in cells cultured in the absence or presence of Trp to shed light on the impact of Trp starvation on mitochondrial homeostasis. Whereas most research on intracellular Trp has concentrated on the cytoplasmic Trp levels, little is known about the free Trp concentrations inside the mitochondria and to what extent these levels are reduced under Trp starvation. However, Trp depletion caused by IFN γ -induced IDO1 activity was shown to only upregulate the cytoplasmic WARS1 expression without influencing WARS2 which binds mitochondrial tRNA_{Trp} (Adam et al., 2018).

The energy state of Trp-deprived cells was again verified indirectly with NAM supplementation, which is a precursor of NAD⁺. On top of serving as a signaling molecule, NAD⁺ as the final metabolite of the KP also generates energy for the cell (Navarro et al., 2021). Even though the amount of NAM synthesized in IECs at baseline may be scarce, NAM supplementation to Trp-lacking cells may generate an insight into the cellular energy state. As expected from ATP labeling, NAM supplementation did not restore STING levels in Trp-starved cells. NAM treatment even impaired the Cxcl10 expression in response to DMXAA in Trp-containing cells (Figure 3.14), conforming with previous publications. In a study on whole human blood stimulated with endotoxin [1 ng/mL] (the concentration represents septic patients), supplementation with NAM inhibited the cytokine response in a dose-dependent manner. NAM at 40 mmol/L nearly completely abolished the secretion of the pro-inflammatory cytokines IL-1 β , IL-6, and TNF α , and, to a lesser extent, IL-8 (Ungerstedt et al., 2003). The connection between NAD⁺ and the cGAS/STING pathway has been investigated in a mouse model of Alzheimer's disease (AD). The APP/PS1 mutant transgenic mice had elevated levels of cytoplasmic DNA which were reduced after nicotinamide riboside (NR) treatment, a precursor of NAD⁺. NR likely exerted its protective functions via induction of mitophagy and via improving double-strand break repair mechanisms. This, in turn, also decreased the activation of the cGAS/STING pathway. Furthermore, NR also reduced STING protein levels in 12 months old AD mice (Hou et al., 2021). This finding confirms the results presented in this project showing that both the lack of Trp and the Trp metabolite NAD⁺ have suppressive functions on the cGAS/SITNG pathway. The correction of the cellular energy state during Trp starvation therefore requires supplementation with another energy source. These findings indicate that analyzing the energy state of Trp-starved cells is complex and may require additional approaches other than supplementing NAD⁺ precursors due to the ambivalent effects of NAD⁺ in the setting.

4.6 Inhibition of autophagy does not restore STING levels under Trp starvation

AA depletion is sensed via GCN2, a protein crucially involved in coordinating the integrated stress response. Activation of this pathway results in a global translational arrest after phosphorylation of eIF2 α , and induction of autophagy (Wek et al., 1989; Dever et al., 1992; Wek et al., 1995).

Since STING is regularly degraded by autophagy after its activation (Saitoh et al., 2009; Prabakaran et al., 2018), it was hypothesized that the induction of autophagy in response to AA depletion leads to STING degradation. First, the effects of autophagy induction by different stimuli were compared to assess whether STING loss is a general phenomenon mediated by excessive autophagy. Surprisingly, only Trp starvation lowered STING protein levels, as neither complete starvation in HBSS nor rapamycin treatment had a significant effect on STING and serum starvation even led to an increase in STING (Figure 3.15). It therefore is possible that the decrease in STING is not a general mechanism elicited by the cell to either save energy or to recycle protein building blocks, but rather a direct process specifically induced by Trp starvation. To further study whether the Trp starvation-mediated STING loss is dependent on autophagy, we created a KO of the CD risk gene *Atg16l1* in ModeK cells using a CRISPR/Cas9-based system.

Atg16l1 KO ModeK cells exhibited strikingly elevated STING levels at baseline conditions compared to WT controls, presumably because STING turnover by autophagy is inhibited. However, even though STING accumulated when Trp was available for uptake, *Atg16l1* KO cells also showed lower STING levels when cultured without Trp (Figure 3.16). In order to investigate the functionality of the accumulated STING, we stimulated cells with DMXAA in the presence and absence of Trp. Interestingly, although *Atg16l1* KO cells responded to DMXAA stimulation with markedly higher pSTING and pTBK1 levels than WT cells, this was not reflected in Cxcl10 mRNA levels. The cytokine response of *Atg16l1* KO cells compared to WT control cells was reduced when cells were cultured either in Trp-containing or Trp-free medium (Figure 3.17). This raises the assumption that *Atg16l1* may regulate the cytokine production downstream of TBK1 activation, and in the future, it will be interesting to further measure IRF3 activation. However, it seems as if Trp starvation does not engage the autophagic machinery to lower STING levels.

Autophagy-deficient mouse models have already been exploited, and although these mice have been more susceptible to DSS colitis, signs of spontaneous inflammation only occurred when both autophagy and the UPR were impaired in IECs (Haq et al., 2019). In line with this, boosting the autophagic response with pharmaceuticals such as rapamycin was shown to be beneficial in murine colitis (Haq et al., 2019). Other previous studies found autophagy-deficient IECs to be unaffected during steady state, but TNF- α treatment led to increased cell death, suggesting that autophagy protects against exacerbated inflammatory cell damage (Haq et al., 2019). In accordance, when

macrophages were treated with LPS, *Atg16l1* deficiency led to increased IL-1 β production compared to autophagy-competent controls. Likewise, a hematopoietic KO of *Atg16l1* rendered mice more susceptible to DSS-induced colitis owing to the elevated inflammatory state which could be alleviated by anti-IL-1 β and anti-IL-18 antibody injection (Saitoh et al., 2008). The stimulation of *Atg16l1* ^{Δ IEC} intestinal organoids with IL-22 augmented the IFN-I response via cGAS-STING-mediated sensing of dsDNA. This upregulation, however, was independent of STING levels as these were equally elevated in both *Atg16l1* ^{Δ IEC} and *Atg16l1*^{fl/fl} organoids upon IL-22 stimulation (Aden et al., 2018). In contrast, direct dsDNA stimulation of *Atg16l1*-deficient murine embryonic fibroblasts (MEFs) did not affect Irfn β production (Saitoh et al., 2009). Interestingly, the autophagic protein Atg9a was found to co-localize with STING after its activation by dsDNA in MEFs. Although loss of *Atg9a* did not influence the translocation of activated STING from the ER to the Golgi apparatus, the assembly of STING with TBK1 was markedly promoted which in turn resulted in augmented IRF3 phosphorylation and the subsequent transcription of the inflammatory mediators Irfn β , IL-6, and Cxcl10 (Saitoh et al., 2009).

This highlights how closely the STING pathway and the autophagic machinery are interrelated, hence, the involvement other autophagy-related proteins was tested. GCN2 was already shown to modulate intestinal inflammation (Ravindran et al., 2016), and a lack of the sensor GCN2 should abrogate the induction of autophagy resulting from AA depletion. However, repressing the GCN2 pathway by knocking down eukaryotic translation initiation factor 2 α kinase 4 (*Eif2ak4*) (encoding GCN2), did not restore DMXAA-mediated STING activation in Trp-deprived cells (Figure 3.18). This was surprising as GCN2-dependent sensing of AA deprivation has previously been shown to suppress inflammation in DSS-challenged mice on a low protein diet. Here, the protective effect was in part due to an impaired T_H17 response without affecting the T_H1 response and was dependent on ROS scavenging and autophagy (Ravindran et al., 2016). Reasons for this difference might be due to the duration of AA deprivation, and in the obvious inequality of the model complexity.

To sum it up, autophagy is unlikely to be the main mechanism by which Trp starvation leads to decreased STING protein levels, as a KO of neither *Atg16l1*, nor *Eif2ak4* could rescue the phenotype. Nevertheless, the KO of *Eif2ak4* also led to an increase in ROS in the study of Ravindran et al. (2016), leaving open the opportunity that increased ROS has impacted on STING in the present study. Indeed, the negative influence of oxidative stress on the STING pathway has been described previously (Zamorano Cuervo et al., 2021), and the correlation between Trp and cellular stress will be discussed next.

4.7 Trp starvation affects STING independent of oxidative stress

ROS refers to a diverse group of reactive molecules and comprise O_2^- , H_2O_2 , O, O_3 , hypohalous acids, and organic peroxides. The many cell functions they influence range from ageing, over cell death, to inflammation, whereby they can be both enhancing and alleviative. They are also produced under steady state from different sources as they are fundamental to cell signaling and feature an atomic specificity as they bind to atomic targets in macromolecules which allows for influencing many pathways simultaneously. ROS also participate in activating transcription. During intestinal inflammation, ROS can arise in high amounts and, on one hand, restrict microbial invasion, but on the other hand damage the epithelium. Low levels of ROS, instead, can suppress inflammation via preventing NF- κ B activation. The clinical importance of ROS is highlighted by the fact that ROS are either produced or scavenged by many medical drugs (Nathan and Cunningham-Bussel, 2013; Gusarov et al., 2021).

Oxidative damage can also impact on the cGAS/STING pathway as it can lead to oxidative posttranslational modifications of STING. Whereas reversible oxidation of human STING Cys¹⁴⁸ takes place under basal conditions but is required for subsequent 2'3'-cGAMP binding, oxidative stress or 2'3'-cGAMP stimulation of human STING can lead to its oxidation of Cys²⁰⁶ rendering it inactive and thus preventing hyperstimulation. STING that is oxidized at Cys²⁰⁶ undergoes a conformational change towards disulfide bonds-containing inactive polymers and it is assumed that this structurally hinders the binding of TBK1 and thus prevents STING phosphorylation at Ser³⁶⁶ (Zamorano Cuervo et al., 2021).

Antioxidative functions have been attributed to IDO because the enzyme uses O_2^- as cofactor and substrate, and because it initiates the metabolism of Trp along the KP. Of the Trp metabolites, especially 5-hydroxytryptophan (5HTrp), 3-HK, xanthurenic acid (XA), and 3-HAA were able to prevent oxidation of soybean phosphatidylcholine (PtdCho) liposomes in an *in vitro* experiment. As only hydroxylated Trp metabolites scavenged peroxy radicals, the antioxidant activity may be mediated by their phenolic moiety (Christen et al., 1990). However, with regard to the high concentration of other antioxidants, the extent to which these metabolites contribute to cellular defense mechanisms is yet unclear, also keeping in mind that the KP in extrahepatic tissue is only boosted under inflammatory conditions (Christen et al., 1990).

Thus, we hypothesized that Trp may be needed to protect the cell from oxidative damage, and that a lack of Trp likewise results in cellular stress. In ModeK cells, Trp deprivation led to an increase in Atf4 transcripts (Figure 3.19A), which indicates cellular stress and, more importantly, is part of the GCN2-peIF2 α -ATF4 axis to upregulate WARS (Adam et al., 2018). Further experiments were conducted with iXBP1 cells, which represent a model to study chronic ER stress and moreover are highly relevant for translational IBD research as genetic variants of *XBP1* have been associated with both CD and UC (Kaser

et al., 2008). Inducing cellular stress by TM or knocking down *Xbp1* resulted in a greater Trp uptake (Figure 3.19B). Considering that ER stress is enhanced in inflamed tissue (Kaser et al., 2008), it is surprising that the expression of the neutral AA transporter SLC6A19/BOAT1 by which Trp is taken up in the intestine was downregulated in both CD and UC patients (Nikolaus et al., 2017). This discrepancy to the here presented results maybe stems from the fact that they used colon biopsies to measure the gene expression. Further, iXBP1 cells were more susceptible to Trp reduction as a decrease in STING was observable when Trp was reduced to at least 10 μ M, compared to 1 μ M in iCtrl cells (Figure 3.20). iXBP1 cells had slightly elevated levels of Cxcl10 at baseline as compared to iCtrl cells. Under Trp control conditions, DMXAA-stimulated iXBP1 cells had a slightly diminished Cxcl10 mRNA expression than iCtrl cells, although not significant. Similar to iCtrl cells, DMXAA-induced STING response was compromised in iXBP1 cells under Trp starvation (Figure 3.21), which matches the expectation derived from the Trp titration experiment. It is published that a KO of *Xbp1* restricted to the intestinal epithelium worsened DSS colitis, increased ER stress, caused apoptosis of Paneth cells, and a state of hyperresponsiveness to TNF α and flagellin in IECs (Kaser et al., 2008). The different capabilities to mount an immune response may be found in the different types of stimuli used.

In order to indirectly assess a possible oxidative damage of STING elicited by Trp starvation, the ROS scavenger NAC was used. Inside the cell, NAC is converted to cysteine and ultimately leads to the synthesis of the antioxidant glutathione (GSH) (Niraula and Kim, 2019). A rescue approach using NAC supplementation failed to restore STING, or pSTING or Cxcl10 levels after DMXAA stimulation (Figure 3.22), indicating that Trp starvation does not lead to oxidative damage of STING. Thereby it is important to mention that adding NAC to the growth media leads to its acidification which in turn impacts on the organisms' health (Gusarov et al., 2021), and likewise led to an increased cell death in iXBP1 cells (Figure 3.23). It is therefore recommended to repeat these cell culture experiments with pH-adjusted NAC. When interpreting the results of the IFN response, it also is important to consider the effect NAC has on degradation pathways. Importantly, NAC can inhibit 26S proteasome function, which is responsible for degrading I κ B α that, in turn, releases NF- κ B. In this way, NAC treatment can result in I κ B α accumulation and consequently prevent NF- κ B activation (Pajonk et al., 2002). Based on this, NAC supplementation may partially have counteracted STING-mediated IFN response, even though the STING pathway mainly engages the TBK1-IRF3 axis and induces NF- κ B to a lesser extent (Chen et al., 2016). It therefore is necessary to validate these experiments with a different kind of ROS scavenger, and further it is advisable to directly measure ROS levels that may arise due to Trp deprivation.

A potential clinical translation of these *in vitro* findings must consider several aspects, which are mostly derived from animal models with a short life span: (1) A lifespan expansion by 3.8 % on average after administration of a NAC-supplemented diet [1 mg/mL] was found in an investigation using *Drosophila*

flies. This was limited to female flies which contrasts with a previous study and may be owing to differences in *Drosophila* strains. Common to both female and male flies, however, was the observation that a high dose of NAC [10 mg/mL] was toxic and even shortened the lifespan by 72 % in female and by 32 % in male flies. An explanation for the toxicity may be the elevated levels of the NAC derivative cysteine that is known to damage the kidney (Niraula and Kim, 2019). (2) Another study on *C. elegans* showed that dietary supplementation of NAC or the natural antioxidant GSH even accelerated the aging when administered chronically. Remarkably, also aged worms did not benefit from NAC supplementation that was started during their adulthood (Gusarov et al., 2021). (3) Likewise, chronic supplementation with antioxidants so far has almost always failed in long-term clinical trials one example being stroke-induced ischemia injury (reviewed in Schmidt et al., 2015). Since mitochondria are a key source of ROS, the detrimental effect of antioxidants may be related to the repressive effect they have on mitochondrial function. Moreover, antioxidants suppress cellular signaling cascades including those involved in stress resistance and homeostasis. Instead of supplementing, it may be advisable to restrict exogenous thiols in order to boost the cellular defense mechanisms when needed. Indeed, animals are capable of balancing their redox status by synthesizing enough GSH in response to sudden increases in ROS (Gusarov et al., 2021). Thus, caution should be taken when supplementing NAC as it is widely available for human use but lacks specific guidelines (Niraula and Kim, 2019).

4.8 Trp starvation decreases *Tmem173* mRNA expression

Although the data so far provided evidence that the Trp starvation-mediated STING decrease neither solely depends on autophagy nor on oxidative damage, it yet remains to be elucidated whether Trp shortage affects STING on the transcriptional or another post-translational level. Trp depletion markedly decreased *Tmem173* mRNA levels and further abolished *Tmem173* mRNA upregulation in response to DMXAA stimulation (Figure 3.24). It is tempting to speculate that Trp shortage blocks STING synthesis either by inhibiting its transcription factors, or by activating other factors that negatively impact on *Tmem173* mRNA stability. Transcription factors that were identified to increase human STING promoter activity are both c-myc and cyclic-AMP response element binding (CREB) (Wang et al., 2016). C-myc was upregulated in response to Trp deprivation (Figure 3.24), which is similar to a previous report on AA starvation. Omitting either proline, isoleucine, methionine, leucine, or any of the essential AAs from the cell culture medium significantly increased c-myc mRNA. Although the overall protein synthesis was reduced and c-myc is known to have a short half-life time, the accumulation of the c-myc mRNA was dependent on protein synthesis (Pohjanpelto and Hölttä, 1990). It has been published that, compared to controls, a KD of either CREB or c-myc with siRNA reduced STING at mRNA and protein levels by 75-80 % and 40-45 %, respectively. Likewise, an overexpression of CREB increased STING mRNA and protein levels by approximately 1.4-fold, and c-myc overexpression did so by 1.4 - 1.9-fold (Wang et al., 2016). Nevertheless, Trp starvation unexpectedly led to a decrease in STING despite a striking upregulation of c-myc (Figure 3.24).

Amongst the signaling pathways that can be activated by AAs is the Nrf2 pathway (He et al., 2018). The transcription factor Nrf2 is inactivated by Kelch-like ECH-associated protein 1 (Keap1) and readily degraded by the proteasome under homeostatic conditions. Upon inactivation of Keap1 during oxidative stress, Nrf2 is activated to induce genes involved in antioxidant processes to relieve cellular stress (Olagnier et al., 2018; Sun et al., 2020). Under inflammatory conditions, the activation of Nrf2 lowers the risk of colitis-associated cancer via preventing excessive tissue damage upon DSS challenge. Its chronic activation in the colonic epithelium, however, may promote tumor growth owing to stress adaptation (Stachel et al., 2014). In human macrophages, stimulation with LPS initiated metabolic changes and the accumulation of itaconate and its derivative 4-octyl-itaconate (4-OI) can activate the Nrf2 pathway via binding of Keap1. Nrf2, in turn, did not directly bind to *Tmem173* mRNA but rather affected its stability (Olagnier et al., 2018). Even though Nrf2 activation did not alter *Tmem173* expression in murine macrophages in the study of Olagnier et al. (2018), the investigation by Sun et al. (2020) showed that the Nrf2 activator RTA-408 could decrease STING expression without affecting the IFN- β production during murine osteoclastogenesis.

Taking these reports as a basis, it was intriguing to investigate whether the Nrf2-STING axis exists in murine IECs and whether this could explain the Trp starvation-mediated downregulation of STING. The data presented so far have shown a marked decrease in *Tmem173* mRNA under Trp starvation (Figure 3.24). Although STING reduction could not be rescued by the addition of NAC (Figure 3.22), the limitations of NAC still render the contribution of Nrf2 a plausible mechanism. Assuming that Nrf2 activation can downregulate *Tmem173* mRNA, *Nfe2l2* KO is expected to upregulate *Tmem173* mRNA and consequently IFN production. SiRNA against *Nfe2l2* neither rescued *Tmem173* mRNA expression nor the *Cxcl10* response after DMXAA treatment in Trp-deprived cells. Nevertheless, there seems to be a connection between Nrf2 and STING in murine IECs as the DMXAA-induced *Cxcl10* signal also was abolished in the siNfe2l2-treated cells cultured with Trp (Figure 3.25). This contrasts with the study of Sun et al. (2020) who observed an effect of Nrf2 on STING but not on the consequent IFN release. Thus, the interplay between STING and the oxidative stress response and particularly Nrf2 seems to be highly complex and dependent on the respective conditions and microenvironments.

4.9 Inhibition of protein synthesis rescues Trp starvation-induced STING loss

As an essential AA, the cell requires Trp for protein synthesis, which raises the question whether the observed STING loss results from a halt of protein synthesis. Importantly, regulation of STING on the synthesis level will only affect total STING levels when it is not replenished after its half-life time is exceeded. Therefore, ModeK cells were treated with CHX, which blocks the translation elongation (Schneider-Poetsch et al., 2010) and is commonly used to study the half-life time of proteins. STING was previously described to feature a half-life time exceeding 12 h (Pokatayev et al., 2020). The clear detection of STING by WB after 24 h of CHX treatment (Figure 3.26) provides evidence that it is stable for a longer period than the selected starvation period, so that a decrease in Tmem173 mRNA expression alone cannot account for the decrease at protein level.

Trp starvation led to decreased STING levels but in combination with CHX, the loss of STING was abrogated (Figure 3.26). Thus, the synthesis of selected proteins can still occur in response to Trp starvation and even is required to impact on STING, raising the assumption that Trp starvation leads to the synthesis of factors yet to be defined that in turn degrade STING. As proteins involved in degradative processes are readily available, a blockage in recycling seems unlikely. The observation that Tmem173 mRNA also is downregulated leads to the suggestion that under Trp starvation some factors are induced that target STING on both transcriptional and post-translational levels. It therefore is desirable to verify the CHX results with actinomycin D (ActD) which blocks RNA transcription by RNA polymerase (Olagnier et al., 2018) to elucidate whether the STING-degrading factor is newly transcribed or translated.

This raises the question how protein synthesis continues to occur despite the lack of Trp. A similar issue with respect to cancer cells has been regarded by the Opitz group who investigated the apparent contradiction how tumors can exploit Trp degradation as evasion strategy but at the same time manage to maintain their high proliferation rate (Adam et al., 2018). Trp is incorporated into proteins after attachment to its tRNA by WARS that competes for Trp utilization with Trp-metabolizing enzymes (Hoagland et al., 1958; Jorgensen et al., 2000; Adam et al., 2018). In the occasion of Trp shortage, uncharged tRNAs accumulate and activate the kinase GCN2, which in turn phosphorylates eIF2 α . The activation of eIF2 α leads to a translational arrest but still induces the expression of ATF4, amongst others (Wek et al., 1989; Dever et al., 1992; Wek et al., 1995; Adam et al., 2018). ATF4 is suggested to increase WARS expression, and activation of the GCN2-peIF2 α -ATF4 axis also increases Trp transporter expression, both mediating an adaptation mechanism to secure protein synthesis under starvation conditions (Adam et al., 2018). WARS further mediates an alternative decoding mechanism by which protein synthesis across tryptophan codons can continue to occur despite Trp shortage in the tumor. In the absence of Trp, WARS can use phenylalanine as a substrate to generate protein substituents by

means of the W>F codon reassignment. Tests with cancer cells confirmed the functionality of these substitutant proteins and further showed that, when presented on the cell surface, they can be successfully recognized by APCs (Pataskar et al., 2022). It will thus be intriguing to extend the study of the tumor microenvironment to chronic inflammation to investigate the prevalence of these substitutants. If somatic W>F substitutants may arise from lower Trp serum levels observed in IBD, analyzing both their functionality and effects on immune responses might open new treatment targets.

4.10 Conclusion

To put it in a nutshell, the intestinal mucosa of IBD patients is likely to experience a reduction of Trp levels, highlighting the urge to investigate the importance of this essential AA for intestinal homeostasis and further encouraging research on Trp as a cheap and non-invasive biomarker for inflammatory diseases. In *in vitro* assays on murine enterocytes, Trp starvation sensitized cells to NF- κ B activation on the one hand, but on the other hand it decreased STING at both protein and mRNA levels and consequently impaired the cGAS/STING response. However, the effect of Trp on STING was reversible as it could be rescued by restoring Trp levels. It can be excluded that Trp starvation activates autophagy to degrade STING, neither does it induce ROS. Moreover, the ATP levels of Trp-starved cells seemed to be unaffected, and protein synthesis of key proteins seemed to continue to occur. Indeed, inhibition of protein translation abrogated the downregulation of STING in response to Trp deprivation, and further confirmed that the half-life time of STING exceeded the selected starvation period. These results taken together raise the assumption that Trp starvation leads to the synthesis of another factor(s) that negatively acts on STING at both mRNA and protein level and was absent when protein translation was blocked. In the future, it will be crucial to determine the STING degrading factor, and it will be interesting to determine STING promoter activity, and to test other factors that act on Tmem173 mRNA stability. Thus, this project has underlined the crucial role and diverse effects of Trp in intestinal immunity *in vitro* and thereby paves the way for further investigations on targeting Trp metabolism as a novel strategy for combined treatment options for IBD. Depending on the presence and type of infection accompanying IBD, it may be beneficial to either boost or block Trp metabolism.

4.11 Outlook

While the STING decrease under Trp starvation was verified in organoids, as next steps it would be advisable to confirm the functional response as well as to elucidate the underlying mechanism in organoids since they provide a more complex 3D model that also includes different differentiated intestinal cell types. Approaches to do so comprise RNA sequencing of Trp-starved and infected organoids in combination with a metabolic screening compared to controls to enable correlating the gene expression with the respective metabolite levels. Whereas the data presented here provide the hint that also the intestinal tissue of IBD patients exhibits a reduction in Trp levels, it still remains unknown whether Trp starvation is a cause or consequence of inflammation. Owing to the negative correlation between Trp levels and disease activity, Trp may represent an interesting candidate for biomarker discovery in the future that would allow a cheap and non-invasive strategy. In order to translate these findings into the clinics, it first will be necessary to perform animal experiments to verify these findings *in vivo*. This will further reveal the effect of Trp starvation on other cell types and their relative contributions as the dynamic interplay can only be studied in a living multicellular organism. Thereby, a Trp-free diet administered to mice for a certain period will reveal whether Trp starvation can cause intestinal inflammation; and simultaneous Trp starvation and infection will elucidate the immune competence of mice. It, however, will not allow any direct conclusions to be drawn as IBD is a complex disease with different subtypes and different prevailing immune signatures. Therein lies the unique possibility to personalize the treatment strategy with either inhibitors of Trp metabolism or Trp supplementation since nutritional intervention provide a cheap and well-tolerated opportunity to benefit combined therapy.

References

- Abraham, C.; Cho, J. H. Inflammatory Bowel Disease. *n engl j med* **2009** (361), pp. 2066-2078.
- Adam, I.; Dewi, D. L.; Mooiweer, J.; Sadik, A.; Mohapatra, S. R.; Berdel, B.; Keil, M.; Sonner, J. K.; Thedieck, K.; Rose, A. J.; Platten, M.; Heiland, I.; Trump, S.; Opitz, C. A. Upregulation of Tryptophanyl-tRNA Synthetase Adapts Human Cancer Cells to Nutritional Stress Caused by Tryptophan Degradation. *Oncolimmunology* **2018**, *7* (12), e1486353.
- Aden, K.; Rehman, A.; Waschina, S.; Pan, W.-H.; Walker, A.; Lucio, M.; Nunez, A. M.; Bharti, R.; Zimmerman, J.; Bethge, J.; Schulte, B.; Schulte, D.; Franke, A.; Nikolaus, S.; Schroeder, J. O.; Vandeputte, D.; Raes, J.; Szymczak, S.; Waetzig, G. H.; Zeuner, R.; Schmitt-Kopplin, P.; Kaleta, C.; Schreiber, S.; Rosenstiel, P. Metabolic Functions of Gut Microbes Associate With Efficacy of Tumor Necrosis Factor Antagonists in Patients With Inflammatory Bowel Diseases. *Gastroenterology* **2019**, *157* (5), 1279-1292.e11.
- Aden, K.; Tran, F.; Ito, G.; Sheibani-Tezerji, R.; Lipinski, S.; Kuiper, J. W.; Tschurtschenthaler, M.; Saveljeva, S.; Bhattacharyya, J.; Häslér, R.; Bartsch, K.; Luzius, A.; Jentzsch, M.; Falk-Paulsen, M.; Stengel, S. T.; Welz, L.; Schwarzer, R.; Rabe, B.; Barchet, W.; Krautwald, S.; Hartmann, G.; Pasparakis, M.; Blumberg, R. S.; Schreiber, S.; Kaser, A.; Rosenstiel, P. ATG16L1 Orchestrates Interleukin-22 Signaling in the Intestinal Epithelium via cGAS–STING. *Journal of Experimental Medicine* **2018**, *215* (11), 2868–2886.
- Adolph, T. E.; Tomczak, M. F.; Niederreiter, L.; Ko, H.-J.; Böck, J.; Martinez-Naves, E.; Glickman, J. N.; Tschurtschenthaler, M.; Hartwig, J.; Hosomi, S.; Flak, M. B.; Cusick, J. L.; Kohno, K.; Iwawaki, T.; Billmann-Born, S.; Raine, T.; Bharti, R.; Lucius, R.; Kweon, M.-N.; Marciniak, S. J.; Choi, A.; Hagen, S. J.; Schreiber, S.; Rosenstiel, P.; Kaser, A.; Blumberg, R. S. Paneth Cells as a Site of Origin for Intestinal Inflammation. *Nature* **2013**, *503* (7475), 272–276.
- Agus, A.; Planchais, J.; Sokol, H. Gut Microbiota Regulation of Tryptophan Metabolism in Health and Disease. *Cell Host & Microbe* **2018**, *23* (6), 716–724.
- Ahn, J.; Son, S.; Oliveira, S. C.; Barber, G. N. STING-Dependent Signaling Underlies IL-10 Controlled Inflammatory Colitis. *Cell Reports* **2017**, *21* (13), 3873–3884.
- Ananthakrishnan, A. N.; Bernstein, C. N.; Iliopoulos, D.; Macpherson, A.; Neurath, M. F.; Ali, R. A. R.; Vavricka, S. R.; Fiocchi, C. Environmental Triggers in IBD: A Review of Progress and Evidence. *Nat Rev Gastroenterol Hepatol* **2018**, *15* (1), 39–49.
- Anderson, G.; Kubera, M.; Duda, W.; Lasoń, W.; Berk, M.; Maes, M. Increased IL-6 Trans-Signaling in Depression: Focus on the Tryptophan Catabolite Pathway, Melatonin and Neuroprogression. *Pharmacological Reports* **2013**, *65* (6), 1647–1654.
- Andreou, N.-P. Inflammatory Bowel Disease Pathobiology: The Role of the Interferon Signature. *aog* **2020**, *33*, 125-133.
- Arlt, A.; Rosenstiel, P.; Kruse, M.-L.; Grohmann, F.; Minkenber, J.; Perkins, N. D.; Fölsch, U. R.; Schreiber, S.; Schäfer, H. IEX-1 Directly Interferes with RelA/P65 Dependent Transactivation and Regulation of Apoptosis. *Biochimica et Biophysica Acta (BBA) - Molecular Cell Research* **2008**, *1783* (5), 941–952.
- Auerbuch, V.; Brockstedt, D. G.; Meyer-Morse, N.; O’Riordan, M.; Portnoy, D. A. Mice Lacking the Type I Interferon Receptor Are Resistant to *Listeria Monocytogenes*. *Journal of Experimental Medicine* **2004**, *200* (4), 527–533.
- Badawy, A.-B. Plasma Free Tryptophan Revisited: What You Need to Know and Do before Measuring It. *J Psychopharmacol* **2010**, *24* (6), 809–815.

- Badawy, A. A.-B. Kynurenine Pathway of Tryptophan Metabolism: Regulatory and Functional Aspects. *International Journal of Tryptophan Research* **2017**, *10*, 117864691769193.
- Badawy, A. A.-B. Tryptophan Metabolism, Disposition and Utilization in Pregnancy. *Bioscience Reports* **2015**, *35* (5), e00261.
- Badawy, A. A.-B.; Evans, M. The Effects of Chemical Porphyrins and Drugs on the Activity of Rat Liver Tryptophan Pyrrolase. *Biochemical Journal* **1973**, *136* (4), 885–892.
- Baeuerle, P. A.; Baltimore, D. Activation of DNA-Binding Activity in an Apparently Cytoplasmic Precursor of the NF- κ B Transcription Factor. *Cell* **1988**, *53*, 211-217.
- Bai, J.; Liu, F. The cGAS-cGAMP-STING Pathway: A Molecular Link Between Immunity and Metabolism. *Diabetes* **2019**, *68* (6), 1099–1108.
- Bartfeld, S. Modeling Infectious Diseases and Host-Microbe Interactions in Gastrointestinal Organoids. *Developmental Biology* **2016**, *420* (2), 262–270.
- Baumgart, D. C.; Le Berre, C. Newer Biologic and Small-Molecule Therapies for Inflammatory Bowel Disease. *N Engl J Med* **2021**, *385* (14), 1302–1315.
- Becker, B.; Wottawa, F.; Bakr, M.; Koncina, E.; Mayr, L.; Kugler, J.; Yang, G.; Windross, S. J.; Neises, L.; Mishra, N.; Harris, D.; Tran, F.; Welz, L.; Schwärzler, J.; Bánki, Z.; Stengel, S. T.; Ito, G.; Krötz, C.; Coleman, O. I.; Jaeger, C.; Haller, D.; Paludan, S. R.; Blumberg, R.; Kaser, A.; Cicin-Sain, L.; Schreiber, S.; Adolph, T. E.; Letellier, E.; Rosenstiel, P.; Meiser, J.; Aden, K. Metabolic Plasticity of Serine Metabolism Is Crucial for cGAS/STING-Signalling and Innate Immune Response to Viral Infections in the Gut. *bioRxiv* [Preprint] **2023** [accessed November 2023], 2022.05.17.492340.
- Bender, D. A. Biochemistry of Tryptophan in Health and Disease. *Molecular Aspects of Medicine* **1983**, *6* (2), 101–197.
- Bosch, S.; Struys, E. A.; Van Gaal, N.; Bakkali, A.; Jansen, E. W.; Diederens, K.; Benninga, M. A.; Mulder, C. J.; De Boer, N. K. H.; De Meij, T. G. J. Fecal Amino Acid Analysis Can Discriminate De Novo Treatment-Naïve Pediatric Inflammatory Bowel Disease From Controls. *Journal of Pediatric Gastroenterology & Nutrition* **2018**, *66* (5), 773–778.
- Buck, M. D.; Sowell, R. T.; Kaech, S. M.; Pearce, E. L. Metabolic Instruction of Immunity. *Cell* **2017**, *169* (4), 570–586.
- Burdette, D. L.; Monroe, K. M.; Sotelo-Troha, K.; Iwig, J. S.; Eckert, B.; Hyodo, M.; Hayakawa, Y.; Vance, R. E. STING Is a Direct Innate Immune Sensor of Cyclic Di-GMP. *Nature* **2011**, *478* (7370), 515–518.
- Chen, L.-W.; Egan, L.; Li, Z.-W.; Greten, F. R.; Kagnoff, M. F.; Karin, M. The Two Faces of IKK and NF- κ B Inhibition: Prevention of Systemic Inflammation but Increased Local Injury Following Intestinal Ischemia-Reperfusion. *Nat Med* **2003**, *9* (5), 575–581.
- Chen, M.; Liu, Y.; Xiong, S.; Wu, M.; Li, B.; Ruan, Z.; Hu, X. Dietary L -Tryptophan Alleviated LPS-Induced Intestinal Barrier Injury by Regulating Tight Junctions in a Caco-2 Cell Monolayer Model. *Food Funct.* **2019**, *10* (5), 2390–2398.
- Chen, Q.; Sun, L.; Chen, Z. J. Regulation and Function of the cGAS–STING Pathway of Cytosolic DNA Sensing. *Nat Immunol* **2016**, *17* (10), 1142–1149.
- Chino, H.; Mizushima, N. ER-Phagy: Quality Control and Turnover of Endoplasmic Reticulum. *Trends in Cell Biology* **2020**, *30* (5), 384–398.
- Christen, S.; Peterhans, E.; Stocker, R. Antioxidant Activities of Some Tryptophan Metabolites: Possible Implication for Inflammatory Diseases. *Proc. Natl. Acad. Sci. U.S.A.* **1990**, *87* (7), 2506–2510.

Cummins, E. P.; Keogh, C. E.; Crean, D.; Taylor, C. T. The Role of HIF in Immunity and Inflammation. *Molecular Aspects of Medicine* **2016**, *47–48*, 24–34.

Darnell, J. E.; Kerr, L. M.; Stark, G. R. Jak-STAT Pathways and Transcriptional Activation in Response to IFNs and Other Extracellular Signaling Proteins. *Science* **1994**, *264* (5164), 1415–1421.

De Veer, M. J.; Holko, M.; Frevel, M.; Walker, E.; Der, S.; Paranjape, J. M.; Silverman, R. H.; Williams, B. R. G. Functional classification of interferon-stimulated genes identified using microarrays. *Journal of Leukocyte Biology* **2001**, *69*, 912–920.

Decker, T.; Stockinger, S.; Karaghiosoff, M.; Müller, M.; Kovarik, P. IFNs and STATs in Innate Immunity to Microorganisms. *J. Clin. Invest.* **2002**, *109* (10), 1271–1277.

Der, S. D.; Zhou, A.; Williams, B. R. G.; Silverman, R. H. Identification of Genes Differentially Regulated by Interferon α , β , or γ Using Oligonucleotide Arrays. *Proc. Natl. Acad. Sci. USA* **1998**, *95*, 15623–15628.

Derynck, R.; Leung, D. W.; Gray, P. W.; Goeddel, D. V. Human interferon γ is encoded by a single class of mRNA. *Nucleic Acids Research* **1982**, *10*, 3605–3615.

Dever, E.; Feng, L.; Wek, C.; Cigan, A. M.; Donahue, F.; Hinnebusch, A. G. Phosphorylation of Initiation Factor 2a by Protein Kinase GCN2 Mediates Gene-Specific Translational Control of GCN4 in Yeast. **1992**.

Duerkop, B. A.; Vaishnava, S.; Hooper, L. V. Immune Responses to the Microbiota at the Intestinal Mucosal Surface. *Immunity* **2009**, *31* (3), 368–376.

Eckmann, L.; Nebelsiek, T.; Fingerle, A. A.; Dann, S. M.; Mages, J.; Lang, R.; Robine, S.; Kagnoff, M. F.; Schmid, R. M.; Karin, M.; Arkan, M. C.; Greten, F. R. Opposing Functions of IKK β during Acute and Chronic Intestinal Inflammation. *Proc. Natl. Acad. Sci. U.S.A.* **2008**, *105* (39), 15058–15063.

Eleftheriadis, T.; Pissas, G.; Antoniadis, G.; Spanoulis, A.; Liakopoulos, V.; Stefanidis, I. Indoleamine 2,3-Dioxygenase Increases P53 Levels in Alloreactive Human T Cells, and Both Indoleamine 2,3-Dioxygenase and P53 Suppress Glucose Uptake, Glycolysis and Proliferation. *International Immunology* **2014**, *26* (12), 673–684.

Ellinger, A.; Flamand, C. Über synthetisch gewonnenes Tryptophan und einige seiner Derivate. *Hoppe-Seyler's Zeitschrift für physiologische Chemie* **1908**, *55* (1), 8–24.

Ely, B.; Pittard, J. Aromatic Amino Acid Biosynthesis: Regulation of Shikimate Kinase in Escherichia Coli K-12. *J Bacteriol* **1979**, *138* (3), 933–943.

Etienne, P.; Young, S. N.; Sourkes, T. L. Inhibition by albumin of tryptophan uptake by rat brain. *Nature* **1976**, *262*, 144–145.

Feng, G. S.; Taylor, M. W. Interferon Gamma-Resistant Mutants Are Defective in the Induction of Indoleamine 2,3-Dioxygenase. *Proc. Natl. Acad. Sci. U.S.A.* **1989**, *86* (18), 7144–7148.

Fullerton, J. N.; Gilroy, D. W. Resolution of Inflammation: A New Therapeutic Frontier. *Nat Rev Drug Discov* **2016**, *15* (8), 551–567.

Galluzzi, L.; Pietrocola, F.; Levine, B.; Kroemer, G. Metabolic Control of Autophagy. *Cell* **2014**, *159* (6), 1263–1276.

Gao, N.; Dou, X.; Yin, T.; Yang, Y.; Yan, D.; Ma, Z.; Bi, C.; Shan, A. Tryptophan Promotes Intestinal Immune Defense through Calcium-Sensing Receptor (CaSR)-Dependent Metabolic Pathways. *J. Agric. Food Chem.* **2021**, *69* (45), 13460–13473.

- Ghosh, S.; Baltimore, D. Activation in vitro of NF- κ B by phosphorylation of its inhibitor I κ B. *Nature* **1990**, *344*, 678-682.
- Ghosh, S.; Gifford, A. M.; Riviere, L. R.; Tempst, P.; Nolan, G.P.; Baltimore, D. Cloning of the p50 DNA Binding Subunit of NF- κ B: Homology to rel and dorsal. *Cell* **1990**, *62*, 1019-1029.
- González-Navajas, J. M.; Lee, J.; David, M.; Raz, E. Immunomodulatory Functions of Type I Interferons. *Nat Rev Immunol* **2012**, *12* (2), 125–135.
- Green, A. C.; Marttila, P.; Kiweler, N.; Chalkiadaki, C.; Wiita, E.; Cookson, V.; Lesur, A.; Eiden, K.; Bernardin, F.; Vallin, K. S. A.; Borhade, S.; Long, M.; Ghahe, E. K.; Jiménez-Alonso, J. J.; Jemth, A.-S.; Loseva, O.; Mortusewicz, O.; Meyers, M.; Viry, E.; Johansson, A. I.; Hodek, O.; Homan, E.; Bonagas, N.; Ramos, L.; Sandberg, L.; Frödin, M.; Moussay, E.; Slipicevic, A.; Letellier, E.; Paggetti, J.; Sørensen, C. S.; Helleday, T.; Henriksson, M.; Meiser, J. Formate Overflow Drives Toxic Folate Trapping in MTHFD1 Inhibited Cancer Cells. *Nat Metab* **2023**, *5* (4), 642–659.
- Günther, C.; Ruder, B.; Stolzer, I.; Dorner, H.; He, G.-W.; Chiriac, M. T.; Aden, K.; Strigli, A.; Bittel, M.; Zeissig, S.; Rosenstiel, P.; Atreya, R.; Neurath, M. F.; Wirtz, S.; Becker, C. Interferon Lambda Promotes Paneth Cell Death Via STAT1 Signaling in Mice and Is Increased in Inflamed Ileal Tissues of Patients With Crohn's Disease. *Gastroenterology* **2019**, *157* (5), 1310-1322.e13.
- Gusarov, I.; Shamovsky, I.; Pani, B.; Gautier, L.; Eremina, S.; Katkova-Zhukotskaya, O.; Mironov, A.; Makarov, A. A.; Nudler, E. Dietary Thiols Accelerate Aging of *C. Elegans*. *Nat Commun* **2021**, *12* (1), 4336.
- Hampe, J.; Franke, A.; Rosenstiel, P.; Till, A.; Teuber, M.; Huse, K.; Albrecht, M.; Mayr, G.; De La Vega, F. M.; Briggs, J.; Günther, S.; Prescott, N. J.; Onnie, C. M.; Häsler, R.; Sipos, B.; Fölsch, U. R.; Lengauer, T.; Platzer, M.; Mathew, C. G.; Krawczak, M.; Schreiber, S. A Genome-Wide Association Scan of Nonsynonymous SNPs Identifies a Susceptibility Variant for Crohn Disease in ATG16L1. *Nat Genet* **2007**, *39* (2), 207–211.
- Haq, S.; Grondin, J.; Banskota, S.; Khan, W. I. Autophagy: Roles in Intestinal Mucosal Homeostasis and Inflammation. *J Biomed Sci* **2019**, *26* (1), 19.
- Hashimoto, T.; Perlot, T.; Rehman, A.; Trichereau, J.; Ishiguro, H.; Paolino, M.; Sigl, V.; Hanada, T.; Hanada, R.; Lipinski, S.; Wild, B.; Camargo, S. M. R.; Singer, D.; Richter, A.; Kuba, K.; Fukamizu, A.; Schreiber, S.; Clevers, H.; Verrey, F.; Rosenstiel, P.; Penninger, J. M. ACE2 Links Amino Acid Malnutrition to Microbial Ecology and Intestinal Inflammation. *Nature* **2012**, *487* (7408), 477–481.
- Havell, E. A.; Berman, B.; Ogburn, C. A.; Berg, K.; Paucker, K.; Vilcek, J. Two Antigenically Distinct Species of Human Interferon. *Proc. Natl. Acad. Sci. U.S.A.* **1975**, *72* (6), 2185–2187.
- He, F.; Wu, C.; Li, P.; Li, N.; Zhang, D.; Zhu, Q.; Ren, W.; Peng, Y. Functions and Signaling Pathways of Amino Acids in Intestinal Inflammation. *BioMed Research International* **2018**, *2018*, 1–13.
- Heath-Pagliuso, S.; Rogers, W. J.; Tullis, K.; Seidel, S. D.; Cenijn, P. H.; Brouwer, A.; Denison, M. S. Activation of the Ah Receptor by Tryptophan and Tryptophan Metabolites. *Biochemistry* **1998**, *37* (33), 11508–11515.
- Hiller, K.; Hangebrauk, J.; Jäger, C.; Spura, J.; Schreiber, K.; Schomburg, D. MetaboliteDetector: Comprehensive Analysis Tool for Targeted and Nontargeted GC/MS Based Metabolome Analysis. *Anal. Chem.* **2009**, *81* (9), 3429–3439.
- Hirata, F.; Hayaishi, O. Studies on Indoleamine 2,3-Dioxygenase. I. Superoxide Anion as Substrate. *Journal of Biological Chemistry* **1975**, *250* (15), 5960–5966.
- Hoagland, M. B.; Stephenson, M. L.; Scott, J. F.; Hecht, L. I.; Zamecnik, P. C. A SOLUBLE RIBONUCLEIC ACID INTERMEDIATE IN PROTEIN SYNTHESIS. *Journal of Biological Chemistry* **1958**, *231* (1), 241–257.

- Hopkins, F. G. Feeding experiments illustrating the importance of accessory factors in normal dietaries. *J Physiol.* **1912**, *44*, 425–60.
- Hou, Y.; Wei, Y.; Lautrup, S.; Yang, B.; Wang, Y.; Cordonnier, S.; Mattson, M. P.; Croteau, D. L.; Bohr, V. A. NAD⁺ Supplementation Reduces Neuroinflammation and Cell Senescence in a Transgenic Mouse Model of Alzheimer's Disease via cGAS–STING. *Proc. Natl. Acad. Sci. U.S.A.* **2021**, *118* (37), e2011226118.
- Hsu, S.-C.; Chen, C.-L.; Cheng, M.-L.; Chu, C.-Y.; Changou, C. A.; Yu, Y.-L.; Yeh, S.-D.; Kuo, T.-C.; Kuo, C.-C.; Chuu, C.-P.; Li, C.-F.; Wang, L.-H.; Chen, H.-W.; Yen, Y.; Ann, D. K.; Wang, H.-J.; Kung, H.-J. Arginine Starvation Elicits Chromatin Leakage and cGAS-STING Activation via Epigenetic Silencing of Metabolic and DNA-Repair Genes. *Theranostics* **2021**, *11* (15), 7527–7545.
- Huang, L.; Li, L.; Lemos, H.; Chandler, P. R.; Pacholczyk, G.; Baban, B.; Barber, G. N.; Hayakawa, Y.; McGaha, T. L.; Ravishankar, B.; Munn, D. H.; Mellor, A. L. Cutting Edge: DNA Sensing via the STING Adaptor in Myeloid Dendritic Cells Induces Potent Tolerogenic Responses. *The Journal of Immunology* **2013**, *191* (7), 3509–3513.
- Irving, P. M.; Gibson, P. R. Infections and IBD. *Nat Rev Gastroenterol Hepatol* **2008**, *5* (1), 18–27.
- Isaacs, A.; Lindenmann, J. Virus Interference. I. The Interferon. **1957**.
- Isaacs, A.; Lindenmann, J.; Valentine, R. C. Virus Interference. II. Some Properties of Interferon. **1957**.
- Ishikawa, H.; Barber, G. N. STING Is an Endoplasmic Reticulum Adaptor That Facilitates Innate Immune Signalling. *Nature* **2008**, *455* (7213), 674–678.
- Ishikawa, H.; Ma, Z.; Barber, G. N. STING Regulates Intracellular DNA-Mediated, Type I Interferon-Dependent Innate Immunity. *Nature* **2009**, *461* (7265), 788–792.
- Islam, J.; Sato, S.; Watanabe, K.; Watanabe, T.; Ardiansyah; Hirahara, K.; Aoyama, Y.; Tomita, S.; Aso, H.; Komai, M.; Shirakawa, H. Dietary Tryptophan Alleviates Dextran Sodium Sulfate-Induced Colitis through Aryl Hydrocarbon Receptor in Mice. *The Journal of Nutritional Biochemistry* **2017**, *42*, 43–50.
- Jia, M.; Qin, D.; Zhao, C.; Chai, L.; Yu, Z.; Wang, W.; Tong, L.; Lv, L.; Wang, Y.; Rehwinkel, J.; Yu, J.; Zhao, W. Redox Homeostasis Maintained by GPX4 Facilitates STING Activation. *Nat Immunol* **2020**, *21* (7), 727–735.
- Jørgensen, R.; Sjøgaard, T. M. M.; Rossing, A. B.; Martensen, P. M.; Justesen, J. Identification and Characterization of Human Mitochondrial Tryptophanyl-tRNA Synthetase. *Journal of Biological Chemistry* **2000**, *275* (22), 16820–16826.
- Kaiko, G. E.; Ryu, S. H.; Koues, O. I.; Collins, P. L.; Solnica-Krezel, L.; Pearce, E. J.; Pearce, E. L.; Oltz, E. M.; Stappenbeck, T. S. The Colonic Crypt Protects Stem Cells from Microbiota-Derived Metabolites. *Cell* **2016**, *165* (7), 1708–1720.
- Kaser, A.; Lee, A.-H.; Franke, A.; Glickman, J. N.; Zeissig, S.; Tilg, H.; Nieuwenhuis, E. E. S.; Higgins, D. E.; Schreiber, S.; Glimcher, L. H.; Blumberg, R. S. XBP1 Links ER Stress to Intestinal Inflammation and Confers Genetic Risk for Human Inflammatory Bowel Disease. *Cell* **2008**, *134* (5), 743–756.
- Kaser, A.; Zeissig, S.; Blumberg, R. S. Inflammatory Bowel Disease. *Annu. Rev. Immunol.* **2010**, *28* (1), 573–621.
- Kieran, M.; Blank, V.; Logeat, F.; Vendekemkove, J.; Lottspelch, F.; Le Ball, O.; Urban, M.B.; Kourllsky, P.; Baeuerle, P. A.; Israel, A. The DNA Binding Subunit of NF- κ B Is Identical to Factor KBFI and Homologous to the Rel Oncogene Product. *Cell* **1990**, *62*, 1007-1018.

Kim, C. J.; Kovacs-Nolan, J. A.; Yang, C.; Archbold, T.; Fan, M. Z.; Mine, Y. L-Tryptophan Exhibits Therapeutic Function in a Porcine Model of Dextran Sodium Sulfate (DSS)-Induced Colitis. *The Journal of Nutritional Biochemistry* **2010**, *21* (6), 468–475.

Lamas, B.; Richard, M. L.; Leducq, V.; Pham, H.-P.; Michel, M.-L.; Da Costa, G.; Bridonneau, C.; Jegou, S.; Hoffmann, T. W.; Natividad, J. M.; Brot, L.; Taleb, S.; Couturier-Maillard, A.; Nion-Larmurier, I.; Merabtene, F.; Seksik, P.; Bourrier, A.; Cosnes, J.; Ryffel, B.; Beaugerie, L.; Launay, J.-M.; Langella, P.; Xavier, R. J.; Sokol, H. CARD9 Impacts Colitis by Altering Gut Microbiota Metabolism of Tryptophan into Aryl Hydrocarbon Receptor Ligands. *Nat Med* **2016**, *22* (6), 598–605.

Lanis, J. M.; Alexeev, E. E.; Curtis, V. F.; Kitzenberg, D. A.; Kao, D. J.; Battista, K. D.; Gerich, M. E.; Glover, L. E.; Kominsky, D. J.; Colgan, S. P. Tryptophan Metabolite Activation of the Aryl Hydrocarbon Receptor Regulates IL-10 Receptor Expression on Intestinal Epithelia. *Mucosal Immunology* **2017**, *10* (5), 1133–1144.

Lee, A.-H.; Iwakoshi, N. N.; Anderson, K. C.; Glimcher, L. H. Proteasome Inhibitors Disrupt the Unfolded Protein Response in Myeloma Cells. *Proc. Natl. Acad. Sci. U.S.A.* **2003**, *100* (17), 9946–9951.

Li, J.-Y.; Xiao, J.; Gao, M.; Zhou, H.-F.; Fan, H.; Sun, F.; Cui, D.-D. IRF/Type I IFN Signaling Serves as a Valuable Therapeutic Target in the Pathogenesis of Inflammatory Bowel Disease. *International Immunopharmacology* **2021**, *92*, 107350.

Li, X.-D.; Wu, J.; Gao, D.; Wang, H.; Sun, L.; Chen, Z. J. Pivotal Roles of cGAS-cGAMP Signaling in Antiviral Defense and Immune Adjuvant Effects. *Science* **2013**, *341* (6152), 1390–1394.

Liu, G.; Tao, J.; Lu, J.; Jia, G.; Zhao, H.; Chen, X.; Tian, G.; Cai, J.; Zhang, R.; Wang, J. Dietary Tryptophan Supplementation Improves Antioxidant Status and Alleviates Inflammation, Endoplasmic Reticulum Stress, Apoptosis, and Pyroptosis in the Intestine of Piglets after Lipopolysaccharide Challenge. *Antioxidants* **2022**, *11* (5), 872.

Lawrence, T.; Gilroy, D. W.; Colville-Nash, P. R.; Willoughby, D. A. Possible New Role for NF- κ B in the Resolution of Inflammation. *Nat Med* **2001**, *7* (12), 1291–1297.

Maddocks, O. D. K.; Berkers, C. R.; Mason, S. M.; Zheng, L.; Blyth, K.; Gottlieb, E.; Vousden, K. H. Serine Starvation Induces Stress and P53-Dependent Metabolic Remodelling in Cancer Cells. *Nature* **2013**, *493* (7433), 542–546.

Maes, M.; Meltzer, H. Y.; Scharpè, S.; Bosmans, E.; Suy, E.; De Meester, I.; Calabrese, J.; Cosyns, P. Relationships between Lower Plasma L-Tryptophan Levels and Immune-Inflammatory Variables in Depression. *Psychiatry Research* **1993**, *49* (2), 151–165.

Mahapatro, M.; Erkert, L.; Becker, C. Cytokine-Mediated Crosstalk between Immune Cells and Epithelial Cells in the Gut. *Cells* **2021**, *10* (1), 111.

Majumdar, T.; Sharma, S.; Kumar, M.; Hussain, Md. A.; Chauhan, N.; Kalia, I.; Sahu, A. K.; Rana, V. S.; Bharti, R.; Haldar, A. K.; Singh, A. P.; Mazumder, S. Tryptophan-Kynurenine Pathway Attenuates β -Catenin-Dependent pro-Parasitic Role of STING-TICAM2-IRF3-IDO1 Signalosome in Toxoplasma Gondii Infection. *Cell Death Dis* **2019**, *10* (3), 161.

Mak, W. Y.; Zhao, M.; Ng, S. C.; Burisch, J. The Epidemiology of Inflammatory Bowel Disease: East Meets West. *Journal of Gastroenterology and Hepatology* **2020**, *35* (3), 380–389.

Maloy, K. J.; Powrie, F. Intestinal Homeostasis and Its Breakdown in Inflammatory Bowel Disease. *Nature* **2011**, *474* (7351), 298–306.

Mayr, L.; Grabherr, F.; Schwärzler, J.; Reitmeier, I.; Sommer, F.; Gehmacher, T.; Niederreiter, L.; He, G.-W.; Ruder, B.; Kunz, K. T. R.; Tymoszuk, P.; Hilbe, R.; Haschka, D.; Feistritzer, C.; Gerner, R. R.; Enrich, B.; Przysiecki, N.; Seifert, M.; Keller, M. A.; Oberhuber, G.; Sprung, S.; Ran, Q.; Koch, R.;

Effenberger, M.; Tancevski, I.; Zoller, H.; Moschen, A. R.; Weiss, G.; Becker, C.; Rosenstiel, P.; Kaser, A.; Tilg, H.; Adolph, T. E. Dietary Lipids Fuel GPX4-Restricted Enteritis Resembling Crohn's Disease. *Nat Commun* **2020**, *11* (1), 1775.

Meiser, J.; Tumanov, S.; Maddocks, O.; Labuschagne, C. F.; Athineos, D.; Van Den Broek, N.; Mackay, G. M.; Gottlieb, E.; Blyth, K.; Vousden, K.; Kamphorst, J. J.; Vazquez, A. Serine One-Carbon Catabolism with Formate Overflow. *Sci. Adv.* **2016**, *2* (10), e1601273.

Miller, C. A. Expression of the Human Aryl Hydrocarbon Receptor Complex in Yeast. *Journal of Biological Chemistry* **1997**, *272* (52), 32824–32829.

Mizushima, N.; Yoshimori, T. How to Interpret LC3 Immunoblotting. *Autophagy* **2007**, *3* (6), 542–545.

Modoux, M.; Rolhion, N.; Mani, S.; Sokol, H. Tryptophan Metabolism as a Pharmacological Target. *Trends in Pharmacological Sciences* **2021**, *42* (1), 60–73.

Murray, M. F.; Srinivasan, A. Nicotinamide inhibits HIV-1 in both acute and chronic in vitro infection. *Biochemical and Biophysical Research Communications* **1995**, *210*(3), 954-959.

Nathan, C.; Cunningham-Bussel, A. Beyond Oxidative Stress: An Immunologist's Guide to Reactive Oxygen Species. *Nat Rev Immunol* **2013**, *13* (5), 349–361.

Navarro, M. N.; Gómez De Las Heras, M. M.; Mittelbrunn, M. Nicotinamide Adenine Dinucleotide Metabolism in the Immune Response, Autoimmunity and Inflammation. *British J Pharmacology* **2021**, 1–18.

Nenci, A.; Becker, C.; Wullaert, A.; Gareus, R.; Van Loo, G.; Danese, S.; Huth, M.; Nikolaev, A.; Neufert, C.; Madison, B.; Gumucio, D.; Neurath, M. F.; Pasparakis, M. Epithelial NEMO Links Innate Immunity to Chronic Intestinal Inflammation. *Nature* **2007**, *446* (7135), 557–561.

Niederreiter, L.; Fritz, T. M. J.; Adolph, T. E.; Krismer, A.-M.; Offner, F. A.; Tschurtschenthaler, M.; Flak, M. B.; Hosomi, S.; Tomczak, M. F.; Kaneider, N. C.; Sarcevic, E.; Kempster, S. L.; Raine, T.; Esser, D.; Rosenstiel, P.; Kohno, K.; Iwawaki, T.; Tilg, H.; Blumberg, R. S.; Kaser, A. ER Stress Transcription Factor Xbp1 Suppresses Intestinal Tumorigenesis and Directs Intestinal Stem Cells. *Journal of Experimental Medicine* **2013**, *210* (10), 2041–2056.

Nikolaus, S.; Schulte, B.; Al-Massad, N.; Thieme, F.; Schulte, D. M.; Bethge, J.; Rehman, A.; Tran, F.; Aden, K.; Häslér, R.; Moll, N.; Schütze, G.; Schwarz, M. J.; Waetzig, G. H.; Rosenstiel, P.; Krawczak, M.; Szymczak, S.; Schreiber, S. Increased Tryptophan Metabolism Is Associated With Activity of Inflammatory Bowel Diseases. *Gastroenterology* **2017**, *153* (6), 1504-1516.e2.

Nikolaus, S.; Waetzig, G. H.; Butzin, S.; Ziolkiewicz, M.; Al-Massad, N.; Thieme, F.; Lövgren, U.; Rasmussen, B. B.; Reinheimer, T. M.; Seegert, D.; Rosenstiel, P.; Szymczak, S.; Schreiber, S. Evaluation of Interleukin-6 and Its Soluble Receptor Components sIL-6R and Sgp130 as Markers of Inflammation in Inflammatory Bowel Diseases. *Int J Colorectal Dis* **2018**, *33* (7), 927–936.

Niraula, P.; Kim, M. S. N-Acetylcysteine Extends Lifespan of Drosophila via Modulating ROS Scavenger Gene Expression. *Biogerontology* **2019**, *20* (4), 533–543.

Nolan, G. P.; Ghosh, S.; Liou, H.-C.; Tempst, P.; Baltimore, D. DNA Binding and I κ B Inhibition of the Cloned p65 Subunit of NF- κ B, a rel-Related Polypeptide. *Cell* **1991**, *64*, 961-969.

Noth, R.; Stüber, E.; Häslér, R.; Nikolaus, S.; Kühbacher, T.; Hampe, J.; Bewig, B.; Schreiber, S.; Aert, A. Anti-TNF- α Antibodies Improve Intestinal Barrier Function in Crohn's Disease. *Journal of Crohn's and Colitis* **2012**, *6* (4), 464–469.

Novick, D.; Cohen, B.; Rubinstein, M. The Human Interferon α /p Receptor: Characterization and Molecular Cloning. *Cell* **1994**, *77*, 391-400.

O'Connell, R. M.; Saha, S. K.; Vaidya, S. A.; Bruhn, K. W.; Miranda, G. A.; Zarnegar, B.; Perry, A. K.; Nguyen, B. O.; Lane, T. F.; Taniguchi, T.; Miller, J. F.; Cheng, G. Type I Interferon Production Enhances Susceptibility to *Listeria Monocytogenes* Infection. *Journal of Experimental Medicine* **2004**, *200* (4), 437–445.

O'Neill, L. A. J.; Kishton, R. J.; Rathmell, J. A Guide to Immunometabolism for Immunologists. *Nat Rev Immunol* **2016**, *16* (9), 553–565.

Olagnier, D.; Brandtoft, A. M.; Gunderstofte, C.; Villadsen, N. L.; Krapp, C.; Thielke, A. L.; Laustsen, A.; Peri, S.; Hansen, A. L.; Bonefeld, L.; Thyrted, J.; Bruun, V.; Iversen, M. B.; Lin, L.; Artegoitia, V. M.; Su, C.; Yang, L.; Lin, R.; Balachandran, S.; Luo, Y.; Nyegaard, M.; Marrero, B.; Goldbach-Mansky, R.; Motwani, M.; Ryan, D. G.; Fitzgerald, K. A.; O'Neill, L. A.; Hollensen, A. K.; Damgaard, C. K.; De Paoli, F. V.; Bertram, H. C.; Jakobsen, M. R.; Poulsen, T. B.; Holm, C. K. Nrf2 Negatively Regulates STING Indicating a Link between Antiviral Sensing and Metabolic Reprogramming. *Nat Commun* **2018**, *9* (1), 3506.

Opitz, C. A.; Somarribas Patterson, L. F.; Mohapatra, S. R.; Dewi, D. L.; Sadik, A.; Platten, M.; Trump, S. The Therapeutic Potential of Targeting Tryptophan Catabolism in Cancer. *Br J Cancer* **2020**, *122* (1), 30–44.

Ortega-Gomez, A.; Perretti, M.; Soehnlein, O. Resolution of inflammation: an integrated view. *EMBO Mol Med* **2013**, *5*, 661-674.

Pajonk, F.; Riess, K.; Sommer, A.; McBride, W. H. N-ACETYL-L-CYSTEINE INHIBITS 26S PROTEASOME FUNCTION: IMPLICATIONS FOR EFFECTS ON NF- κ B ACTIVATION. *Free Radical Biology & Medicine* **2002**, *32* (6), 536-543.

Palego, L.; Betti, L.; Rossi, A.; Giannaccini, G. Tryptophan Biochemistry: Structural, Nutritional, Metabolic, and Medical Aspects in Humans. *Journal of Amino Acids* **2016**, *2016*, 1–13.

Parzych, K. R.; Klionsky, D. J. An Overview of Autophagy: Morphology, Mechanism, and Regulation. *Antioxidants & Redox Signaling* **2014**, *20* (3), 460–473.

Pataskar, A.; Champagne, J.; Nagel, R.; Kenski, J.; Laos, M.; Michaux, J.; Pak, H. S.; Bleijerveld, O. B.; Mordente, K.; Navarro, J. M.; Blommaert, N.; Nielsen, M. M.; Lovecchio, D.; Stone, E.; Georgiou, G.; De Gooijer, M. C.; Van Tellingen, O.; Altelaar, M.; Joosten, R. P.; Perrakis, A.; Olweus, J.; Bassani-Sternberg, M.; Peeper, D. S.; Agami, R. Tryptophan Depletion Results in Tryptophan-to-Phenylalanine Substitutants. *Nature* **2022**, *603* (7902), 721–727.

Perkins, N. D. Integrating Cell-Signalling Pathways with NF- κ B and IKK Function. *Nat Rev Mol Cell Biol* **2007**, *8* (1), 49–62.

Pfefferkorn, E. R. Interferon Gamma Blocks the Growth of *Toxoplasma Gondii* in Human Fibroblasts by Inducing the Host Cells to Degrade Tryptophan. *Proc. Natl. Acad. Sci. U.S.A.* **1984**, *81* (3), 908–912.

Podolsky, D. K. Inflammatory Bowel Disease. *The New England Journal of Medicine* **2002**.

Pohjanpelto, P.; Hölttä, E. Deprivation of a Single Amino Acid Induces Protein Synthesis Dependent Increases in *C-Jun*, *c-Myc*, and Ornithine Decarboxylase mRNAs in Chinese Hamster Ovary Cells. *Molecular and Cellular Biology* **1990**, *10* (11), 5814–5821.

Pokatayev, V.; Yang, K.; Tu, X.; Dobbs, N.; Wu, J.; Kalb, R. G.; Yan, N. Homeostatic Regulation of STING Protein at the Resting State by Stabilizer TOLLIP. *Nat Immunol* **2020**, *21* (2), 158–167.

Prabakaran, T.; Bodda, C.; Krapp, C.; Zhang, B.; Christensen, M. H.; Sun, C.; Reinert, L.; Cai, Y.; Jensen, S. B.; Skouboe, M. K.; Nyengaard, J. R.; Thompson, C. B.; Lebbink, R. J.; Sen, G. C.; Van Loo, G.; Nielsen, R.; Komatsu, M.; Nejsun, L. N.; Jakobsen, M. R.; Gyrd-Hansen, M.; Paludan, S. R. Attenuation

of c GAS - STING Signaling Is Mediated by a P62/ SQSTM 1-dependent Autophagy Pathway Activated by TBK1. *The EMBO Journal* **2018**, *37* (8), e97858.

Rashid, H.-O.; Yadav, R. K.; Kim, H.-R.; Chae, H.-J. ER Stress: Autophagy Induction, Inhibition and Selection. *Autophagy* **2015**, *11* (11), 1956–1977.

Ravindran, R.; Loebbermann, J.; Nakaya, H. I.; Khan, N.; Ma, H.; Gama, L.; Machiah, D. K.; Lawson, B.; Hakimpour, P.; Wang, Y.; Li, S.; Sharma, P.; Kaufman, R. J.; Martinez, J.; Pulendran, B. The Amino Acid Sensor GCN2 Controls Gut Inflammation by Inhibiting Inflammasome Activation. *Nature* **2016**, *531* (7595), 523–527.

Rieder, F.; Fiocchi, C. Intestinal Fibrosis in IBD—a Dynamic, Multifactorial Process. *Nat Rev Gastroenterol Hepatol* **2009**, *6* (4), 228–235.

Roda, G. Intestinal Epithelial Cells in Inflammatory Bowel Diseases. *WJG* **2010**, *16* (34), 4264.

Roers, A.; Hiller, B.; Hornung, V. Recognition of Endogenous Nucleic Acids by the Innate Immune System. *Immunity* **2016**, *44* (4), 739–754.

Rogler, G. Resolution of Inflammation in Inflammatory Bowel Disease. *The Lancet Gastroenterology & Hepatology* **2017**, *2* (7), 521–530.

Rogler, G.; Zeitz, J.; Biedermann, L. The Search for Causative Environmental Factors in Inflammatory Bowel Disease. *Dig Dis* **2016**, *34* (Suppl. 1), 48–55.

Rosenstiel, P.; Fantini, M.; Bräutigam, K.; Kühbacher, T.; Waetzig, G. H.; Seegert, D.; Schreiber, S. TNF- α and IFN- γ Regulate the Expression of the NOD2 (CARD15) Gene in Human Intestinal Epithelial Cells. *Gastroenterology* **2003**, *124* (4), 1001–1009.

Rubinstein, M.; Levy, W. P.; Moschera, J. A.; Lai, C.-Y.; Hershberg, R. D.; Bartlett, R. T.; Pestka, S. Human Leukocyte Interferon: Isolation and Characterization of Several Molecular Forms. *Archives of Biochemistry and Biophysics* **1981**, *210* (1), 307–318.

Sadler, A. J.; Williams, B. R. G. Interferon-Inducible Antiviral Effectors. *Nat Rev Immunol* **2008**, *8* (7), 559–568.

Saeid Seyedian, S.; Nokhostin, F.; Forogh Nokhostin, Dargahi Malamir, M. A Review of the Diagnosis, Prevention, and Treatment Methods of Inflammatory Bowel Disease. *JMedLife* **2019**, *12* (2), 113–122.

Saitoh, T.; Fujita, N.; Hayashi, T.; Takahara, K.; Satoh, T.; Lee, H.; Matsunaga, K.; Kageyama, S.; Omori, H.; Noda, T.; Yamamoto, N.; Kawai, T.; Ishii, K.; Takeuchi, O.; Yoshimori, T.; Akira, S. Atg9a Controls dsDNA-Driven Dynamic Translocation of STING and the Innate Immune Response. *Proc. Natl. Acad. Sci. U.S.A.* **2009**, *106* (49), 20842–20846.

Saitoh, T.; Fujita, N.; Jang, M. H.; Uematsu, S.; Yang, B.-G.; Satoh, T.; Omori, H.; Noda, T.; Yamamoto, N.; Komatsu, M.; Tanaka, K.; Kawai, T.; Tsujimura, T.; Takeuchi, O.; Yoshimori, T.; Akira, S. Loss of the Autophagy Protein Atg16L1 Enhances Endotoxin-Induced IL-1 β Production. *Nature* **2008**, *456* (7219), 264–268.

Schmidt, H. H. H. W.; Stocker, R.; Vollbracht, C.; Paulsen, G.; Riley, D.; Daiber, A.; Cuadrado, A. Antioxidants in Translational Medicine. *Antioxidants & Redox Signaling* **2015**, *23* (14), 1130–1143.

Schneider, W. M.; Chevillotte, M. D.; Rice, C. M. Interferon-Stimulated Genes: A Complex Web of Host Defenses. *Annu. Rev. Immunol.* **2014**, *32* (1), 513–545.

Schneider-Poetsch, T.; Ju, J.; Eyler, D. E.; Dang, Y.; Bhat, S.; Merrick, W. C.; Green, R.; Shen, B.; Liu, J. O. Inhibition of Eukaryotic Translation Elongation by Cycloheximide and Lactimidomycin. *Nat Chem Biol* **2010**, *6* (3), 209–217.

- Schreiber, S. Activation of Signal Transducer and Activator of Transcription (STAT) 1 in Human Chronic Inflammatory Bowel Disease. *Gut* **2002**, *51* (3), 379–385.
- Schreiber, S.; Rosenstiel, P.; Albrecht, M.; Hampe, J.; Krawczak, M. Genetics of Crohn Disease, an Archetypal Inflammatory Barrier Disease. *Nat Rev Genet* **2005**, *6* (5), 376–388.
- Schreiber, S.; Aden, K.; Bernardes, J. P.; Conrad, C.; Tran, F.; Höper, H.; Volk, V.; Mishra, N.; Blase, J. I.; Nikolaus, S.; Bethge, J.; Kühbacher, T.; Röcken, C.; Chen, M.; Cottingham, I.; Petri, N.; Rasmussen, B. B.; Lokau, J.; Lenk, L.; Garbers, C.; Feuerhake, F.; Rose-John, S.; Waetzig, G. H.; Rosenstiel, P. Therapeutic Interleukin-6 Trans-Signaling Inhibition by Olamkicept (sgp130Fc) in Patients With Active Inflammatory Bowel Disease. *Gastroenterology* **2021**, *160* (7), 2354-2366.e11.
- Schreiber, S.; Heinig, T.; Thiele, H.-G.; Raedler, A. Immunoregulatory Role of Interleukin 10 in Patients with Inflammatory Bowel Disease. *Gastroenterology* **1995**, *108* (5), 1434–1444.
- Schroecksadel, K.; Kaser, S.; Ledochowski, M.; Neutrauer, G.; Mur, E.; Herold, M.; Fuchs, D. Increased Degradation of Tryptophan in Blood of Patients with Rheumatoid Arthritis. *The Journal of Rheumatology* **2003**, *1935-1939*.
- Sen, R.; Baltimore, D. Multiple Nuclear Factors Interact with the Immunoglobulin Enhancer Sequences. *Cell* **1986**, *46*, 705-716.
- Sina, C.; Arlt, A.; Gavrilova, O.; Midtling, E.; Kruse, M.-L.; Mürköster, S. S.; Kumar, R.; Fölsch, U. R.; Schreiber, S.; Rosenstiel, P.; Schäfer, H. Ablation of Gly96/Immediate Early Gene-X1 (Gly96/lex-1) Aggravates DSS-Induced Colitis in Mice: Role for Gly96/lex-1 in the Regulation of NF-κB: *Inflammatory Bowel Diseases* **2010**, *16* (2), 320–331.
- Sofia, M. A.; Ciorba, M. A.; Meckel, K.; Lim, C. K.; Guillemin, G. J.; Weber, C. R.; Bissonnette, M.; Pekow, J. R. Tryptophan Metabolism through the Kynurenine Pathway Is Associated with Endoscopic Inflammation in Ulcerative Colitis. *Inflammatory Bowel Diseases* **2018**, *24* (7), 1471–1480.
- Sonner, J. K.; Keil, M.; Falk-Paulsen, M.; Mishra, N.; Rehman, A.; Kramer, M.; Deumelandt, K.; Röwe, J.; Sanghvi, K.; Wolf, L.; Von Landenberg, A.; Wolff, H.; Bharti, R.; Oezen, I.; Lanz, T. V.; Wanke, F.; Tang, Y.; Brandao, I.; Mohapatra, S. R.; Epping, L.; Grill, A.; Röth, R.; Niesler, B.; Meuth, S. G.; Opitz, C. A.; Okun, J. G.; Reinhardt, C.; Kurschus, F. C.; Wick, W.; Bode, H. B.; Rosenstiel, P.; Platten, M. Dietary Tryptophan Links Encephalogenicity of Autoreactive T Cells with Gut Microbial Ecology. *Nat Commun* **2019**, *10* (1), 4877.
- Stachel, I.; Geismann, C.; Aden, K.; Deisinger, F.; Rosenstiel, P.; Schreiber, S.; Sebens, S.; Arlt, A.; Schäfer, H. Modulation of Nuclear Factor E2-Related Factor-2 (Nrf2) Activation by the Stress Response Gene Immediate Early Response-3 (IER3) in Colonic Epithelial Cells. *Journal of Biological Chemistry* **2014**, *289* (4), 1917–1929.
- Stengel, S. T.; Fazio, A.; Lipinski, S.; Jahn, M. T.; Aden, K.; Ito, G.; Wottawa, F.; Kuiper, J. W. P.; Coleman, O. I.; Tran, F.; Bordononi, D.; Bernardes, J. P.; Jentsch, M.; Luzius, A.; Bierwirth, S.; Messner, B.; Henning, A.; Welz, L.; Kakavand, N.; Falk-Paulsen, M.; Imm, S.; Hinrichsen, F.; Zilbauer, M.; Schreiber, S.; Kaser, A.; Blumberg, R.; Haller, D.; Rosenstiel, P. Activating Transcription Factor 6 Mediates Inflammatory Signals in Intestinal Epithelial Cells Upon Endoplasmic Reticulum Stress. *Gastroenterology* **2020**, *159* (4), 1357-1374.e10.
- Stewart, W. E.; LeGoff, S.; Wiranowska-Stewart, M. Characterization of Two Distinct Molecular Populations of Type I Mouse Interferons. *Journal of General Virology* **1977**, *37* (2), 277–284.
- Sun, L.; Wu, J.; Du, F.; Chen, X.; Chen, Z. J. Cyclic GMP-AMP Synthase Is a Cytosolic DNA Sensor That Activates the Type I Interferon Pathway. *Science* **2013**, *339* (6121), 786–791.

- Sun, X.; Xie, Z.; Hu, B.; Zhang, B.; Ma, Y.; Pan, X.; Huang, H.; Wang, J.; Zhao, X.; Jie, Z.; Shi, P.; Chen, Z. The Nrf2 Activator RTA-408 Attenuates Osteoclastogenesis by Inhibiting STING Dependent NF-Kb Signaling. *Redox Biology* **2020**, *28*, 101309.
- Takaoka, A.; Yanai, H. Interferon Signalling Network in Innate Defence. *Cell Microbiol* **2006**, *8* (6), 907–922.
- Tanaka, M.; Tóth, F.; Polyák, H.; Szabó, Á.; Mándi, Y.; Vécsei, L. Immune Influencers in Action: Metabolites and Enzymes of the Tryptophan-Kynurenine Metabolic Pathway. *Biomedicines* **2021**, *9* (7), 734.
- Tashita, C.; Hoshi, M.; Hirata, A.; Nakamoto, K.; Ando, T.; Hattori, T.; Yamamoto, Y.; Tezuka, H.; Tomita, H.; Hara, A.; Saito, K. Kynurenine Plays an Immunosuppressive Role in 2,4,6-Trinitrobenzene Sulfate-Induced Colitis in Mice. *WJG* **2020**, *26* (9), 918–932.
- Taylor, C. T.; Colgan, S. P. Hypoxia and Gastrointestinal Disease. *J Mol Med* **2007**, *85* (12), 1295–1300.
- Taylor, C. T.; Colgan, S. P. Regulation of Immunity and Inflammation by Hypoxia in Immunological Niches. *Nat Rev Immunol* **2017**, *17* (12), 774–785.
- Tesser, A.; Piperno, G. M.; Pin, A.; Piscianz, E.; Boz, V.; Benvenuti, F.; Tommasini, A. Priming of the cGAS-STING-TBK1 Pathway Enhances LPS-Induced Release of Type I Interferons. *Cells* **2021**, *10* (4), 785.
- Tontini, G. E.; Vecchi, M.; Pastorelli, L.; Neurath, M. F.; Neumann, H. Differential Diagnosis in Inflammatory Bowel Disease Colitis: State of the Art and Future Perspectives. *WJG* **2015**, *21* (1), 21-46.
- Török, N.; Tanaka, M.; Vécsei, L. Searching for Peripheral Biomarkers in Neurodegenerative Diseases: The Tryptophan-Kynurenine Metabolic Pathway. *IJMS* **2020**, *21* (24), 9338.
- Tschurtschenthaler, M.; Adolph, T. E.; Ashcroft, J. W.; Niederreiter, L.; Bharti, R.; Saveljeva, S.; Bhattacharyya, J.; Flak, M. B.; Shih, D. Q.; Fuhler, G. M.; Parkes, M.; Kohno, K.; Iwawaki, T.; Janneke Van Der Woude, C.; Harding, H. P.; Smith, A. M.; Peppelenbosch, M. P.; Targan, S. R.; Ron, D.; Rosenstiel, P.; Blumberg, R. S.; Kaser, A. Defective ATG16L1-Mediated Removal of IRE1 α Drives Crohn's Disease-like Ileitis. *Journal of Experimental Medicine* **2017**, *214* (2), 401–422.
- Ungerstedt, J. S.; Blombäck, M.; Söderström, T. Nicotinamide Is a Potent Inhibitor of Proinflammatory Cytokines. *Clinical and Experimental Immunology* **2003**, *131* (1), 48–52.
- Vidal, K.; Grosjean, I.; Revillard, J.-P.; Gespach, C.; Kaiserlian, D. Immortalization of mouse intestinal epithelial cells by the SV40-arge T gene. *Journal of Immunological Methods* **1993**, *166*, 63-73.
- Waetzig, G. H.; Chalaris, A.; Rosenstiel, P.; Suthaus, J.; Holland, C.; Karl, N.; Vallés Uriarte, L.; Till, A.; Scheller, J.; Gröttinger, J.; Schreiber, S.; Rose-John, S.; Seegert, D. N-Linked Glycosylation Is Essential for the Stability but Not the Signaling Function of the Interleukin-6 Signal Transducer Glycoprotein 130. *Journal of Biological Chemistry* **2010**, *285* (3), 1781–1789.
- Wang, Y.-Y.; Jin, R.; Zhou, G.-P.; Xu, H.-G. Mechanisms of Transcriptional Activation of the Stimulator of Interferon Genes by Transcription Factors CREB and C-Myc. *Oncotarget* **2016**, *7* (51), 85049–85057.
- Wek, R. C.; Jackson, B. M.; Hinnebusch, A. G. Juxtaposition of Domains Homologous to Protein Kinases and Histidyl-tRNA Synthetases in GCN2 Protein Suggests a Mechanism for Coupling GCN4 Expression to Amino Acid Availability. *Proc. Natl. Acad. Sci. U.S.A.* **1989**, *86* (12), 4579–4583.

- Wek, S. A.; Zhu, S.; Wek, R. C. The Histidyl-tRNA Synthetase-Related Sequence in the eIF-2 α Protein Kinase GCN2 Interacts with tRNA and Is Required for Activation in Response to Starvation for Different Amino Acids. *Molecular and Cellular Biology* **1995**, *15* (8), 4497–4506.
- Wen, Z.; Fiocchi, C. Inflammatory Bowel Disease: Autoimmune or Immune-Mediated Pathogenesis? *Clinical and Developmental Immunology* **2004**, *11* (3–4), 195–204.
- Wheelock, E. F. Interferon-Like Virus-Inhibitor Induced in Human Leukocytes by Phytohemagglutinin. *Science* **1965**, *149* (3681), 310–311.
- Wu, J.; Zhao, L.; Hu, H.; Li, W.; Li, Y. Agonists and Inhibitors of the STING Pathway: Potential Agents for Immunotherapy. *Med Res Rev* **2020**, *40* (3), 1117–1141.
- Yusufu, I.; Ding, K.; Smith, K.; Wankhade, U. D.; Sahay, B.; Patterson, G. T.; Pacholczyk, R.; Adusumilli, S.; Hamrick, M. W.; Hill, W. D.; Isales, C. M.; Fulzele, S. A Tryptophan-Deficient Diet Induces Gut Microbiota Dysbiosis and Increases Systemic Inflammation in Aged Mice. *IJMS* **2021**, *22* (9), 5005.
- Yuwiler, A.; Oldendorf, W. H.; Geller, E.; Braun, L. EFFECT OF ALBUMIN BINDING AND AMINO ACID COMPETITION ON TRYPTOPHAN UPTAKE INTO BRAIN. *J Neurochem* **1977**, *28* (5), 1015–1023.
- Zamorano Cuervo, N.; Fortin, A.; Caron, E.; Chartier, S.; Grandvaux, N. Pinpointing Cysteine Oxidation Sites by High-Resolution Proteomics Reveals a Mechanism of Redox-Dependent Inhibition of Human STING. *Sci. Signal.* **2021**, *14* (680), eaaw4673.
- Zeissig, S.; Rosati, E.; Dowds, C. M.; Aden, K.; Bethge, J.; Schulte, B.; Pan, W. H.; Mishra, N.; Zuhayra, M.; Marx, M.; Paulsen, M.; Strigli, A.; Conrad, C.; Schuldt, D.; Sinha, A.; Ebsen, H.; Kornell, S.-C.; Nikolaus, S.; Arlt, A.; Kabelitz, D.; Ellrichmann, M.; Lützen, U.; Rosenstiel, P. C.; Franke, A.; Schreiber, S. Vedolizumab Is Associated with Changes in Innate Rather than Adaptive Immunity in Patients with Inflammatory Bowel Disease. *Gut* **2019**, *68* (1), 25–39.
- Zhang, C.; Shang, G.; Gui, X.; Zhang, X.; Bai, X.; Chen, Z. J. Structural Basis of STING Binding with and Phosphorylation by TBK1. *Nature* **2019**, *567* (7748), 394–398.
- Zhong, B.; Yang, Y.; Li, S.; Wang, Y.-Y.; Li, Y.; Diao, F.; Lei, C.; He, X.; Zhang, L.; Tien, P.; Shu, H.-B. The Adaptor Protein MITA Links Virus-Sensing Receptors to IRF3 Transcription Factor Activation. *Immunity* **2008**, *29* (4), 538–550.

Appendix

Materials

Chemicals

Table 2 List of chemicals

Substance	Supplier	Catalogue Number	CAS Number
0.5M EDTA pH 8.0	Invitrogen	15575-020	
3-Hydroxyanthranilic acid	Sigma Aldrich	148776-250MG	
6-Aminocaproic acid 99% powder	Merck	A2504-100g	60-32-2
Agar-agar, bacteriological	Carl Roth	2266.2	9002-18-0
Anthranilic acid	Sigma Aldrich	10680-25G	118-92-3
Ammonium persulfate (APS)	Serva	13376.01	7727-54-0
BisAcrylamide 30%	BioRad	1610158	
BIS-TRIS	Carl Roth	9140.2	6976-37-0
Bromophenol blue	AppliChem	A2331,0025	115-39-9
Dithiothietol (DTT)	Serva	20710,03	578517
Dimethylsulfoxid (DMSO)	Carl Roth	A994.2	67-68-5
Ethanol absolute	Supelco	1.00983.1000	64-17-5
Glycerol	AppliChem	A2926,0500	56-81-5
Glycine BioUltra	Sigma Aldrich	50046-50G	56-40-6
Hydrochloric acid 32%	Supelco	1.00319.1000	
Hydrogen peroxide solution 3%	Sigma Aldrich	88597-100ML-F	7722-84-1
Methanol	ChemSolute	1428.2500	67-56-1
Paraformaldehyde	Sigma Aldrich	15127-5g	30525-89-4
Propionic acid	Sigma Aldrich	94425-1ML-F	79-09-4
Roti-Stock 20 % SDS	Carl Roth	1057.1	
Saponin	Sigma Aldrich	47036-50G-F	8047-15-2
SDS Pellets	Carl Roth	CN30.3	151-21-3
Sodium acetate	Sigma Aldrich	S2889-250G	127-09-3
Sodium butyrate	Sigma Aldrich	B5887-250mg	156-54-7
Sodium chloride	Sigma Aldrich	S9625-5kg	7647-14-5
Sodium citrate tribasic dihydrate	Sigma Aldrich	S4641-500G	
Sodium dihydrogen phosphate dihydrate	Supelco	1.06342.1000	
Sodium deoxycholate	Sigma Aldrich	30970-100G	
Sodium hydrogen sulfite	Sigma Aldrich	8.06356.1000	
Sodium hydroxide pellets	Merck	1.06482.1000	1310-73-2
Sodium propionate	Sigma Aldrich	P5436-100G	
Sulfuric acid	Sigma Aldrich	258105-500ML	7664-93-9
Tetramethylethylenediamine (TEMED)	BioRad	1610801	110-18-9
Trichloroacetic acid, Bio Ultra	Sigma Aldrich	91228-100G	
Trifluoressigsäure (TFA)	Carl Roth	P088.1	
Tris (hydroxymethyl) aminomethane	Merck	1.08382.1000	77-86-1
Triton x-100	Sigma Aldrich	T9284-500ML	9002-93-1
Trypan Blue Solution	Gibco	15250-061	72-57-1
Tween 20	Merck	8.22184.0500	

Consumables

Table 3 List of consumables

Substance	Supplier	Catalogue Number
Advanced DMEM/F12	Gibco	12634-010
Amersham ECL Prime WB Reagents	Cytiva	RPN2232
Amersham 0.2 PVDF Membran	Cytiva	10600021
Bacilol	Paul Hartmann AG	973380
Blotting-Pads, Sorte 707, thik WB Filter	VWR	732-0597
Blotto, non-fat dry milk	Santa Cruz	sc-2325
Clarity Max Western ECL Substrate	Biorad	1705062
Cell culture flasks and plates	Sarstedt	
CryoStor® CS10	Stem cell	7930
Dialyzed Fetal Bovine Serum	Sigma Aldrich / Merck	F0392-100ML
DMEM GlutaMax	Thermofisher	61965-059
DPBS	Gibco	14190-169
Eppendorf tubes	Sarstedt	
Falcons	Sarstedt	
Foetal Bovine Serum (FBS) - Triple 0.1 µm	Serana	S-FBS-SA-015
Halt™ Protease Inhibitor Cocktail (100X)	Thermo Scientific	87786
HEPES	Sigma Aldrich	H0887-100ML
LB-Medium	Carl Roth	X968.2
Lipofectamine 3000 Transfection Reagent	Thermo Fisher	L3000-008
Lipofectamine RNAiMAX	Invitrogen	13778-150
Lyovec	Invivogen	lyec-1
Matrigel Growth factor reduced, Phenol red free	BD	356231
NEAA, non-essential amino acids	Gibco	11140-035
Nuclease-free Water	Qiagen	AM9937
Optimem	Gibco	31985-062
Penicillin-Streptomycin	Life Technologies	15140-122
Phosphate Buffered Saline (PBS) tablet	Sigma Aldrich	P4417-50TAB
PrimeTime Gene Expression Master Mix	IDT	1055771
Restore™ WB Stripping-Puffer	Thermofisher	21059
RIPA Lysis and Extraction Buffer	Thermo Scientific	89901
Page Ruler Plus Prestained Protein Ladder	Thermo Fisher	26619
Pipette tips	Starlab	
RNase ZAP 250ml	Sigma	R2020-250ML
Rotiphorese 50x TAE Puffer	Carl Roth	CL86.1
Serological pipettes	Sarstedt	
TGS 10x	Biorad	
Thin Blot Paper	Biorad	1620118
Trypsin EDTA	Gibco	25200-056

Kits

Table 4 List of kits

Kit	Supplier	Catalogue Number
CellTiter 96® AQueous Non-Radioactive Cell Proliferation Assay (MTS)	Promega	G5421
Monarch Total RNA Miniprep Kit	Bio Labs	T2010S
Maxima H Minus FirstStrand cDNA Kit	Thermo Scientific	K1652
GeneJET Plasmid Miniprep Kit	ThermoScientific	K0503
GeneArt® CRISPR Nuclease Vector with CD4 Enrichment Kit	Life Technologies	A21175
HiPure Plasmid Filter Midiprep Kit	Life Technologies	K210015

Media/Buffer compositions

The media and buffers were prepared according to the following protocols:

Table 5 Overview of buffer compositions

Buffer	Composition
5x Loading buffer	Tris at pH 6.8 [250 mM], SDS [10 %], Glycerol [50 %], DTT [500 mM], Bromphenolblau
4x Separation buffer	Tris at pH 8.8 [1.5 M], SDS [0.4 %]
4x Stacking buffer	Tris at pH 6.8 [0.5 M], SDS [0.4 %]
Cathode buffer	Tris [25 mM], 6-aminocaproic acid [40 mM], methanol [20 %]
Anode buffer 1	Tris [30 mM], methanol [20 %]
Anode buffer 2	Tris [300 mM], methanol [20 %]
10x TBS	Tris at pH 7.6 [200 mM], NaCl [1.37 M]
TBS-T	1x TBS + 0.1 % Tween20
LB medium	Tryptone [10 g], Yeast [5 g], NaCl [5 g] in 1 L dH ₂ O
LB agar	Tryptone [10 g], Yeast [5 g], NaCl [5 g], agar [15 g] in 1 L dH ₂ O

Table 6 Protocol to cast gels for SDS-PAGE

12 % gel	Composition
Separation gel	3.5 mL dH ₂ O, 2.5 mL 4x separation buffer, 4 mL Bis-acrylamide, 10 µL TEMED, 100 µL APS (10 %)
Stacking gel	1.95 mL dH ₂ O, 0.75 mL 4x stacking buffer, 300 µL Bis-acrylamide, 3 µL TEMED, 30 µL APS (10 %)

Table 7 Overview of the organoid media compositions

Organoid media	Composition
2x basal medium	46.8 mL Advanced DMEM/F12, 1 mL HEPES [1 M], 1 mL Glutamax [100x], 1 mL P/S, 200 µL NAC [500 mM]
ENR conditioned medium	70 % 2x basal medium, 10 % Noggin conditioned medium, 20 % R-Spondin conditioned medium, 0.1 % rhEGF [50 µg/mL]
Customized starvation medium	Glucose and amino acid concentrations given in the table below, 20 mM HEPES, 100 ng/mL rhNoggin, 1 µg/mL rhR-Spondin, 50 ng/mL rhEGF

Following components were added to prepare the cell starvation and control media:

Table 8 Components added to the customized DMEM powder to prepare starvation medium for ModeK cells

Substance	Supplier	Catalogue Number	cell culture
D-(+)-Glucose	Sigma Aldrich	G7021-100G	3060.0
Glycine	Sigma	50046-50G	30.0
L-Glutamine	Sigma	G3126-10G	292.3
L-Serine	Sigma	84959-25G	42.0
L-Tryptophan	Sigma	T0254-5G	16.0
Sodium Bicarbonate 99,5%	Sigma	S6297	3700.0

Following components were added to prepare the organoid starvation and control media:

Table 9 Components added to the customized ADF medium to prepare starvation medium for organoids

Substance	Supplier	Catalogue Number	organoids
Glycine	Sigma	50046-50G	18.75
L-Alanine (25g)	Carl Roth	3076,1	4.45
L-Arginin Monohydrochlorid (CellPure)	Carl Roth	1689,1	147.5
L-Asparagin Monohydrat (CellPure)	Carl Roth	KK37.1	7.5
L-Asparaginsäure (CellPure)	Carl Roth	1690,1	6.65
L-Cystein Hydrochlorid Monohydrat (CellPure)	Carl Roth	1694,1	17.56
L-Cystin -dihydrochlorid	Merck	C6727-25G	31.29
L-Glutaminsäure (CellPure)	Carl Roth	1743,1	7.35
L-Histidin Hydrochlorid Monohydrat	Carl Roth	1697,1	31.48
L-Isoleucin (CellPure)	Carl Roth	1698,1	54.47
L-Leucin (CellPure)	Carl Roth	1699,1	59.05
L-Lysin Hydrochlorid	Carl Roth	1700,1	91.25
L-Methionin (CellPure)	Carl Roth	1702,1	17.24
L-Phenylalanin (CellPure)	Carl Roth	1709,1	35.48
L-Prolin	Carl Roth	1713,1	17.25
L-Serine	Sigma	84959-25G	26.25
L-Threonin (CellPure)	Carl Roth	1738,1	53.45
L-Tryptophan	Sigma	T0254-5G	9.02
L-Tyrosin Dinatriumsalz Hydrat	Sigma Aldrich	T1145	55.79
L-Valin (CellPure)	Carl Roth	1742,1	52.85

Stimulants and inhibitors

Table 10 List of stimulants and inhibitors used in cell culture experiments

Substance	Supplier	Catalogue number
2'3'-cGAMP	Invivogen	tlrl-nacga23-02
3'3'-cGAMP	Invivogen	tlrl-nacga
3-Hydroxy-DL-kynurenin	Sigma Aldrich	H1771-25MG
Bafilomycin A1	Enzo	BML-CM110-0100
Cycloheximide (CHX)	Merck	239765-1ML
DMXAA	Hözel	HY-10964
dsDNA	InvivoGen	tlrl-ecdna
hEGF	R&D	236-EG-01M
L-Kynurenine	InvivoGen	tlrl-kyn
LPS	Sigma	L2880-10MG
N-Acetyl-L-cystein (NAC)	Merck	A7250-25g
Nicotinamide	Sigma Aldrich	N0636-100G
rhNoggin	PeptoTech	120-10C
rhR-Spondin	PeptoTech	120-38
rm IFN gamma	Immunotools	12343534
rm IFN-beta Protein (with carrier)	R&D Systems	8234-MB-010
rm IL-1 β	PeptoTech	211-11B
Rapamycin	Sigma	R0395-1MG
Tunicamycin	Enzo	BML-CC104
Y-27632	Abcam	ab120129

siRNAs

Following siRNAs were used for KD studies:

Table 11 List of siRNAs used in cell culture experiments

Name	Supplier	Order number
FlexiTube GeneSolution GS27103 for Eif2ak4	Qiagen	1027416
FlexiTube GeneSolution GS18024 for Nfe2l2	Qiagen	1027416
TBK1	Qiagen	3255271

qPCR Assays/Primers

Table 12 List of qPCR assays and primers

Gene name	ID	RefSeq Number	Supplier
18S rRNA	Mm03928990_g1		Invitrogen
Atf4	Mm.PT.58.31755577	NM_009716(1)	IDT
Eif2ak4	Mm.PT.58.10993494	NM_001177806(2)	IDT
c-myc	Mm.PT.58.13590978		IDT
Cxcl10	Mm.PT.58.43575827	NM_021274(1)	IDT
Tmem173	Mm.PT.58.12798185	NM_028261(1)	IDT
Cxcl1	Mm.PT.58.42076891	NM_008176(1)	IDT
Gclm	Mm.PT.58.17443532	NM_008129(1)	IDT
Ifnb1	Mm.PT.58.30132453		IDT
IL-6	Mm.PT.58.10005566	NM_031168	IDT
Wars	Wars_Mm00457097_m1		Thermo Fisher Scientific
Nfe2l2	Mm.PT.58.29108649	NM_010902(1)	IDT

Antibodies for WB

Table 13 List of primary and secondary antibodies used in WB

Primary Antibodies	Supplier	Catalogue number	Dilution factor
Atg16L1 (D6D5)	CST	8089	1,000
beta-actin (mono mouse)	Sigma	A-5441	10,000
cGAS (D3080)	CST	31659	1,000
c-Myc (D84C12)	CST	5605S	1,000
IκBα (L35A5)	CST	4814S	1,000
LC3A/B	CST	4108	1,000
NFκB P65 XP (D14E12)	CST	8242T	1,000
p-IκBα (Ser32)	CST	2859	1,000
P-P65 (S536)	CST	3033S	1,000
p-STING (S365) (D8F4W)	CST	72971	1,000
p-TBK1 / NAK (S172) (D52C2)	CST	5483	1,000
STING (D2P2F)	CST	13647	1,000
TBK1 /NAK	CST	3013	1,000
Secondary Antibodies	Supplier	Catalogue number	Dilution factor
ECL Anti-rabbit IgG Horseradish peroxidase-linked	Cytiva	NA934V	1,000
ECL Anti-mouse IgG Horseradish peroxidase-linked	Cytiva	NA931V	1,000

Supplements

List of Figures

Figure 1.1 Tryptophan metabolism through the kynurenine pathway (KP)	24
Figure 3.1 IBD patients have reduced mucosal Trp levels	37
Figure 3.2 Trp starvation for 24 h induces <i>Wars</i> expression and decreases cell viability	38
Figure 3.3 Trp starvation potentiates NF- κ B activation	40
Figure 3.4 Trp starvation impairs Cxcl10 induction after IFN treatment	41
Figure 3.5 Trp starvation reduces STING expression in ModeK cells and murine SI organoids	42
Figure 3.6 Trp starvation-induced STING loss does not depend on TBK1	43
Figure 3.7 Trp-starved cells scarcely respond to DMXAA	44
Figure 3.8 Trp starvation impairs the cGAS/STING response	45
Figure 3.9 Replenishing Trp levels rescues the phenotype	46
Figure 3.10 Starvation-induced STING decrease is specific to Trp	47
Figure 3.11 Trp starvation does not affect the glycolytic activity in ModeK cells	48
Figure 3.12 TCA cycle activity is reduced under Trp starvation	50
Figure 3.13 Intracellular ATP levels are not affected by Trp starvation	51
Figure 3.14 Supplementation of the Trp derivative NAM does not restore STING levels	52
Figure 3.15 General autophagy inducers do not lead to a decrease in STING	53
Figure 3.16 STING is reduced in autophagy-deficient cells upon Trp starvation	54
Figure 3.17 Trp starvation-induced STING decrease does not depend on Atg16l1-mediated autophagy	55
Figure 3.18 Trp starvation-induced STING loss is independent of Gcn2-mediated autophagy	56
Figure 3.19 Cellular stress and Trp starvation positively correlate	57
Figure 3.20 ER-stressed cells are more sensitive to Trp reduction	57
Figure 3.21 ER-stressed cells are more sensitive to Trp starvation	58
Figure 3.22 The impaired STING response under Trp starvation is independent of oxidative stress	59
Figure 3.23 NAC supplementation increased cell death in Trp-starved iXBP1 cells	60
Figure 3.24 Trp starvation impacts on Tmem173 mRNA levels	61
Figure 3.25 Trp starvation does not impair STING response via engaging Nrf2 pathway	62
Figure 3.26 Trp starvation requires protein translation for STING degradation	63

List of Tables

Table 1 Information on the primer used for the crRNA targeting the Atg16l1 gene	28
Table 2 List of chemicals	96
Table 3 List of consumables	97
Table 4 List of kits	98
Table 5 Overview of buffer compositions	98
Table 6 Protocol to cast gels for SDS-PAGE	98
Table 7 Overview of the organoid media compositions	99
Table 8 Components added to the customized DMEM powder to prepare starvation medium for ModeK cells	99
Table 9 Components added to the customized ADF medium to prepare starvation medium for organoids	100
Table 10 List of stimulants and inhibitors used in cell culture experiments	101
Table 11 List of siRNAs used in cell culture experiments	101
Table 12 List of qPCR assays and primers	102
Table 13 List of primary and secondary antibodies used in WB	102

Acknowledgements

My sincere gratitude goes to my principal supervisor Prof. Dr. Philip Rosenstiel for his excellent professional support, and I am extremely grateful for this indispensable contribution to my academic career.

I genuinely thank Prof. Dr. Konrad Aden for his supervision and guidance throughout my doctoral studies, and for making this doctoral thesis possible for me.

I would like to acknowledge all members of the Try-IBD research consortium, and I especially thank Dr. Björn Becker for his excellent advice and the scientific discussions. Thanks goes to the German Federal Ministry of Education and Research for supporting me and my project financially.

I also express my gratitude to Prof. Dr. Sabrina Jabs for the helpful scientific discussions.

My deepest appreciation belongs to my dear colleagues who supported me and made me laugh no matter how difficult the times were, especially Guang Yang, Hang Xiang, Dr. Lina Welz, Dr. Nami Kim, Qicong Wu, Mohamed Bakr, Silke Van Den Bossche, and Dr. Mhmd Oumari. I further thank the technicians Maren Reffelmann, Sabine Kock, and Stefanie Rentzow for their kind support during my onboarding and for their technical assistance. I also want to thank all other members of the Aden lab, Jabs lab, and Rosenstiel lab who, for reasons of space, I cannot all mention by name.

Most importantly, I am profoundly moved by the emotional support I received from my family, particularly from my parents and my sister. Without you I would not have made it this far and I thank you for everything.

Eidesstattliche Erklärung

Hiermit erkläre ich, Julia Kugler, an Eides statt, dass ich die vorliegende Dissertation unter der wissenschaftlichen Leitung von Prof. Dr. Philip Rosenstiel selbständig und ohne fremde Hilfe verfasst habe. Die Abhandlung stellt nach Form und Inhalt meine eigene Arbeit dar und ich habe außer der Beratung meiner Betreuer, Prof. Dr. Philip Rosenstiel und Prof. Dr. Konrad Aden, keine weitere Hilfe in Anspruch genommen wurde. Weiterhin habe ich keine anderen als die von mir angegebenen Quellen und Hilfsmittel benutzt und die den verwendeten Werken wörtlich und inhaltlich entnommenen Stellen als solche kenntlich gemacht. Die Arbeit wurde unter der Einhaltung der Regeln guter wissenschaftlicher Praxis der Deutschen Forschungsgemeinschaft erstellt. Die Arbeit wurde bis jetzt weder vollständig noch in Teilen einer anderen Stelle im Rahmen eines Prüfungsverfahrens vorgelegt, veröffentlicht, oder zur Veröffentlichung eingereicht. Ich versichere, dass ich weder an der Christian-Albrechts-Universität zu Kiel noch anderweitig bisher versucht habe, eine Dissertation einzureichen oder mich einer Promotionsprüfung zu unterziehen. Weiterhin wurde mir kein akademischer Grad entzogen.

Kiel, den _____

Julia Kugler